

ผลของขนาดอนุภาคและอัตราส่วนซีลิกอนต่ออุณหภูมิเนียมต่อความเสถียรทางความร้อนและความชื้น
ของซีไอไลต์บีต้า พอลิคริสตัลไลน์



นางสาวอุษณีย์ ฐูปหอม

สถาบันวิทยบริการ

จุฬาลงกรณ์มหาวิทยาลัย

วิทยานิพนธ์นี้เป็นส่วนหนึ่งของการศึกษาตามหลักสูตรปริญญาวิศวกรรมศาสตรมหาบัณฑิต

สาขาวิชาวิศวกรรมเคมี ภาควิชาวิศวกรรมเคมี


คณะวิศวกรรมศาสตร์ จุฬาลงกรณ์มหาวิทยาลัย

ปีการศึกษา 2545

ISBN 974-17-2492-6

ลิขสิทธิ์ของจุฬาลงกรณ์มหาวิทยาลัย

EFFECT OF PARTICLE SIZE AND SILICON TO ALUMINIUM RATIO ON THE HYDROTHERMAL
STABILITY OF POLYCRYSTALLINE ZEOLITE BETA



Miss Usnee Toophorm

สถาบันวิทยบริการ
จุฬาลงกรณ์มหาวิทยาลัย

A Thesis Submitted in Partial Fulfillment of the Requirements
for the Degree of Master of Engineering in Chemical Engineering

Department of Chemical Engineering

Faculty of Engineering

Chulalongkorn University

Academic Year 2002

ISBN 974-17-2492-6

Thesis Title EFFECT OF PARTICLE SIZE AND SILICON TO ALUMINIUM
RATIO ON THE HYDROTHERMAL STABILITY OF
POLYCRYSTALLINE ZEOLITE BETA
By Miss Usnee Toophorn
Field of Study Chemical Engineering
Thesis Advisor Professor Piyasan Prasertthdam, Dr.Ing.

Accepted by the Faculty of Engineering, Chulalongkorn University in Partial
Fulfillment of the Requirements for the Master's Degree

.....Dean of Faculty of Engineering
(Professor Somsak Panyakeow, D.Eng.)

THESIS COMMITTEE

..... Chairman
(Montree Wongsri, D.Sc.)

..... Thesis Advisor
(Professor Piyasan Prasertthdam, Dr.Ing.)

..... Member
(Associate Professor Tharathon Mongkhonsi, Ph.D.)

..... Member
(Waraporn Tanakulrungsank, D.Eng.)

..... Member
(Suphot Phatanasri, D.Eng.)

อุษณีย์ รูปหอม : ผลของขนาดอนุภาคและอัตราส่วนซิลิกอนต่ออลูมิเนียมต่อความเสถียรทางความร้อนและความชื้นของซีโอไลต์บีต้า พอลิคริสตัลไลน์ (EFFECT OF PARTICLE SIZE AND SILICON TO ALUMINIUM RATIO ON THE HYDROTHERMAL STABILITY OF POLYCRYSTALLIN ZEOLITE BETA)

อ. ที่ปรึกษา : ศ.ดร.ปิยะสาร ประเสริฐธรรม, 87 หน้า. ISBN 974-17-2492-6

การสังเคราะห์ผลึกบีต้าซีโอไลต์โดยวิธีไฮโดรเทอร์มอลที่สภาวะต่างๆ ได้ผลึกบีต้าซีโอไลต์ที่มีขนาดอนุภาคอยู่ในช่วง 0.2 ถึง 0.9 ไมโครเมตร นำผลึกที่สังเคราะห์ได้มาให้ความร้อนที่อุณหภูมิ 800 องศาเซลเซียสโดยมีน้ำ 10 โมลเปอร์เซ็นต์เป็นเวลา 30 นาที ทำการศึกษาความเสถียรต่อความร้อนและความชื้น โดยทำการวัดการเปลี่ยนแปลงของผลึกก่อนและหลังให้ความร้อนด้วย พบว่าหลังจากผ่านการให้ความร้อนอลูมิเนียมบางส่วนของที่อยู่ในโครงสร้างจะหลุดออกมาซึ่งสามารถวัดได้จาก ^{27}Al MAS NMR พื้นที่ผิวมีการเปลี่ยนแปลงลดลงโดยวัดจาก BET surface area ในขณะที่ผลจาก XRD แสดงให้เห็นว่าอนุภาคทุกขนาดมีการเปลี่ยนแปลงความเป็นผลึกเพียงเล็กน้อย อนุภาคที่มีขนาดเล็กจะเกิดการเปลี่ยนแปลงมากกว่าอนุภาคที่มีขนาดใหญ่ โดยอนุภาคที่มีขนาดเล็กจะเกิดการสูญเสียอะลูมิเนียมเตรดราฮีดรอลมีที่อยู่ในโครงสร้างมากกว่าอนุภาคที่มีขนาดใหญ่ อย่างไรก็ตามอัตราส่วนของซิลิกอนต่ออลูมิเนียมในโครงสร้างของซีโอไลต์บีต้าที่มีขนาดอนุภาคต่างกันหลังจากผ่านความร้อนและความชื้นจะมีค่าใกล้เคียงกัน ความว่องไวในการทำปฏิกิริยาของอนุภาคขนาดเล็กมากกว่าขนาดใหญ่แต่จะลดลงมากกว่าและจะมีความว่องไวใกล้เคียงกันเมื่อผ่านการให้ความร้อน ความร้อนและความชื้น นอกจากนี้พบว่าในขนาดของอนุภาคที่เท่ากันผลึกที่มีอัตราส่วนซิลิกอนต่ออลูมิเนียมต่ำจะเกิดการสูญเสียอะลูมิเนียมเตรดราฮีดรอลมีที่อยู่ในโครงสร้างมากกว่าผลึกที่มีอัตราส่วนอัตราส่วนซิลิกอนต่ออลูมิเนียมสูง

สถาบันวิทยบริการ
จุฬาลงกรณ์มหาวิทยาลัย

ภาควิชา.....วิศวกรรมเคมี..... ลายมือชื่อนิสิต.....
สาขาวิชา.....วิศวกรรมเคมี..... ลายมือชื่ออาจารย์ที่ปรึกษา.....
ปีการศึกษา.....2545.....

##4370631921 : MAJOR CHEMICAL ENGINEERING

KEY WORD: PARTICEL SIZE / ZEOLITE BETA / HYDROTHERMAL STABILITY

USNEE TOOPHORM : EFFECT OF PARTICEL SIZE AND SILICON TO ALUMINIUM RATIO ON THE HYDROTHERMAL STABILITY OF POLYCRYSTALLINE ZEOLITE BETA. THESIS ADVISOR: PROFESSOR PIYASAN PRASERTHDAM, Dr.Ing. 87 pp. ISBN 974-17-2492-6

Polycrystalline zeolite betas have been synthesized by hydrothermal method at various conditions. The particle sizes in the range of 0.2 to 0.9 μm were obtained. The samples were treated at 800 °C with 10 mole percent of water for 30 min. The changes of each size of zeolite beta before and after treatment were observed by ^{27}Al MAS NMR spectrometer, BET surface area measurement and X-ray diffraction. It was found that hydrothermal treatment caused dealumination. The relative area of tetrahedral ^{27}Al MAS NMR decreased similarly in accordance with the BET surface area while the crystallinity obtained from XRD was slightly changed for all sizes. It was found that change of the small particle size was easily occurred than that of the large one. However, the silicon to aluminium ratio in the zeolite framework of the sample after treatment decreased to constant values. The fresh catalysts for small particle size showed higher activity than that for large one but a significant change of activity with time on stream was pronounced. However, the similar activity for both size after hydrothermal treatment was observed. In addition, it was also observed that for the same particle size sample, extent of dealumination of the high Si/Al ratio is lower than that of the low one.

Department.....Chemical Engineering... Student's signature.....
 Field of study...Chemical Engineering... Advisor's signature.....
 Academic year.....2002.....

ACKNOWLEDGEMENTS

The author would like to express her greatest gratitude to her advisor, Professor Dr. Piyasan Prasertthdam for his invaluable guidance throughout this study. In addition, she is also grateful to Dr. Montree Wongsri, as the chairman and Associate Professor Tharathon Mongkonsri, Dr. Suphot Phatanasri and Dr. Waraporn Tanakulrungsank as the member of the thesis committee.

Special thank to petrochemical laboratory member who has encouragement and guided her over the year of this study

Finally she also would like to manifest her greatest gratitude to her parent and her family for their support and encouragement.



สถาบันวิทยบริการ
จุฬาลงกรณ์มหาวิทยาลัย

CONTENTS

	page
ABSTRACT (IN THAI).....	iv
ABSTRACT (IN ENGLISH).....	v
ACKNOWLEDGMENTS.....	vi
CONTENTS.....	vii
LIST OF TABLES.....	x
LIST OF FIGURES.....	xi
CHAPTER	
I INTRODUCTION.....	1
1.1 The objective of this work.....	1
1.2 The scopes of this study.....	1
II LITERATER REVIEWS.....	4
III THEORY.....	11
3.1 Structure of Zeolite.....	11
3.2 Category of Zeolite.....	15
3.3 Zeolite Active sites.....	21
3.3.1 Acid sites.....	21
3.3.2 Generation of Acid Centers.....	22
3.3.3 Basic sites.....	25
3.4 Shape Selective.....	26
3.5 Zeolite Synthesis.....	27
3.6 Zeolite beta.....	29
3.7 Thermal stability.....	30
IV EXPERIMENTS.....	31
4.1 Preparation of Na, NH ₃ and H- zeolite bata	31
4.1.1 Gel composition and reagents.....	31
4.1.2 Crystallization.....	33
4.1.3 First calcinations.....	33
4.1.4 Ammonium ion – exchange.....	33
4.1.5 Second calcination.....	33

CONTENTS(CONT.)

	page
4.2 Hydrothermal Pretreatment.....	34
4.3 Characterization studies.....	34
4.3.1 Scanning Electron Microscopy (SEM).....	34
4.3.2 X- Ray Diffraction analysis (XRD).....	34
4.3.3 ²⁷ Al Magnetic Angle Spinning Nuclear Magnetic Resonance (²⁷ Al MAS NMR).....	35
4.3.4 BET surface area measurement.....	35
4.3.4.1 BET apparatus.....	35
4.3.4.2 Measurement.....	35
4.3.5 X-Ray Fluorescence analysis (XRF).....	36
4.4 Reaction Testing.....	37
4.4.1 Chemicals and Reagents.....	37
4.4.2 Instruments and Apparatus.....	37
4.4.3 Reaction Method.....	38
V RESULTS AND DISCUSSION.....	40
5.1 The effect of crystallites size.....	40
5.1.1 Crystallite size of H-Beta Zeolite samples.....	40
5.1.2 BET surface area.....	40
5.1.3 Percent relative crystallinity.....	45
5.1.4 ²⁷ Al MAS NMR Spectra.....	53
5.1.5 Reaction testing.....	61
5.2 The effect of silica to alumina ratio.....	63
5.2.1 Silica to alumina ratio by XRF measurement.....	63
5.2.2 Crystallite size of H-Beta Zeolite sample.....	63
5.2.3 BET surface area.....	63
5.2.4 Percent relative crystallinity.....	66
5.2.5 ²⁷ Al MAS NMR Spectra.....	70
VI CONCLUSIONS AND RECOMMENDATIONS.....	75
REFERENCES.....	76

CONTENTS(CONT.)

	page
APPENDICES.....	79
A-1 Calculation of Si/Al Atomic for Zeolite beta preparation.....	80
A-2 Calculation of vapor pressure of water.....	81
A-3 Calculation of % crystallinity.....	81
A-4 Calculation of the relative area of tetrahedral aluminum(%).....	82
A-5 Calculation of the specific surface area.....	82
A-6 Calculation of reaction flow rate.....	84
A-7 Calculation of methanol conversion reaction.....	85
B-1 The result of hydrothermal treatment condition: 600 °C, 24 h with 10 mole percent of water.....	86
B-2 The result of hydrothermal treatment condition: 700 °C, 24 h with 10 mole percent of water.....	86
VITA.....	87



 สถาบันวิทยบริการ
 จุฬาลงกรณ์มหาวิทยาลัย

LIST OF TABLES

Table	page
3.1 Zeolites and their secondary building units.....	14
3.2 Structural characteristics of selected zeolites.....	16
4.1 Reagents used for the preparation of Na – zeolite beta	32
4.2 Operating condition of gas chromatograph (GOW-MAC).....	36
4.3 Operating condition for gas chromatograph.....	38
5.1 BET surface area and percent crystallinity.....	44
5.2 Percent relative area of ²⁷ Al NMR signals.....	54
5.3 Si/Al content in zeolite beta	63
5.4 BET surface area and percent crystallinity, Si/Al ratio.....	65
5.5 Percent relative area of ²⁷ Al NMR signals.....	71
B.1 The result of hydrothermal treatment condition: 600 °C, 24 h with 10 mole percent of water.....	86
B.2 The result of hydrothermal treatment condition: 700 °C, 24 h with 10 mole percent of water.....	86

สถาบันวิทยบริการ
จุฬาลงกรณ์มหาวิทยาลัย

LIST OF FIGURES

Figure	page
3.1 TO ₄ tetrahedra (T=Si or Al)	12
3.2 Secondary building units (SBU's) found in zeolite structures	13
3.3 Structure of ZSM-5	17
3.4 Structure of Faujasite.....	18
3.5 Structure of zeolite beta	18
3.6 Structure of zeolite ZSM-12	19
3.7 Structure of Mordenite.....	20
3.8 Framework structure of MCM-22	21
3.9 Diagram of the surface of a zeolite framework	23
3.10 Water molecules co-ordinated to polyvalent cation are dissociated by heat treatment yielding Brønsted acidity.....	24
3.11 Lewis acid site developed by dehydroxylation of Brønsted acid site	24
3.12 Steam dealumination process in zeolite	25
3.13 The enhancement of the acid strength of OH groups by their interaction with dislodged aluminum species.....	26
3.14 Diagram depicting the three type of selectivity	27
4.1 Preparation procedures of zeolite beta.....	32
4.2 Schematic diagram of the reaction apparatus for reaction.....	39
5.1 Scanning electron micrographs of H-zeolite beta particle size.....	41
5.2 BET surface area (m ² /g) of H-zeolite beta, fresh and treated with different size.....	44
5.3 The percent crystallinity of treated H-zeolite beta at different size.....	46
5.4 XRD spectra of H-zeolite beta crystalite size 0.2 μm.....	47
5.5 XRD spectra of H-zeolite beta crystalite size 0.3 μm.....	48
5.6 XRD spectra of H-zeolite beta crystalite size 0.4 μm.....	49
5.7 XRD spectra of H-zeolite beta crystalite size 0.5 μm.....	50
5.8 XRD spectra of H-zeolite beta crystalite size 0.7 μm.....	51
5.9 XRD spectra of H-zeolite beta crystalite size 0.9 μm.....	52
5.10 The percentage relative area of tetrahedral ²⁷ Al MAS NMR changed of treated H-zeolite beta at different size.....	54

LIST OF FIGURES (CONT.)

xi

Figure	page
5.11 ^{27}Al MAS NMR spectra of H-zeolite beta, particle size 0.2 μm	55
5.12 ^{27}Al MAS NMR spectra of H-zeolite beta, particle size 0.3 μm	56
5.13 ^{27}Al MAS NMR spectra of H-zeolite beta, particle size 0.4 μm	57
5.14 ^{27}Al MAS NMR spectra of H-zeolite beta, particle size 0.5 μm	58
5.15 ^{27}Al MAS NMR spectra of H-zeolite beta, particle size 0.7 μm	59
5.16 ^{27}Al MAS NMR spectra of H-zeolite beta, particle size 0.9 μm	60
5.17 Methanol conversion over zeolite beta compared between small and large particle size both fresh and treated.....	62
5.18 Scanning electron micrographs of H-zeolite beta, Si/Al=17, 27 and 45.....	64
5.19 Relationship between the single point BET surface area (m^2/g) and the Si/Al ratio of H-zeolite beta, both fresh and treated by hydrothermal treatment at different Si/Al ratio.....	61
5.20 XRD spectra of H-zeolite beta, Si/Al ratio = 17.....	67
5.21 XRD spectra of H-zeolite beta, Si/Al ratio = 27.....	68
5.22 XRD spectra of H-zeolite beta, Si/Al ratio = 45.....	69
5.23 Percent relative area of tetrahedral ^{27}Al NMR changed of treated H- zeolite beta with different Si/Al ratio.....	71
5.24 ^{27}Al MAS NMR spectra of H-zeolite beta, Si/Al ratio = 17.....	72
5.25 ^{27}Al MAS NMR spectra of H-zeolite beta, Si/Al ratio = 27.....	73
5.26 ^{27}Al MAS NMR spectra of H-zeolite beta, Si/Al ratio = 47.....	74

CHAPTER I

INTRODUCTION

Zeolite beta is a crystalline aluminosilicate of large pores synthesized from a gel with alkali metal and tetraethylammonium cations. It was first synthesized in 1967 by Wadlinger et al.[1]. Its structure is a 12-member ring (12 MR) tridirectional zeolite with two different types of channels having about 7.0 and 5.5 Å. It can be synthesized within a large range of silica to alumina ratio (12-200) [2]. This zeolite may offer interesting opportunities as a catalyst, since it combines three important characteristics: large pores, high silica to alumina synthesis ratio and a tridirectional network of pores.

Zeolite beta is potentially an important catalyst because, like other zeolites with high silica content, it can possess high thermal and acid treatment stability, high strength acid sites and hydrophobicity [3]. Because of its pore system and high acidity, it is of great potential industrial interest, especially, in reactions such as catalytic cracking isomerization, aromatic alkylation with alkenes, aromatic acylation [4,5] and indole synthesis [6] aromatic nitration.

Zeolite beta is generally formed as a very small catalyst, less than 1 µm which diminishes its stability. On the other hand, it is known that the crystal size of a zeolite catalyst can influence the reaction activity and selectivity. The crystallite size of medium pore zeolites, for example, has a pronounced influence in the selectivity of formation of para-dialkylated aromatic compounds [7]. Zeolite beta has been used as a cracking catalyst for higher production of olefins, and an increase in the formation of these products was observed, as well as in the catalyst stability by increasing the crystallite size [8]

Several parameters influence the choice of the optimum size of zeolite crystals: (a) shape-selective catalysis requires larger crystals; (b) catalyst effectiveness is larger for smaller crystals; (c) in bifunctional catalysts, crystal size can influence the average distance between acidic and metallic sites, and modify the product

distribution; (d) catalyst deactivation by coke can be more severe for larger crystals; (e) diffusion of matrix components is easier in the case of smaller crystals; (f) template extraction, cation exchange, even distribution of metal functions are more easily performed for smaller crystals; (g) diffusion of water and extra-framework species as a function of crystal size affect the hydrothermal stability in activation conditions; (h) regeneration of used catalysts can be more difficult for larger crystals; (i) filtration and recovery of very small crystals is a technological challenge [9].

However, little attempt has been made to characterize the stability of zeolite beta, especially, the effect of zeolite crystal size on the hydrothermal properties has not been well established in the literature [10].

Multinuclear solid-state NMR is a powerful tool to characterize the structure of zeolite and other heterogeneous catalysts [11-13]. It can provide specific information on zeolite structure and properties can distinguish framework Al and nonframework Al.

In this work we have studied the effect of particle size on hydrothermal stability of zeolite beta. The hydrothermal stabilities with crystal size in range of 0.2 to 0.9 μm (for the same crystallite Si/Al ratio 50) and the Si / Al ratio in the range of 30 to 80, for the same size as are investigated by using multinuclear solid-state NMR techniques combined with BET surface area measurement and X-ray diffraction.

1.1 The objective of this work

To study the effect of particle size and the silicon to aluminium ratio on the hydrothermal stability of polycrystalline zeolite beta.

1.2 The scope of this study

- 1.2.1 Preparation of the H-form zeolites beta using hydrothermal method in order to varying particle size and Si/Al ratio
- 1.2.2 Treatment the zeolite beta under hydrothermal treatment condition at 800 °C with 10 mole percent of water for 30 min.

- 1.2.3 Characterization of zeolite beta samples by the following methods
- (a) Structure and crystallinity of samples by X-ray diffractometer (XRD).
 - (b) Morphology of sample by Scanning Electron Microscopy (SEM).
 - (c) Specific surface area by N₂ adsorption based on BET method (BET).
 - (d) Determination of chemical composition of catalysts by X-ray Fluorescence (XRF).
 - (e) Quantitative analysis of tetrahedral aluminium in samples by ²⁷Al nuclear magnetic resonance (²⁷Al NMR).

The present thesis is arranged as follows:

Chapter II presents the literature reviews of investigation, synthesis, properties, stability and reaction of zeolite beta.

Chapter III presents the theoretical consideration on zeolite beta.

Chapter IV presents the experimental systems and operation procedures. The experimental results obtained from the laboratory scale and standard measurements are reported and discussed in chapter V.

The last chapter gives overall conclusion emerged from this work. Finally the calculation of zeolite beta preparation, calculation of percent crystallinity and data experiments are included in appendices at the end of this thesis.

CHAPTER II

LITERATURE REVIEWS

The crystallite size and Si/Al ratio are important parameters for the application of zeolite. Zeolite beta is a three dimensional wide-pore, a high silica zeolite, which has potential technological applications in petrochemical process and organic synthesis [14].

Zeolite beta synthesized by a hydrothermal method [15] always has a low product yield and could not be synthesized with $\text{SiO}_2/\text{Al}_2\text{O}_3$ ratio above 250 using TEAOH (tetraethylammonium hydroxide), TEAOH-diethanolamine, TEABr(tetraethylammonium bromide)-triethanolamine [15,16].

The development of method for producing zeolites with controllable macroshape and crystal size is of great technological importance. Spherical form is often preferable e.g. for catalytic applications due to limit attrition and easy handling [17]. Further, the size and the arrangement of the particles building up a catalyst have a crucial role for its performance.

The synthesis of zeolite beta has been studied. Most synthetic zeolite are made by hydrothermal method using the following templating agent: (1) tetraethylammonium hydroxide (TEA) (2) tetraethylammonium bromide-diethanolamine (3) tetraethylammonium hydroxide-tetraethylammonium bromide triethanolamine. The crystal display truncated square bipyramidal morphology with diameter from 0.5 to 1.0 μm and Si/Al ratio from 14 to 72 in a wide range of crystallization temperature and time. The intensity of the X-ray lines was strongly influenced by the condition of calcination the best results were obtained by calcination under water vapor [18, 19]. The more increase of the silicon content in reaction mixture led only to a small enhancement of the Si/Al ratio in the crystal. Wilma N. M. [3] studied the synthesis of zeolite beta with lower template content and observes the influence in its crystallization and crystal size. They obtained that the

average crystallite size increases as template content was decreased, especially, when temperature was increased from 130 to 150°C and longer crystallization times was set.

The high Si/Al ratio was prepared using a new crystallization method called “Dry Gel Conversion Technique, using TEAOH as a structure-directing agent. The crystal size by this method had uniform particles of about 60 nm. This method allowed one to prepare zeolite-beta with higher SiO₂/Al₂O₃ ratio (30 to infinity) than those which have been obtained by the conventional hydrothermal synthesis method. Highly crystalline stable spherical macroparticles of zeolite beta were prepared using a macroporous anion exchanger as a macrotemplate resin [17].

Perez Pariente et al. [20] studied the efficiency of the synthesis of zeolite beta and the chemical composition of crystals. It was very difficult to effectively synthesize siliceous crystal of zeolite beta. From aluminum-rich gels (SiO₂/Al₂O₃ = 30), high yield of zeolite beta could easily be obtained, whereas from siliceous gels (SiO₂/Al₂O₃ = 900), zeolite beta was found in small amount. The crystals were enriched in aluminium. This synthesis insufficiency was due to the inefficiency use of silicon, the mother liquor always being exhausted in aluminium at the end of the crystallization. The incorporation of silicon in zeolite beta could be improved by several means. When ethanol was kept in the system, when aluminium was excluded from the gel particles, or when the synthesis temperature was increased from 100 to 120°C, reasonable yields of siliceous Zeolite beta crystals were obtained.

Bellussi et al. [21] studied the catalytic performance of zeolite beta in liquid phase alkylation of benzene with ethylene and propylene to ethylbenzene and cumene (isopropylbenzene), respectively. They found that zeolite beta was more active and more selective than phosphoric acid (PA), ultrastable Y zeolite (USY) and H-ZSM-5. Furthermore, they studied the influence of Si/Al ratio and particle size of catalyst on activity and selectivity because of intraparticle diffusion. They found that decreasing the framework Al content (by direct synthesis or by partial substitution of Al for B) produced a decrease in both conversion and selectivity in cumene and ethylbenzene. When USY used as catalyst, higher aromatics (triisopropylbenzene) increased because the presence of super cages.

Camiloti et al. [22] studied acidity of zeolite beta with Si /Al ratios ranging from 18 to 33 by temperature programmed desorption (TPD) of ammonia and its catalytic behavior was evaluated by disproportionation of ethylbenzene. The acid strength of zeolite beta determined by TPD of ammonia increased as the Si /Al ratio was increased from 18 to 33. Despite of carrying out TPD measurements under very careful condition, the NH_3/Al ratios were always higher than unity and this result was probably a consequence of Lewis acid sites formed by structural defects present in H-zeolite beta. The ammonia desorbed between 380 °C and 600 °C seemed to be very appropriate to quantify the number of Brönsted acid sites in this zeolite. The results correlated very well with the catalytic behavior of this zeolite: the catalysts with stronger acid sites, determined by NH_3 -TPD, present also higher catalytic activity in the disproportionation of benzene. The induction period of this reaction had no dependence on zeolite Si/Al ratio.

The recent studies demonstrated that part of aluminium atom disconnected from the framework during calcination or steaming could reinsert by post-synthesis hydrothermal treatments [23,24]. The state of the aluminium atoms in actual catalysts would then strongly depend on the nature and severity of the activation treatments as well as on the composition and structure of parent solid. Careful characterization of the local environment of the aluminium atom was therefore essential for the understanding of the catalytic properties of zeolite. Bourgeat-Lami. et al. [25] and Muller et al. [26] independently studied the state of aluminium in zeolite beta by nuclear magnetic ^{27}Al , ^1H and ^{29}Si MAS NMR combined with elemental analysis. In the presence of water the distorted sites may feature an octahedral symmetry or undergo hydrolysis of the Al-O bonds. Partially hydrolyzed aluminium sites would account for the various hydroxylated species evidenced by infrared and for the NMR invisible aluminium.

The hydrothermal treatment was found to cause dealumination of the zeolite lattice and formation of extralattice aluminium species of low symmetry which remain within the pores of zeolite [10, 27, 28]. The effect of hydrothermal treatment on the structure and properties of zeolite with a range of aluminium contents has been investigated. Characterization of the treated zeolite was undertaken with solid-state

NMR (^{27}Al and ^{29}Si), Infrared water adsorption, X-ray diffraction [10, 28], Chemical analysis [28]. On the other hand, dealumination was used to increase the Si/Al ratio of the zeolitic framework, while increase the thermal stability but also because the amount of acidit [10, 29]. Dealumination was performed various treatment by various thermal or hydrothermal treatments complexation by oxalic acid, direct replacement of aluminium by silicon with gaseous silicon tetrachloride [10], HCl treatment [30] dicarboxylic acid treatment [31].

Zhang et al. [10] studied the thermal and hydrothermal stability of nanosized and microsized HZSM-5 zeolite. The samples were treated at varies temperature as 400-700 °C and under 100% water vapor for 2 h. Both nanosizes and microsized were slightly decreased as the hydrothermal temperature increased. The hydrothermal treatment of nanosizes and microsized also caused the zeolite framework to dealuminate. The peak intensity of the framework Al at 52 ppm in the ^{27}Al MAS NMR spectra of the nanosizes decreased more readily than that of microsized and the line width of the ^{27}Al MAS NMR spectra also broadened slightly after the hydrothermal treatment. The result from XRD measurement relative crystallinity of nanosizes was because more decreases slowly than that of the microsized. By nuclear solid-state NMR combine with BET surface and XRD investigations the hydrothermal stability of the nanosizes was almost the same that of the microsized. In addition, with low aluminaium contact it was found to be more resistant to dealumination was calcination and hydrothermal treatment and degree of dealumination was greater when steam was present in the treatment [28].

The extent of dealumination decreased in the same order as the number of T-sites in four-ring: Beta > Mordinite > ZSM-5 > terricirite . Factors such as the zeolite structure type, the Si/Al ratio of the framework, the crystal size, and the number of Brönsted acid sites interacting with the framework or the number of defect sites influenced the dealumination behavior of an individual zeolite sample. Zeolite beta can be very easily dealuminated. After the deep bed calcination, only about one-fourth of the aluminium atoms remained in the lattice and a large amount of EFAI was present. The XRD powder patterns and the surface areas showed that the crystallinity of the sample was retained after treatment [27].

Kunkeler et. al. [32] studied the influence of hydrothermal treatment on the catalytic activity of zeolite beta in the Lewis acid-catalyzed Meerwein-Ponndorf-Varley reaction Ketones. The activity of (H) beta could be increased by several orders of magnitude by mild steaming. The catalytic activity of the materials following reactivation could be diminished again by adsorption of ammonia followed by an induction period. For these changes, an explanation was offered in terms of Lewis acidic framework aluminium atoms which underwent a change of configuration depending on the ligands present, rather than becoming extraframework aluminum. FTIR, ^{29}Si and ^{27}Al MAS NMR spectroscopy were applied to investigate the changes induced by the hydrothermal procedure.

The acid properties and resultant catalytic activity of zeolite material were known to be related to the degree of substitution of aluminum for silicon in the framework [33]. The concentration of acid sites in non-dealuminated ($\text{Si}/\text{Al} = 10$), and dealuminated ($\text{Si}/\text{Al} = 20-90$) H- zeolite betas has been studied by quantitative IR measurements of pyridine sorption [27]. The number of Brønsted sites was found to be less than that of Al atom. Most probably this was due to the presence of Al in extraframework position (Al-OH groups and Lewis acid sites were found). Some positively charged extraframework Al species may neutralize the charge of AlO_4^- and lower the concentration of protonic sites.

Dealumination decreased the amount of extraframework Al species and, hence, the difference between the amounts of Al and Brønsted sites. Dealumination also decreased the number of Lewis acid sites [31]. IR studies of pyridine desorption evidenced that, as well as strong Brønsted sites (Si-OH-Al), there were also weak Brønsted sites, not Si-OH-Al; their nature is not clear. The contribution of such weak Brønsted sites decreased with the extent of dealumination. Dealumination removed the less acidic hydroxy groups first.

The high silica zeolites are attractive catalytic materials because of their thermal and hydrothermal stabilities, acid strength, good resistance for dealumination and hydrophobicity [34].

Frederic et al studied the influence of composition and size of the parent crystals of zeolite beta on its acidity, stability and catalytic activity [35]. The optimum in catalytic activity of zeolite beta was strongly influenced by dealumination during the activation process. Dealumination was generally favored in the case of aluminium-rich zeolites and, within an isostructural series, the stability of tetrahedral aluminium decreased as the aluminium molar ratio increased. Smaller crystals with higher aluminium contents were formed under synthesis condition that generated tetrahedra distortions and silanol defects, with a significant decrease of the thermal stability.

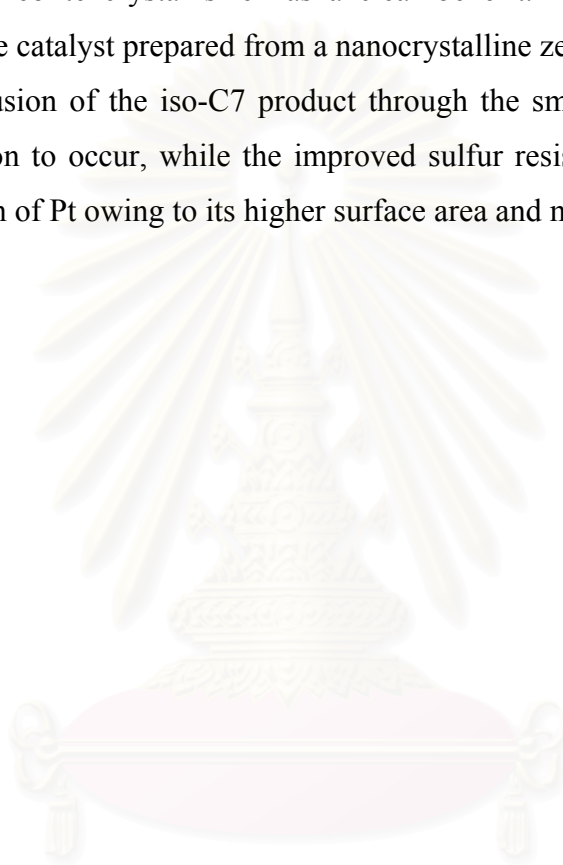
The importance of the lattice stability for the formation of Brønsted acid sites was further stressed by the influence of crystal size on the catalytic activity. The preparation of small grain zeolite beta has been considered as a desirable target in order to increase the effectiveness of the catalyst [36].

Bonetto et al [37] studied the optimum of zeolite beta in cracking catalyst. The zeolite betas with different crystal sized have been used as catalysts for gas-oil cracking. An optimum compromise between stability, activity and selectivity has been found for a sample with an average crystal size of 0.4 μm . This sample, before and after steaming, gave a slightly lower selectivity for gasoline and coke than a high and a low unit cell size USY zeolite, respectively. The optimized zeolite beta produced more liquefied petroleum gas alkenes and a relatively high iso-butane yield that were useful for methyl tert butyl ether and alkylation gasoline production. Zeolite beta with the same silica-to-alumina ratio, but with crystallite size in a narrow distribution countered at ca. 0.17, 0.40 and 0.70 μm , was used to study the stability. The percentage of crystallinity retention during steaming was reported. The stability increased with increasing crystallite size but this increase was not very high.

It was shown previously, the small crystallite zeolite beta was relative unstable to the conventional calcination procedures used for activation, and a loss of properties occurred during this process [38]. This limitation could be overcome by preparing the zeolite with a larger crystal size. However, the crystal size had to be optimized since too large crystallites, whilst being more thermally and hydrothermally stable, were

less active and selective due to higher diffusion limitations, as has been shown to occurred on zeolite Y.

Arribas et al [39] investigated the influence of zeolite crystal size on the catalytic performance of Pt/Beta catalysts for the simultaneous hydroconversion of n-C7 and benzene either the absence or in the presence of sulfur. It was shown that decreasing the zeolite crystal size has a clear benefit. The higher isomerization selectivity of the catalyst prepared from a nanocrystalline zeolite beta can be adsorbed to a faster diffusion of the iso-C7 product through the small crystallites preventing cracking reaction to occur, while the improved sulfur resistance can be related to a better dispersion of Pt owing to its higher surface area and mesoporosity.



สถาบันวิทยบริการ
จุฬาลงกรณ์มหาวิทยาลัย

CHAPTER III

THEORY

3.1 Structure of Zeolite

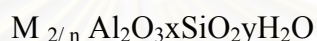
Zeolites are highly crystalline, hydrated aluminosilicates that upon dehydration develop in the ideal crystal a uniform pore structure having minimum channel diameters (aperture) of from about 0.3 to 1.0 nm. The size depends primarily on the type of zeolites and secondarily on the cations present and the nature of treatments such as calcination, leaching, and various chemical treatments. Zeolites have been of intense interest as catalysts for some three decades because of the high activity and unusual selectivity they provide, mostly in a variety of acid-catalyzed reactions. In many cases, but not all, the unusual selectivity is associated with the extremely fine pore structure, which permits only certain molecules to penetrate into the interior of the catalyst particles, or only certain products to escape from the interior. In some cases unusual selectivity seems to stem instead from constraints that the pore structure sets on allowable transition states, sometimes termed spatio-selectivity.

The structure of the zeolite consists of a three-dimensional framework of the SiO_4 and AlO_4 tetrahedra as presented in Figure 3.1 [40], each of which contains a silicon or aluminum atom in the center. In 1982, Barrer defined zeolites as the porous tectosilicates [38], that is, three-dimensional networks built up of TO_4 tetrahedra where T is silicon or aluminum. The oxygen atoms are sheared between adjoining tetrahedra, which can be present in various ratios and arranged in a variety of ways. The framework thus obtained has pores, channels, and cages, or interconnected voids.

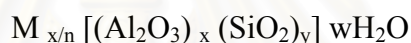
A secondary building unit (SBU) consists of selected geometric groupings of those tetrahedra. There are sixteen such building units, which can be used to describe all of known zeolite structures; for example, 4 (S4R), 6 (S6R), and 8 (S8R) – member single rings, 4-4 (D6R), 8-8 (D8R) – member double rings. The topologies of these units are shown in Figure 3.2 [41]. Also listed are the symbols used to describe them. Most zeolite frameworks can be generated from several different SBU's. Descriptions

of known zeolite structures based on their SBU's are list in Table 3.1 [42]. Both zeolite ZSM-5 and Ferrierite are described by their 5-1 building units. Offertile, Zeolite L, Cancrinite, and Erionite are generated using only single 6-member rings. Some zeolite structures can be described by several buildings. The sodalite framework can be built from either the single 6-member ring or the single 4-member ring. Faujasite (type X or type Y) and zeolite be constructed using 4 ring or 6 ring building units. Zeolite a can also be formed using double 4 ring building units, whereas Faujasite cannot.

Zeolites may be represented by the empirical formula:



or by a structural formula:



Where the bracketed term is the crystallographic unit cell. The metal cation (of valence n) is present it produces electrical neutrality since for each aluminum tetrahedron in the lattice there is an overall charge of -1 . Access to the channels is limited by aperture consisting of a ring of oxygen atoms of connected tetrahedra. There may be 4, 5, 6, 8, 10, or 12 oxygen atoms in the ring. In some cases an interior cavity exists of larger diameter in the aperture; in others, the channel is of uniform diameter like a tube [43].

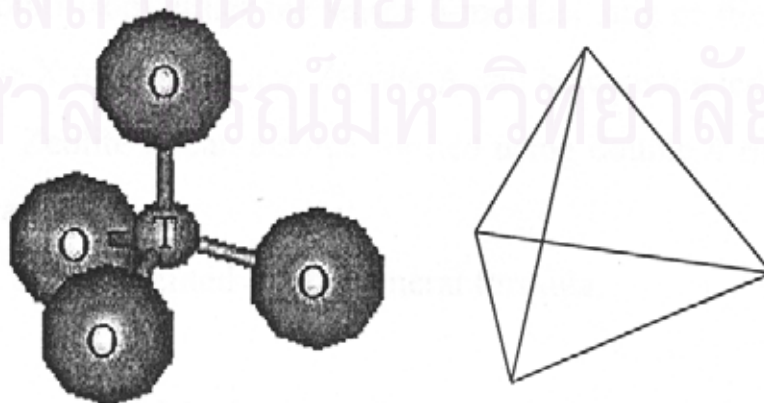


Figure 3.1 TO_4 tetrahedra (T=Si or Al) [40]

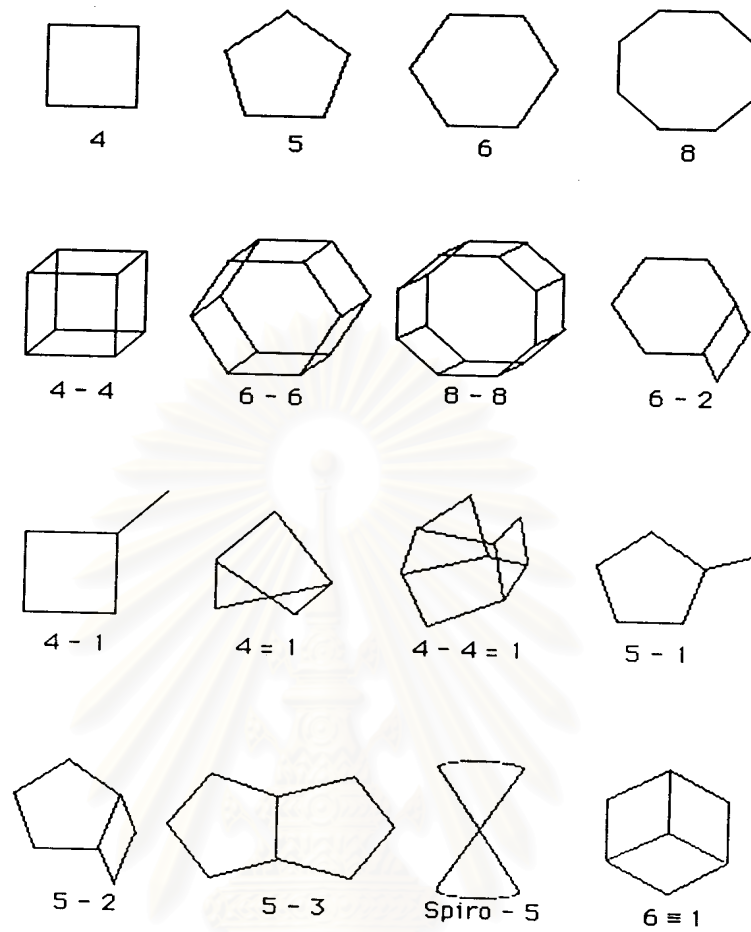


Figure 3.2 Secondary building units (SBU's) found in zeolite structures [41]

สถาบันวิทยบริการ
จุฬาลงกรณ์มหาวิทยาลัย

Table 3.1 Zeolites and their secondary building units. The nomenclature used is consistent with that presented in Figure 3.4 [42]

ZEOLITE	SECONDARY BUILDING UNITS							
	6	4	4-4	6-6	8-8	4-1	5-1	4-4=1
Bikilaite							X	
Li-A (BW)	X	X	X					
Analcime	X	X						
Yagawaralite	X		X					
Episibite							X	
ZSM-5							X	
ZSM-11							X	
Ferrierite							X	
Cachiardite							X	
Brewsterite	X							
Laumontite		X						
Modenite							X	
Sodalite	X	X						
Henulandite								X
Stibite								X
Natrolite						X		
Thomdonite						X		
Edingtonite						X		
Cancrinite		X						
Zeolite L		X						
Mazzite	X							
Merlinoite	X		X		X			
Philipsite	X		X					
Zeolite Losod		X						
Erionite	X	X						
Paulingite	X							
Offeretite		X						
TMA-E(AB)	X	X						
Gismondine	X		X					
Levyne		X						
ZK-5	X	X	X		X			
Chabazite	X	X			X			
Gmelinite	X	X	X		X			
Rho	X	X	X			X		
Type A	X	X	X	X				
Faujasite	X	X			X			

3.2 Category of Zeolite

There are over 40 known natural zeolites and more than 150 synthetic zeolites have been reported [44]. The number of synthetic zeolites with new structure morphologies grows rapidly with time. Based on size of their pore opening, zeolites can be roughly divided into five major categories, namely 8-, 10-, and 12-member oxygen ring systems, dual pore systems and mesoporous systems [2]. Their pore structures can be characterized by crystallography, adsorption, measurements and/or through diagnostic reactions. One such diagnostic characterization test is the “constraint index” test. The concept of constraint index was defined as the ratio of the cracking rate constant of n-hexane to 3-methylpentane. The constraint index of a typical medium-pore zeolite usually ranges from 3 to 12 and those of the large-pore zeolites are the range 1-3. For materials with an open porous structure, such as amorphous silica alumina, their constraint indices are normally less than 1. On the index for erionite is 38.

A comprehensive bibliography of zeolite structures has been published by the International Zeolite Association [44]. The structural characteristics of assorted zeolites are summarized in Table 3.2

Zeolite with 10-membered oxygen rings normally possesses a high siliceous framework structure. They are of special interest in industrial applications. In fact, they were the first family of zeolite that was synthesized with organic ammonium salts. With pore openings close to the dimensions of many organic molecules, they are particularly useful in shape selective catalysis. The 10-membered oxygen ring zeolites also possess other important characteristic properties including high activity, high tolerance to coking and high hydrothermal stability. Among the family of 10-membered oxygen ring zeolites, the MFI - type (ZSM-5) zeolite as presented in Figure 3.3 is probably the most useful one. ZSM-5 zeolite has two types of channel systems of similar sized, one with a straight channel of pore opening $5.3 \times 5.6 \text{ \AA}$ and the other with a tortuous channel of pore opening $5.1 \times 5.5 \text{ \AA}$. Those intersecting channels are perpendicular to each other, generating a three dimensional framework. ZSM-5 zeolites with a wide range of $\text{SiO}_2/\text{Al}_2\text{O}_3$ ratio can easily be synthesized. High siliceous ZSM-5 zeolites are more hydrophobic and hydro thermally stable compared

with many other zeolites. Although the first synthetic ZSM-5 zeolite was discovered more than two decades ago (1972) new interesting applications are still emerging to this day. For example, its recent application in NO_x reduction, especially in the exhaust of lean-burned engine, has drawn much attention. Among various zeolite catalysts, ZSM-5 zeolite has the greatest number of industrial applications, covering from petrochemical production and refinery processing to environmental treatment.

Table 3.2 Structural characteristics of selected zeolite [45]

Zeolite	Number of rings	Pore opening Å	Pore/Channel structure	Void volume (ml/g)	D _{Frame} ^a (g/ml)	CI ^b
<i>8-membered oxygen ring</i>						
Erionite	8	3.6x5.1	Intersecting	0.35	1.51	38
<i>10-membered oxygen ring</i>						
ZSM-5	10	5.3x5.6 5.1x5.5	Intersecting	0.29	1.79	8.3
ZSM-11	10	5.3x5.4	Intersecting	0.29	1.79	8.7
ZSM-23	10	4.5x5.2	One-dimensional	-	-	9.1
<i>Dual pore system</i>						
Ferrierite (ZSM-35, FU-9)	10,8	4.2x5.4 3.5x4.8	One-dimensional 10:8 intersecting	0.28	1.76	4.5
MCM-22	12	7.1	Capped by 6 rings	-	-	1-3
Mordenite	10	Elliptical				
	12	6.5x7.0	One-dimensional	0.28	1.70	0.5
	8	2.6x5.7	12:8 intersecting			
Omega (ZSM-4)	12	7.4	One-dimensional	-	-	2.3
	8	3.4x5.6	One-dimensional	-	-	0.6
<i>12membered oxygen ring</i>						
ZSM-12	12	5.5x5.9	One-dimensional	-	-	2.3
Beta	12	7.6x6.4 5.5x5.5	Intersecting	-	-	0.6
Faujasite (X,Y)	12	7.4	Intersecting	0.48	1.27	0.4
	12	7.4x6.5	12:12 intersecting			
<i>Mesoporous system</i>						
VPI-5	18	12.1	One-dimensional	-	-	-
MCM41-S	-	16-100	One-dimensional	-	-	-

^aFramework density

^bConstraint index

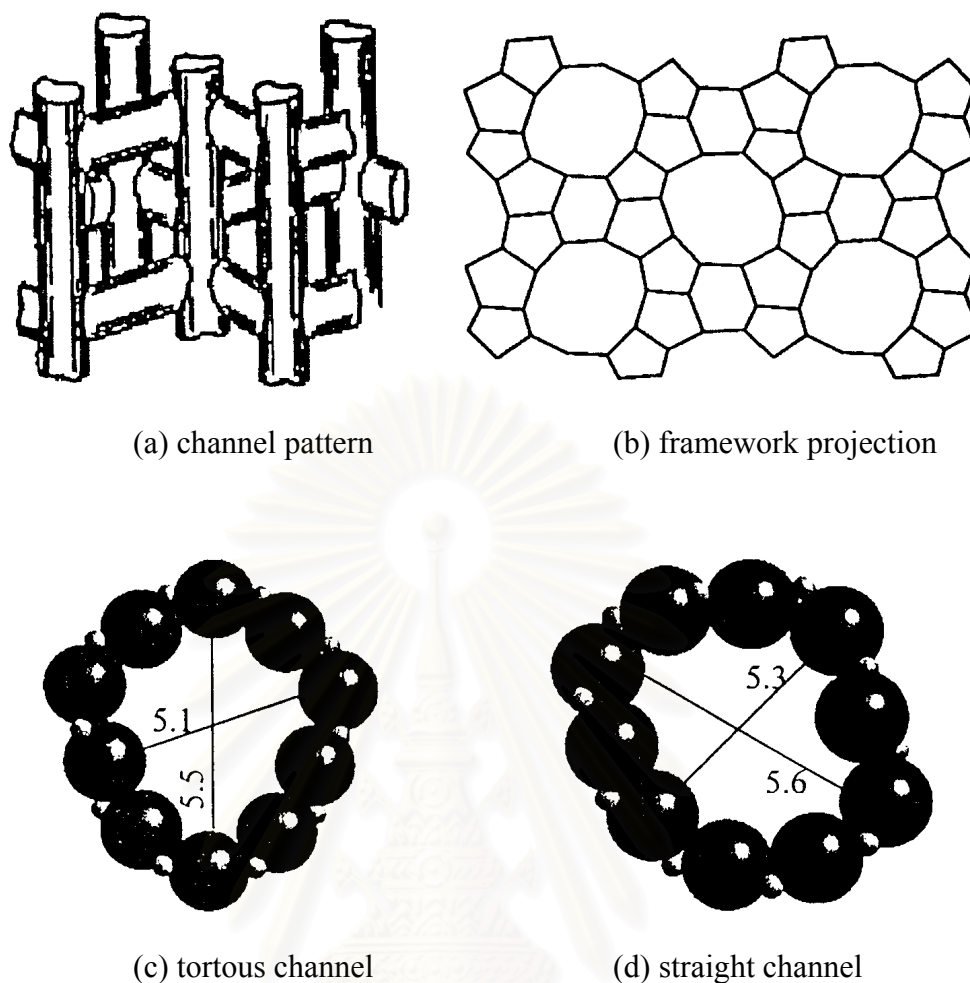


Figure 3.3 Structure of ZSM-5 [44]

Although the 10-membered oxygen ring zeolite were found to possess remarkable shape selectivity, catalysis of large molecules may require a zeolite catalyst with a large-pored opening. Typical 12-membered oxygen ring zeolites, such as faujasite-type zeolites, normally have pore opening greater than 5.5 Å and hence are more useful in catalytic applications with large molecules, for example in trimethylbenzene (TMB) conversions. Faujasite (X or Y; Figure 3.4 [44]) zeolites can be synthesized using inorganic salts and have been widely used in catalytic cracking since 1960s. The framework structures of zeolite beta and ZSM-12 are shown in Figure 3.5 and 3.6 , respectively.

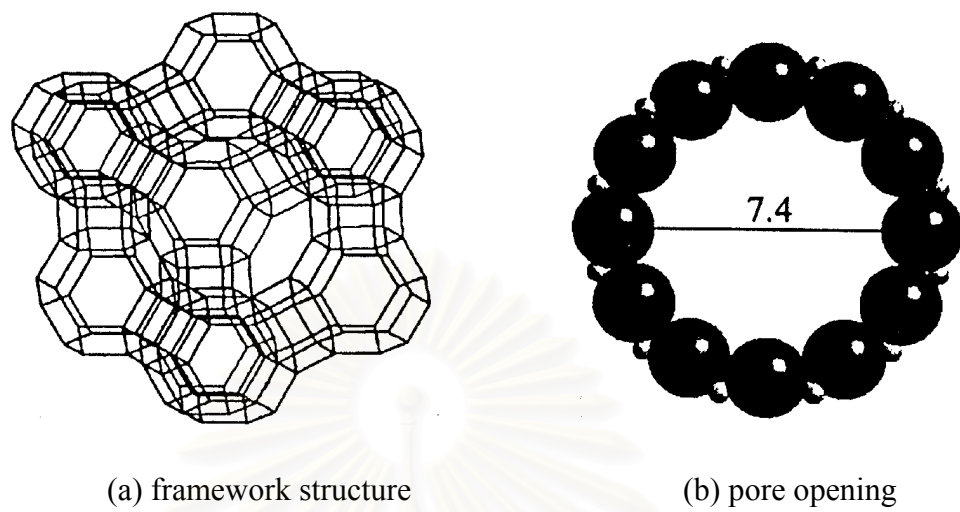


Figure 3.4 Structure of Faujasite [44]

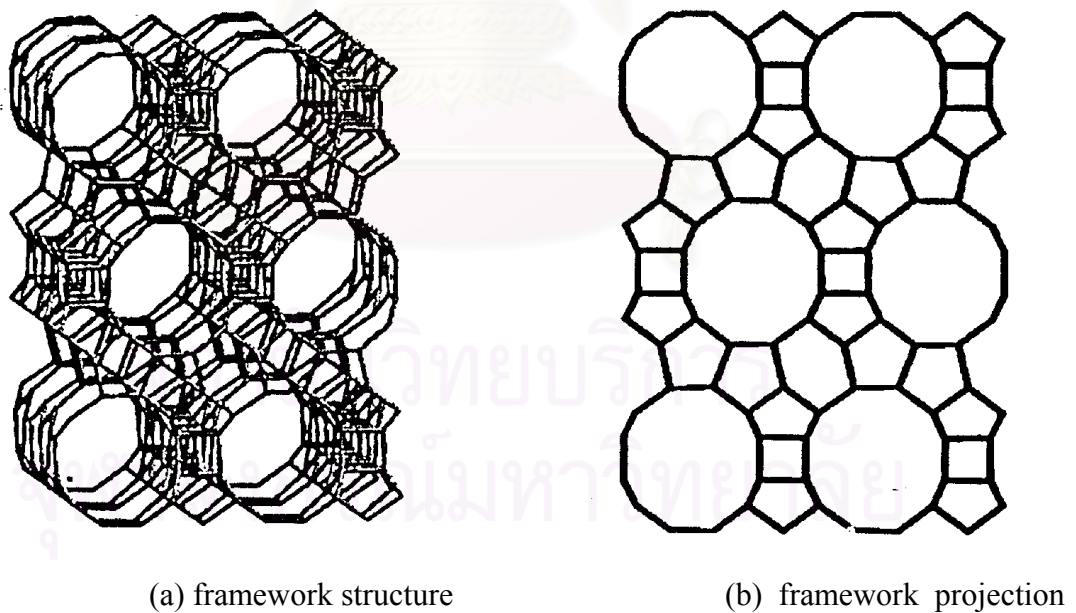


Figure 3.5 Structure of zeolite beta [44]

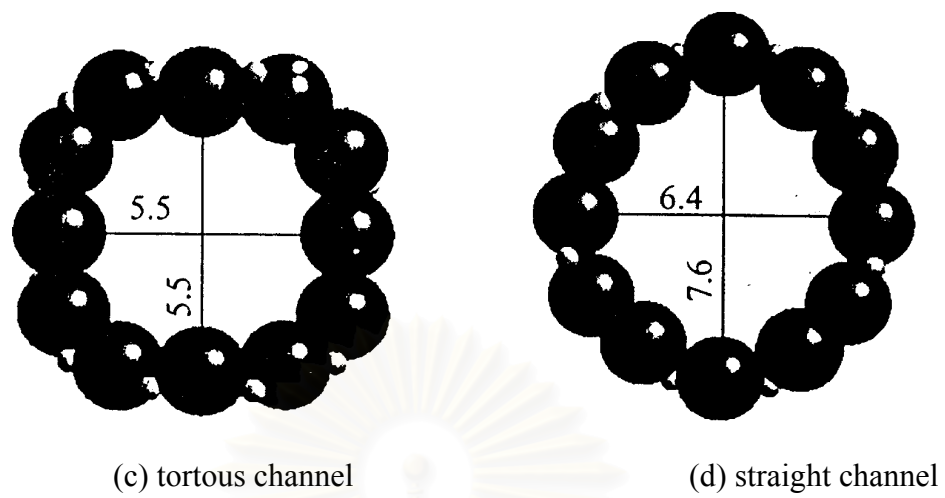


Figure 3.5 Structure of zeolite beta [44]

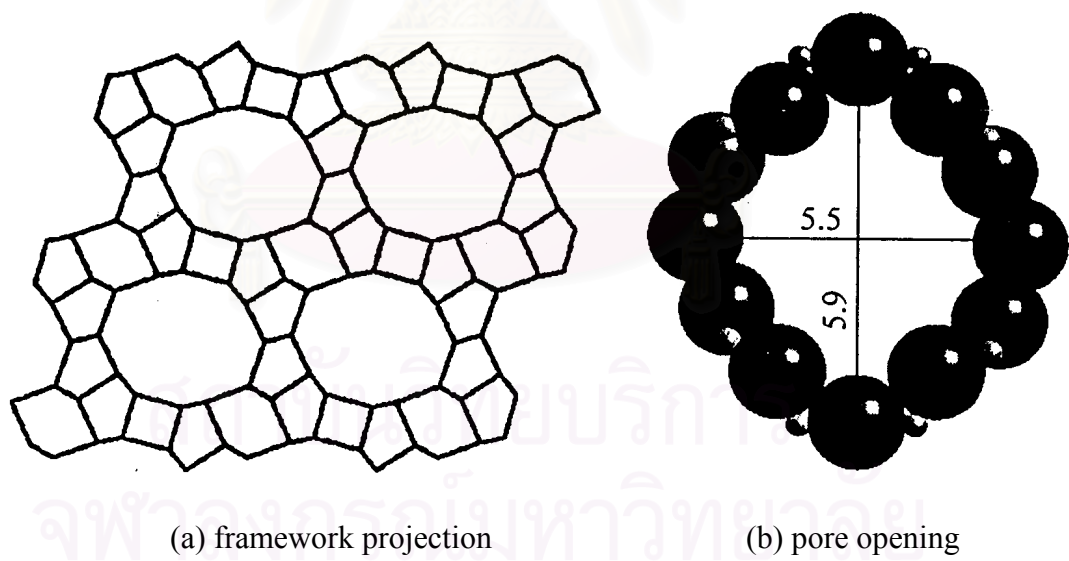


Figure 3.6 Structure of zeolite ZSM-12 [44]

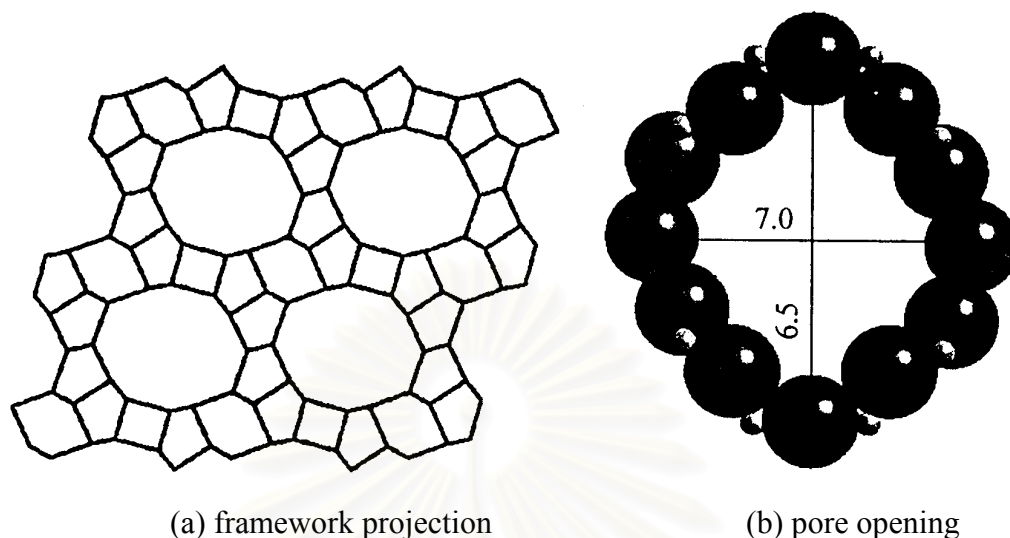


Figure 3.7 Structure of Mordenite [44]

Zeolites with a dual pore system normally possess interconnecting pore channels with two different pore opening sizes. Mordenite is a well-known dual pore zeolite having a 12-membered oxygen ring channel with pore opening $6.5 \times 6.7 \text{ \AA}$ which is interconnected to 8-membered oxygen ring channel with opening $2.6 \times 5.7 \text{ \AA}$ (Figure 3.7 [44]). MCM-22, which was found more than 10 years ago, also possesses a dual pore system. Unlike Mordenite, MCM-22 consists of 10- and 12-membered oxygen rings (Figure 3.8 [44]) and thus shows prominent potential in future applications.

In the past decade, many research efforts in synthetic chemistry have been invested in the discovery of large-pored zeolite with pore diameter greater than 12-membered oxygen rings. The recent discovery of mesoporous materials with controllable pore opening (from 12 to more than 100 \AA) such as VPI-5, MCM-41S undoubtedly will shed new light on future catalyst applications.

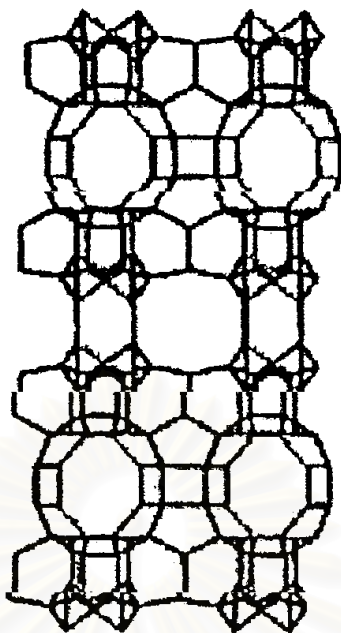


Figure 3.8 Framework structure of MCM-22 [44]

3.3 Zeolite Active sites

3.3.1 Acid sites

Classical Brønsted and Lewis acid models of acidity have used to classify the active sites on zeolites. Brønsted acidity is proton donor acidity; a tridiagonally coordinated alumina atom is an electron deficient and can accept an electron pair, therefore behaves as a Lewis acid [46, 47].

In general, the increase in Si/Al ratio will increase acidic strength and thermal stability of zeolite [48]. Since the numbers of acidic OH groups depend on the number of aluminium in zeolites framework, decrease in Al content is expected to reduce catalytic activity of zeolite. If the effect of increase in the acidic centers, increase in Al content, shall result in enhancement of catalytic activity

Based on electrostatic consideration, the charge density at a cation site increase with increase Si/Al ratio. It was conceived that these phenomena are related to reduction of electrostatic interaction between framework sites, and possibly to

difference in the order of aluminum in zeolite crystal-the location of Al in crystal structure [47].

An improvement in thermal or hydrothermal stability has been ascribed to the lower density of hydroxyl groups, which is parallel to that of Al content [46]. A longer distance between hydroxyl groups decrease the probability of dehydroxylation that generates defects on structure of zeolites.

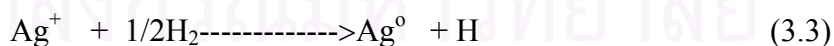
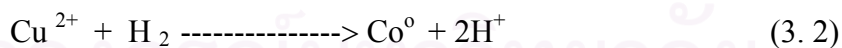
3.3.2 Generation of Acid Centers

Protonic acid centers of zeolite are generated in various ways. Figure 3.9 depicts the thermal decomposition of ammonium-exchanged zeolite yielding the hydrogen form [43].

The Brønsted acidity due to water ionization on polyvalent cations, described below, is depicted in Figure 3.10 [49].



The exchange of monovalent ions by polyvalent cations could improve the catalytic property. Those highly charged cations create very centers by hydrolysis phenomena. Brønsted acid sites are also generated by the reduction of transition metal cations. The concentration of OH groups of zeolite containing transition metals was noted to increase by hydrogen at 2.5 – 450 °C to increase with the rise of the reduction temperature [49].



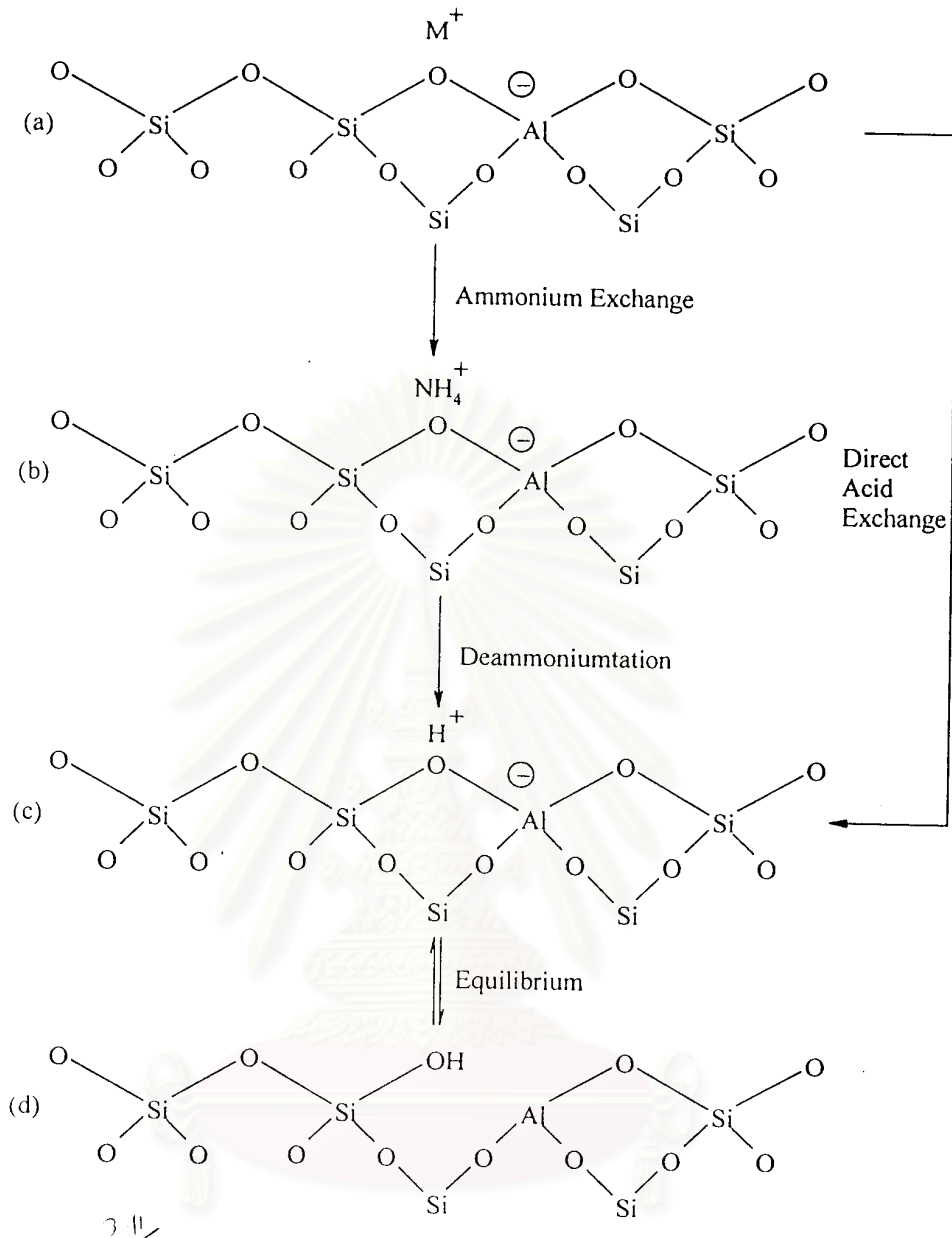


Figure 3.9 Diagram of the surface of a zeolite framework [42].

- In the as-synthesis form M^+ either an organic cation or an alkali metal cation.
- Ammonium in exchange produces the NH_4^+ exchanged form.
- Thermal treatment is used to remove ammonia, producing the H^+ , acid form.
- The acid form in (c) is in equilibrium with the shown in (d), where is a silanol group adjacent to tricoordinate aluminium.

The formation of Lewis acidity from Brønsted acid sites is depicted in Figure 3.11 [49]. The dehydration reaction decrease the number of protons and increases that of Lewis sites. Brønsted (OH) and Lewis (-Al-) sites can be present simultaneously in the structure of zeolite at high temperature. Dehydroxylation is thought to occur in ZSM-5 zeolite above at 500 °C and calcination at 800 to 900 °C produces irreversible dehydroxylation, which causes defection in crystal structure of zeolite.

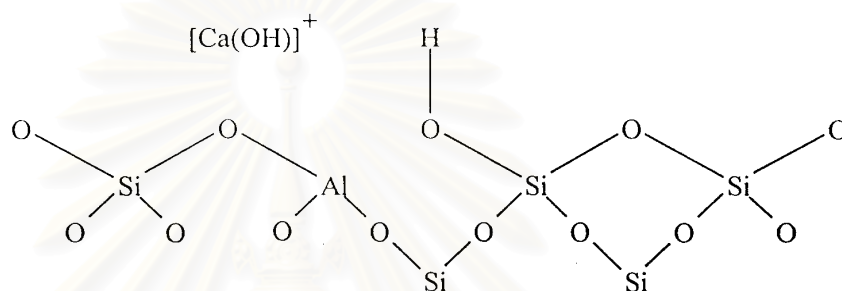


Figure 3.10 Water molecules co-ordinated to polyvalent cation are dissociated by heat treatment yielding Brønsted acidity [49].

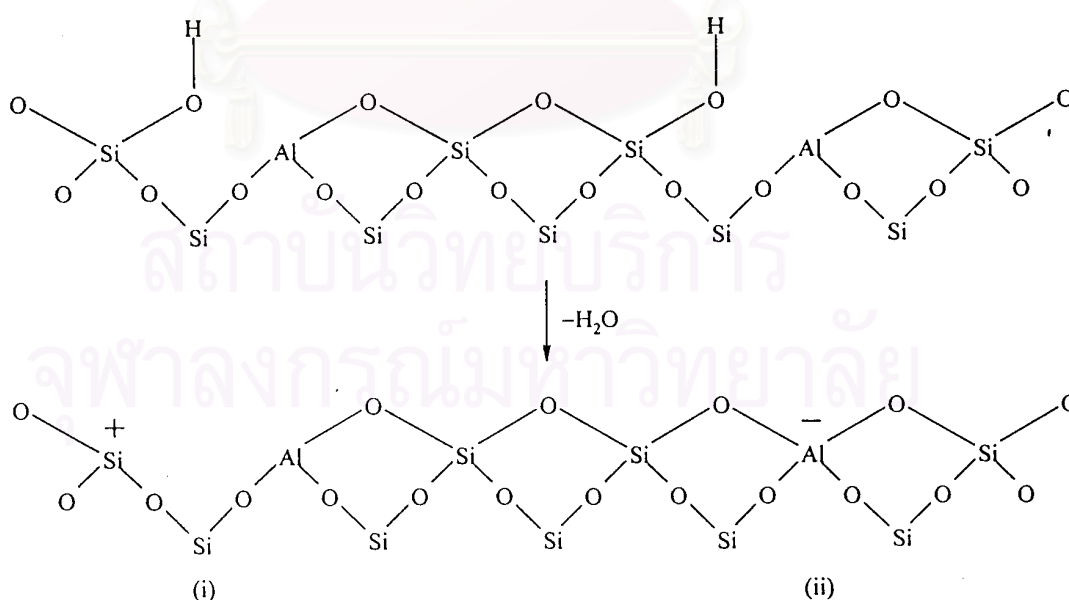


Figure 3.11 Lewis acid site developed by dehydroxylation of Brønsted acid site [49].

Dealumination is believed to occur during dehydroxylation, which may result from the steam generation within the sample. The dealumination is indicated by an increase in the surface concentration of aluminum on the crystal. The dealumination process is expressed in Figure 3.12 [49]. The extent of dealumination monotonously increases with the partial pressure of steam.

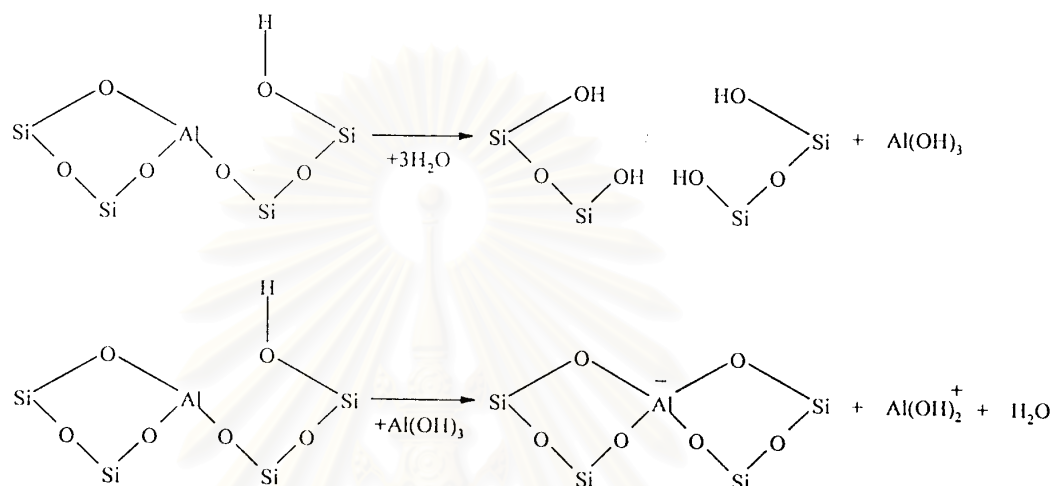


Figure 3.12 Steam dealumination process in zeolite [49]

The enhancement of the acid strength of OH groups is recently proposed to be pertinent to their interaction with those aluminum species sites tentatively expressed in Figure 3.13 [49]. Partial dealumination might therefore yield a catalyst of higher activity while severe steaming reduces the catalytic activity.

3.3.3 Basic Sites

In certain instances reactions have been shown to be catalyzed at basic (cation) site in zeolite without any influences from acid sites. The best-characterized example of this is that K-Y which splits n-hexane isomers at 500°C . The potassium cation has been shown to control the unimolecular cracking (β -scission). Free radical mechanisms also contribute to surface catalytic reactions in these studies.

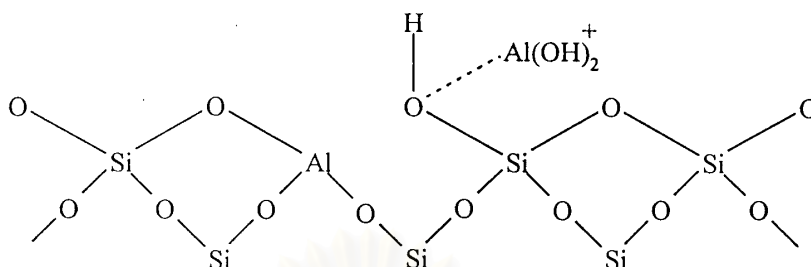


Figure 3.13 The enhancement of the acid strength of OH groups by their interaction with dislodged aluminum species [49].

3.4 Shape Selective

Many reactions involving carbonium intermediates are catalyzed by acidic zeolite. With respects to a chemical standpoint the reaction mechanisms are not fundamentally different with zeolites or with any the acidic oxides. What zeolite add is shape selectivity effect. The shape selective characteristics of zeolites influence their catalytic phenomena by three modes: shape selectivity, reactants shape selectivity, products shape selectivity and transition states shape selectivity. These types of selectivity are illustrated in Figure 3.14.

Reactants of charge selectivity results from the limited diffusibility of some of the reactants, which cannot effectively enter and diffuse inside crystal pore structures of the zeolites. Product shape selectivity occurs as slowly diffusing product molecules cannot escape from the crystal and undergo secondary reaction. This reaction path is established by monitoring changes in product distribution as a function of varying contact time.

Restricted transition state shape selectivity is a kinetic effect from local environment around the active site, the rate constant for a certain reaction mechanism is reduced of the space required for formation of necessary transition state is restricted.

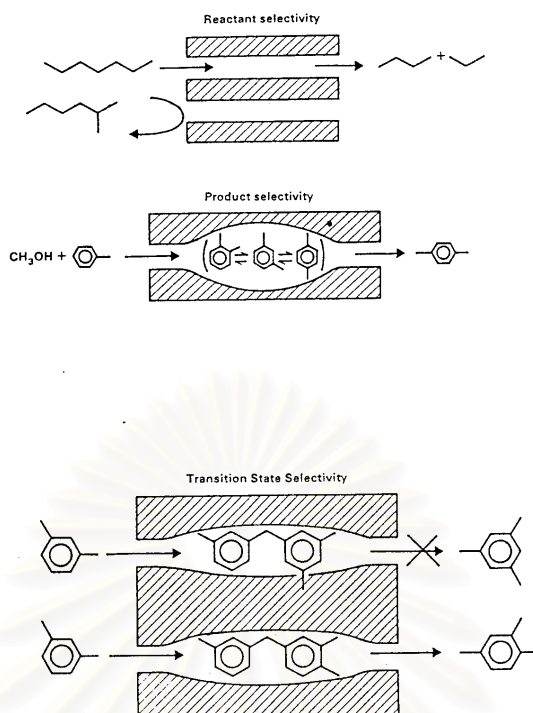


Figure 3.14 Diagram depicting the three type of selectivity [42]

The critical diameter (as opposed to the length) of the molecules and the pore channel diameter of zeolites are important in predicting shape selective effects. However, molecules are deformable and can pass through opening, which are smaller than their critical diameters. Hence, not only size but also the dynamics and structure of the molecules must be taken into account.

3.5 Zeolite Synthesis

Zeolites are generally synthesized by a hydrothermal process from a source of alumina (e.g., sodium aluminate or aluminium sulfate) and of silica (e.g., a silica sol, fumed silica, or sodium water glass) and an alkali such as NaOH, and/or a quaternary ammonium compound. An inhomogeneous gel is produced which gradually crystallizes, in some cases forming more than one type of zeolite in succession. Nucleation effects can be important, and an initial induction period at near ambient temperature may be followed by crystallization temperature that may range up to 200 °C or higher. The pressure is equal to the saturated vapor pressure of the water present.

The final product depends on a complex interplay between many variables including $\text{SiO}_2/\text{Al}_2\text{O}_3$ ratio in the starting medium, nucleating agents, temperature, pH, water content, aging, stirring, and the presence of various inorganic and organic cations. Much remains to be learned about how the initial reaction mixture forms the precursor species and how these arrange into the final crystalline products. A key concept is that the cations present give rise to a templating action, but clearly the process is more complex.

Bauer and coworkers in the early 1960s developed the use of reaction mixtures containing quaternary ammonium ions or other or other cations to direct the crystallization process. In their work and succeeding studies, a primary motivation was to attempt to synthesize zeolites with large apertures than X and Y. This did not occur, but instead organic species were found to modify the synthesis process in a variety of ways that led to the discovery of many new zeolites, and new methods of synthesizing zeolite with structures similar to previously know zeolite.

The mechanism of action of the organic species is still controversial. It was originally thought to be primarily a templating effect, but later it was found that at least some of zeolites could be synthesized without an organic template. Further, organic species other than quaternary ammonium compounds had directing effects not readily ascribed to their size or shape. However, an important result was the zeolites of higher $\text{SiO}_2/\text{Al}_2\text{O}_3$ ratio than before could be synthesized. Previously, only structures with $\text{SiO}_2/\text{Al}_2\text{O}_3$ ratios of about 10 or less could be directly forms, but with organic additives, zeolites with ratio of 20 to 100 or more can be directly prepared.

After synthesis the zeolite are washed, dried, heated to remove water of crystallization, and calcined in air, e.g., at about 550°C . Organic species are also thus removed. For most catalytic purpose, the zeolite is converted into acidic form. For some zeolites this can be achieved by treatment with aqueous HCl without significantly altering the framework structure. For other zeolites Na^+ is replaced with NH_4^+ via an ammonium compound such as NH_4OH , NH_4Cl or NH_4NO_3 . Upon heating NH_3 is driven off, leaving the zeolite in the acid form. For some reaction a

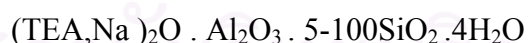
hydrogenation component such as platinum or nickel is introduced by impregnation or ion exchange [43].

3.6 Zeolite beta

Zeolite beta is an old zeolite discovered before Mobil began the “ZSM” naming sequence. Zeolite beta was initially synthesized by Wadlinger et al. [1] using tetraethylammonium hydroxide as the organic template. The structure of zeolite beta was recently determined because the structure is very complex and interest was not high until it becomes important for some dewaxing process.

The tetrahedral framework structure of zeolite beta is disordered along the [001]. The disordered structure and the three simple ordered polytypes are related through layer displacements on 001 planes. These polytypes have mutually perpendicular 12-ring channel systems, and zeolite beta exhibits characteristic properties of the presence of 12-member-ring channels and the intersecting 6.5 x 5.6 and 7.5x5.7Å. The smaller building units are double six-ring units connected by two four-rings and four five –rings unit. These are connected to form chains along the [001] direction. Polytypes A and B contain 9 unique T sites, whereas polytype C contain 32 [46].

The chemical composition of zeolite beta is:



The zeolite may offer interesting opportunities as a catalyst, since it combines three important characteristics: large pore (12 membered oxygen ring), high silica to alumina synthesis ratio, three dimension network or pores. In addition, the dimensions of on type of pores (5.5Å) can give a certain level of shape selectivity. This has been suitable for isomerization of C₄-C₇ hydrocarbons to gasoline fraction with increasing octane number [22,50], to transalkylation of xylenes [51], and to condensation of benzene and formaldehyde [52].

3.7 Thermal stability

The thermal stability of zeolites increase with increasing silica content and by exchange with rare earth cations. Most sieves are uncharged by dehydrating to 400°C; high silica (ultrastabilized forms prepared by steam pre-treatment) and rare earth-exchanged sieves are stable to 700-800 °C. Generally, extensive dehydration causes loss of Brønsted acidity due to the removal of OH or silanol surface groups.

Thermal treatment of zeolites in the presence of water normally leads to dealumination. In fact, it is one of the recommended methods for preparing ultrastable zeolites. Moderate dealuminating generally increases catalytic activity or leaves it unchanged, whereas advanced dealumination leads to a decrease in activity due to a loss of active sites and ultimately collapse of the zeolite structure. For example, dealumination of mordenite significantly changes important chemical and physical properties such as crystal structure, thermal stability, sorption capacity and acidity, as well as catalytic properties. Maximum thermal stability is reached for an $\text{SiO}_2:\text{Al}_2\text{O}_3$ ratio of about 19. The sorption capacity towards water is highly reduced after dealumination because of the absence of strong polarizing cations which can dissociate water to strongly adsorbed hydroxy groups; accordingly, the number of Brønsted acid sites also decrease. Nevertheless, the hydrocarbon cracking activity of mordenite increase with increasing Si:Al ratio. For further details on zeolite stability, the reader is referred to the comprehensive review of McDaniel and Maher [53].

CHAPTER IV

EXPERIMENT

The synthesis of zeolite beta samples, hydrothermal treatment, reaction testing and its characterization are explained in the following section.

4.1 Preparation of H - Zeolite beta

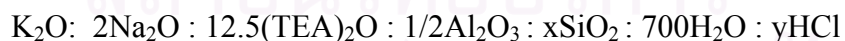
The preparation procedures and the reagents used in this study are shown in Figure 4.1 and Table 4.1 (for calculation see Appendix A-1).

4.1.1 Gel composition and reagents

All synthesis mixtures were prepared with the following reagents:

- tetraethylammonium hydroxide (Fluka, 40% by weight aqueous solution)
- cataloid as a source of SiO₂ (SiO₂ 30% by weight aqueous solution)
- sodium aluminate (Wako, Lot LeH 3.73, Al/NaOH about 0.81)
- sodium hydroxide (MERCK, analytical grade)
- potassium chloride (AJAX CHEMICALS, analytical grade)
- sodium chloride (MERCK, analytical grade).

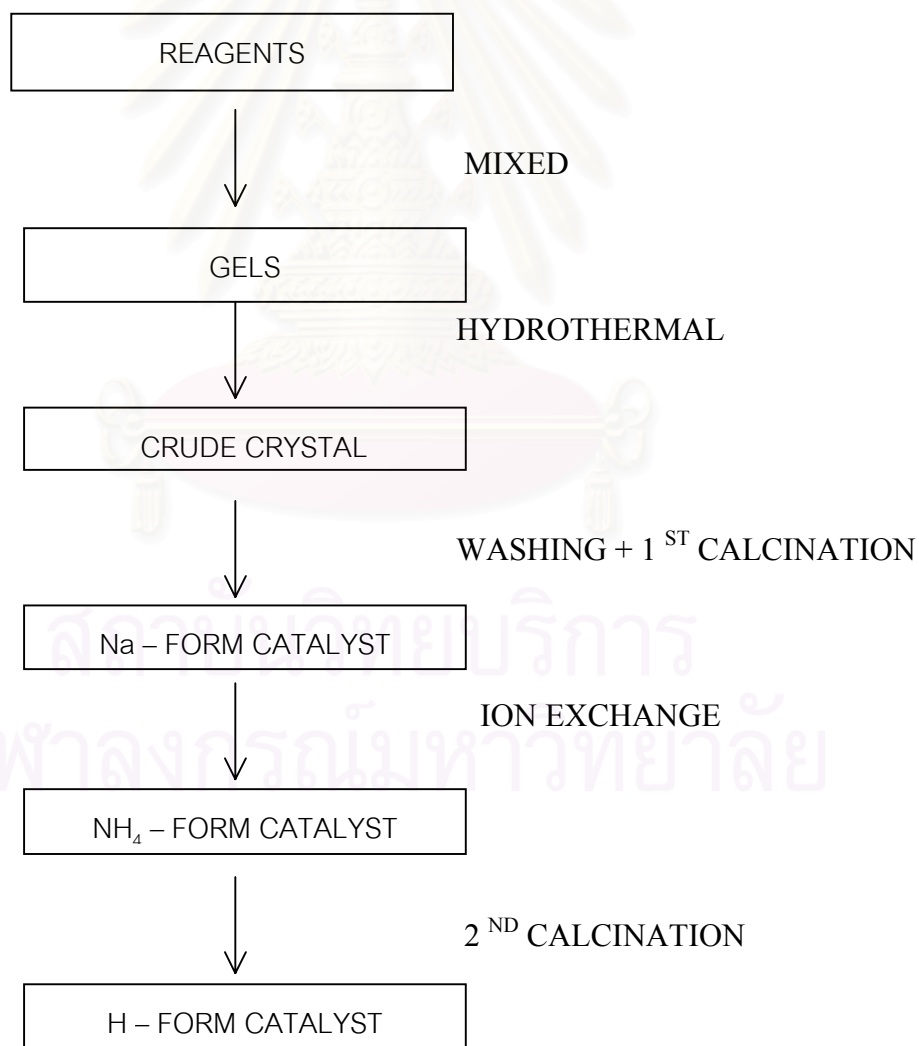
Gels of the following oxide molar composition were prepared for the synthesis:



x was varied from 30 to 80 and y from 0 to 3 by adding the appropriate amounts of NaCl, NaOH and KCl.

Table 4.1 Reagents used for the preparation of Na-zeolite beta

Name	weight
TEAOH	61.36 g
Cataloid For Si/Al=30	40.00 g
Si/Al=50	66.66 g
Si/Al=80	106.67 g
KCl	0.498 g
NaOH	0.458 g
NaAlO ₂	0.702 g
NaCl	0.39 g

**Figure 4.1** Preparation procedure of zeolite beta

4.1.2 Crystallization

The obtained gel was stirred thoroughly before transferring to a stainless-steel autoclave. The gel was heated for crystallization in the autoclave from room temperature to 135 °C in 1 h under a pressure of 3 kg_f/cm² (gauge) of nitrogen gas and maintained at this temperature for 40 hr. After selected time intervals, the autoclave was immersed in cold water to quench the crystallization process. The obtained solid material was centrifuged at 2,500 r.p.m. (about 15 min for each time) and the recovered solids were washed until pH≈9 and dried in an oven at 110 °C overnight.

4.1.3 The first calcination

The dry crystal was calcined in an air stream at 540 °C for 3.5 hr by heating it from room temperature to 540 °C in 60 min. This step was to burn off the organic template and to leave the cavities and channels in the crystals. Then, the calcined crystals were cooled to room temperature in a desiccator. After this step the crystals formed were called Na-zeolite beta.

4.1.4 Ammonium ion-exchange

The ion exchange step was carried out by mixing the calcined crystal with 2 M NH₄NO₃ (ratio of catalyst and solution is 1 g: 30 ml) and heated on a stirring hot plate at 80 °C for 1 h. Then, the mixture was cooled down to room temperature. Then, the ion exchange step was repeated again. After that, the ion exchange crystal was washed twice with deionized water by using a centrifugal separator. Then, the ion exchange crystal was dried at 110 °C for at least 3 h. in oven. The dried crystals (NH₄ – zeolite beta) were then obtained.

4.1.5 The second calcination

The removable species, i.e., NH₃ and NO_x, were decomposed by thermal treatment of the ion exchange crystals in a furnace by heating from the room temperature to 500 °C in air stream and maintained at this temperature for 2 hr After

this step, the obtained crystals were H-zeolite beta which was ready for hydrothermal pretreatment

4.2 Hydrothermal treatment

In order to investigate the effect of hydrothermal treatment on the stability of catalyst with different crystallite size, the catalyst was heated in a He stream while elevating temperature from room temperature to 600 °C and from 600 to 800 °C with constant heating rates of 10 and 1.7 °C/min, respectively. The catalyst sample was then kept at the desired temperature for 30 min under 10 mol % of water vapor. Subsequently, the catalyst was cooled down to room temperature in He stream.

4.3 Characterization studies

4.3.1 Scanning Electron Microscopy (SEM)

The shape and size of the crystal of prepared catalysts were observed by using JEOL JSM-35 CF Scanning Electron Microscope (SEM) at the Scientific and Technological Research Equipment Centre, Chulalongkorn University (STREC).

4.3.2 X- Ray Diffraction analysis (XRD)

Crystallinity and X-ray diffraction (XRD) patterns of the catalysts were performed by a X-ray diffractometer SEIMENS D500 connected with a personal computer with Diffract AT version 3.3 program for fully control of the XRD analyzer. The experiments were carried out by using CuK α radiation with Ni filter and the operating condition of measurement are shown as follows:

2 θ range of detection	:	4 – 60 °
Resolution	:	0.04 °
Number of Scan	:	10

The functions of based line subtraction and smoothing were used in order to get the well formed XRD spectra.

4.3.3 ^{27}Al Magnetic Angle Spinning Nuclear Magnetic Resonance (^{27}Al MAS NMR)

Quantitative analysis of aluminum tetrahedral in zeolites was conformed by ^{27}Al Al-magnetic angle spinning nuclear magnetic resonance (^{27}Al MAS NMR, BRUKER DPX-300 spectroscopy operating at 78.2 MHz) at National Metal and Materials Technology Center (MTEC) Rama VI Road, Bangkok. The signal of alumina tetrahedral could be detected at around 50 ppm.

4.3.4 BET surface area measurement

Physical adsorption isotherms are measured near the boiling point of a gas (e.g., nitrogen, at -196°C). From these isotherms the amount of gas needed to form a monolayer can be determined. If the area occupied by each adsorbed gas molecule is known, the surface area can be determined for all finely divided solids, regardless of their chemical composition.

The specific surface area of samples was calculated using the Brunauer-Emmett-Teller single point method on the basis of nitrogen uptake measured at liquid-nitrogen boiling point temperature equipped with a gas chromatograph.

4.3.4.1 BET apparatus

The reaction apparatus of BET surface area measurement consisted of two feed lines of helium and nitrogen. The flow rate of the gases was adjusted by means of fine-metering valve on the gas chromatograph. The sample cell made from pyrex glass. The operation condition of gas chromatograph (GOW-MAC) is shown in Table 4.2.

4.3.5 X-Ray Fluorescence analysis (XRF)

Quantities of Si and Al in the sample were determined by using XRF analyzer at the Science Service Department, Rama VI Road, Bangkok.

Table 4.2 Operating condition of gas chromatograph (GOW-MAC)

Model	GOW-MAC
Detector	TCD
Helium flow rate	30 ml/min
Detector temperature	80 ° C
Detector current	80 mA

4.3.4.2 Procedure

The mixture gas of helium and nitrogen was flown through the system at the nitrogen relative pressure of 0.3. The catalyst sample was placed in the sample cell, ca. 0.3-0.5 g, which was then heated up to 160°C and held at that temperature for 2 h. Then the catalyst sample was cooled down to room temperature and the specific surface area was measured. There were three steps to measure the specific surface area.

Adsorption step: The catalyst that set in the sample cell was dipped into the liquid nitrogen. Nitrogen gas that was introduced into the system was adsorbed on the surface of the catalyst sample until equilibrium was reached.

Desorption step : The sample cell with nitrogen gas-adsorbed catalyst sample was dipped into a water bath at room temperature. The adsorbed nitrogen gas was desorbed from the surface of the catalyst sample. This step was completed when the integrator line was back in the position of the base line.

Calibration step: 1 ml of nitrogen gas at atmospheric pressure was injected through the calibration port of the gas chromatograph and the area was measured. The area was the calibration peak. The calculation method is explained in Appendix A-5.

4.4 Reaction Testing

4.4.1 Chemicals and Reagents

Methanol is available from MERCK, 99.9 % for methanol conversion.

4.4.2 Instruments and Apparatus

(a) Reactor: The reactor is a conventional micro reactor made from a quartz tube with 6 mm inside diameter. The reaction was carried out under N₂ gas flow and atmospheric pressure.

(b) Automatic Temperature Controller: This consists of a magnetic switch connected to a variable voltage transformer and a RKC temperature controller connected to a thermocouple attached to the catalyst bed in reactor. A dial setting establishes a set point at any temperatures within the range between 0° C to 600° C.

(c) Electric Furnace: This supply the required heated to the reactor for reaction. The reactor can be operated from room temperature up to 700° C at maximum voltage of 220 volt.

(d) Gas Controlling Systems: Nitrogen is equipped with pressure regulator (0-120 psig), an on-off valve and a needle valve were used to adjust flow rate of gas.

(e) Gas Chromatographs: Operating conditions are shown in Table 4.3.

Table 4.3 Operating condition for gas chromatograph

Gas chromatograph	Shimadzu GU-14A
Detector	TCD
Column	Porapak-Q
Carrier gas	He(99.999%)
Column temperature	
-Initial	90°C
-Final	90°C
Detector temperature	100°C
Injector temperature	100°C
Analyzed gas	CH ₃ OH

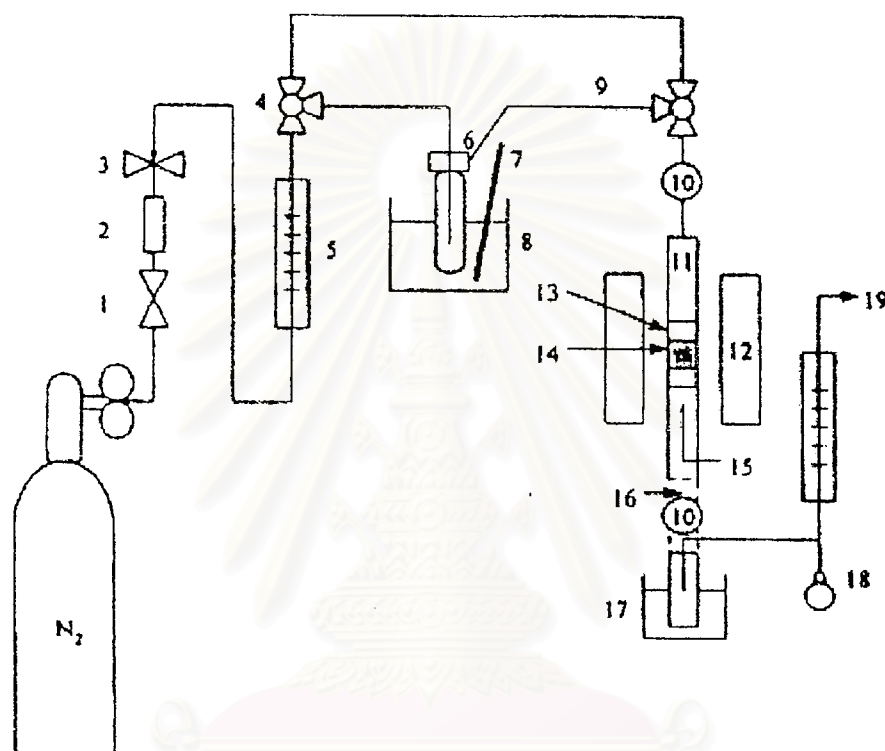
4.4.3 Reaction Method

The methanol conversion was carried out by using a conventional flow as shown in Figure 4.2. A 0.1 portion of the catalyst was packed in the quartz tubular reactor. The reaction was carried out under the following procedure:

- 1) Adjust the pressure of nitrogen to 1 kg/cm², and allow the gas to flow through a rotameter (See Appendix A-6), measure the outlet gas flow rate by using a bubble flowmeter. Gas flow rate was about 11.31 ml/min at GHSV about 4000 h⁻¹.
- 2) Heat up the reactor (under N₂ flow) by raising the temperature from room temperature to 450° C in 45 min and then hold at this temperature about 30 min for preheating catalyst.
- 3) Put methanol 20 ml in saturator and set the temperature of water bath at 25°C at this temperature. The cocentrations of methanol in saturator were 20% mol.

4) Start to run the reaction by adjusting 2 three way valves to allow nitrogen gas to pass through reactants inside saturator in water bath.

5) Take sample for analyzed by gas chromatograph after the reaction ran for 1 h.



- | | | | |
|-----------------|-------------------------|---------------------|----------------------|
| 1. On-off valve | 2. Gas filter | 3. Needle valve | 4. Three-way valve |
| 5. Flow meter | 6. Saturator | 7. Thermocouple | 8. Water bath |
| 9. Heating line | 10. Sampling port | 11. Tubular reactor | 12. Electric furnace |
| 13. Quartz wool | 14. Catalyst | 15. Thermocouple | 16. Heating tape |
| 17. Trap | 18. Soap-film flowmeter | | 19. Purge |

Figure 4.2 Schematic diagram of the reaction apparatus for reaction

CHAPTER V

RESULTS AND DISCUSSION

In this chapter, the results and discussion are divided into two sections. First, the effect of particle size on hydrothermal stability of zeolite beta is presented in section 5.1. Second, the effect of the silica to alumina ratio on hydrothermal stability presented in section 5.2. This is analyzed by ^{27}Al MAS NMR combined with SEM, XRD and BET surface area measurement.

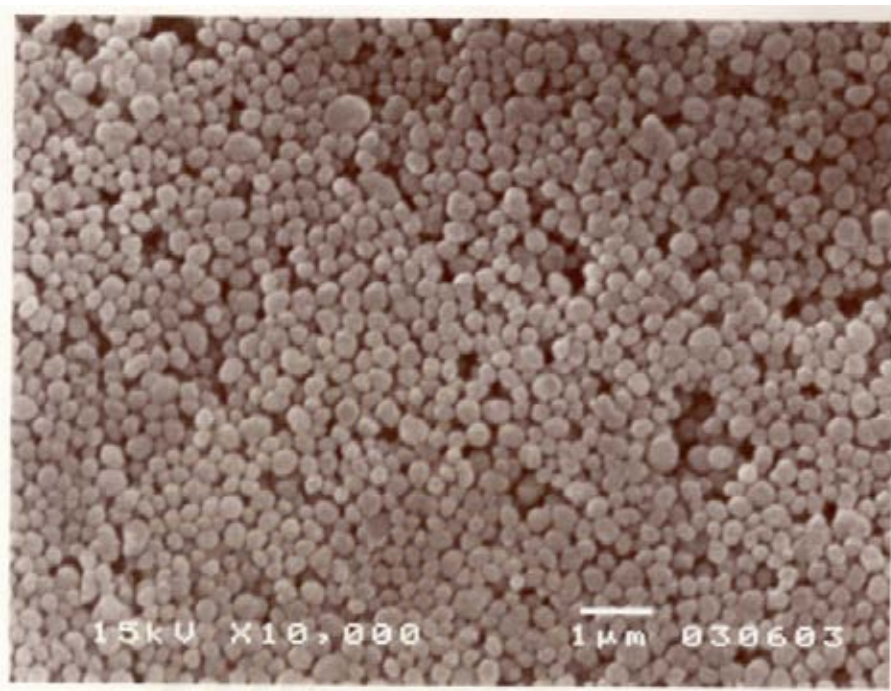
5.1 Hydrothermal stability of zeolite beta for the different particle size

5.1.1 The morphology and particle size of H-zeolite beta samples

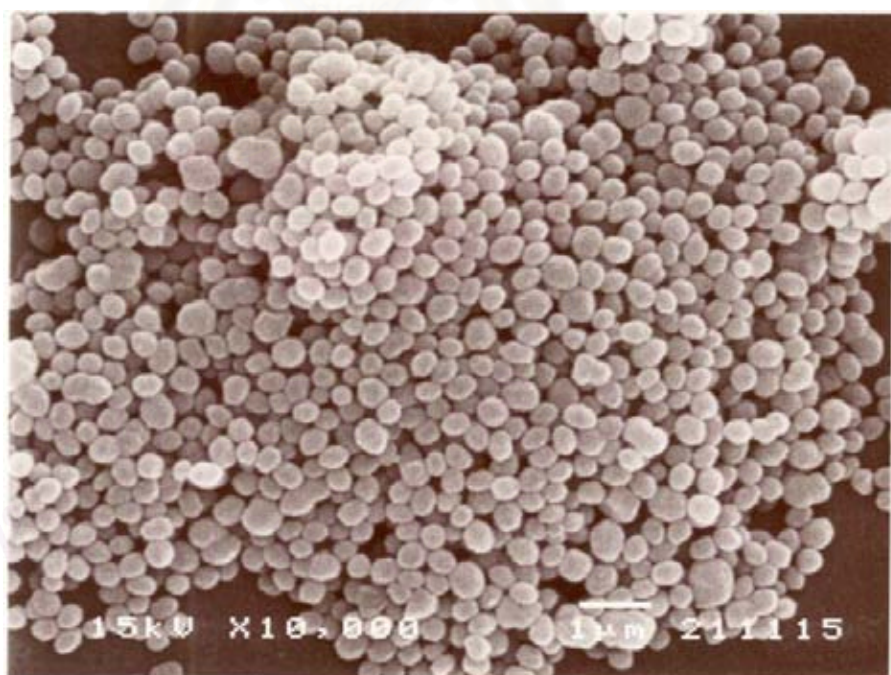
The crystallite H-zeolite betas were synthesized with the same silicon-to-aluminium ratio ($\text{Si}/\text{Al}=27$). The crystal morphology of parent samples with different particle size, average 0.2, 0.3, 0.4, 0.5, 0.7, and 0.9 μm of spheroid shape and a narrow particle size distribution can be seen from the scanning electron microscopy (SEM) picture as shown in Figures 5.1 (a), (b), (c), (d), (e), and (f), respectively. The morphology of the crystals were observed in the SEM picture of the treated samples not changed significantly compared to the fresh samples (not shown here).

5.1.2 The single point BET surface area.

The single point BET surface area of H-zeolite beta, both fresh and treated by hydrothermal treatment procedure under 10 mol % of water vapor, are shown in Table 5.1 and Figure 5.2. It is clear that the BET surface area for all H-zeolite beta decrease due to hydrothermal treatment. However, compared with a large particle size, the BET surface area of a smaller particle size decreases significantly. This suggests that the structure of H-zeolite beta for small particle size may be easily changed. This is possible due to collapses of zeolite framework [10].

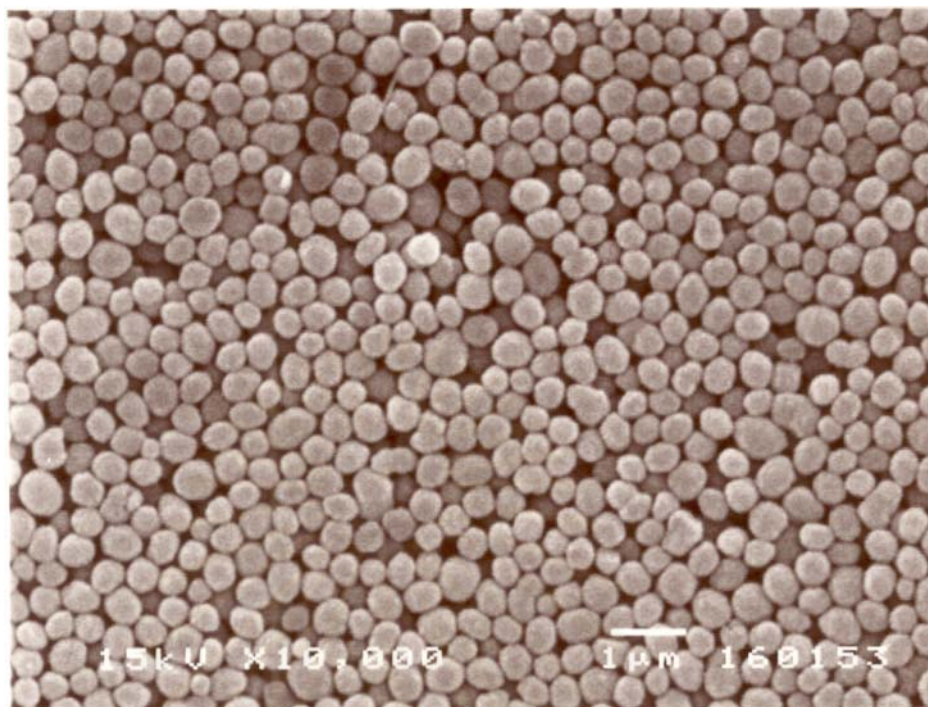


(a)

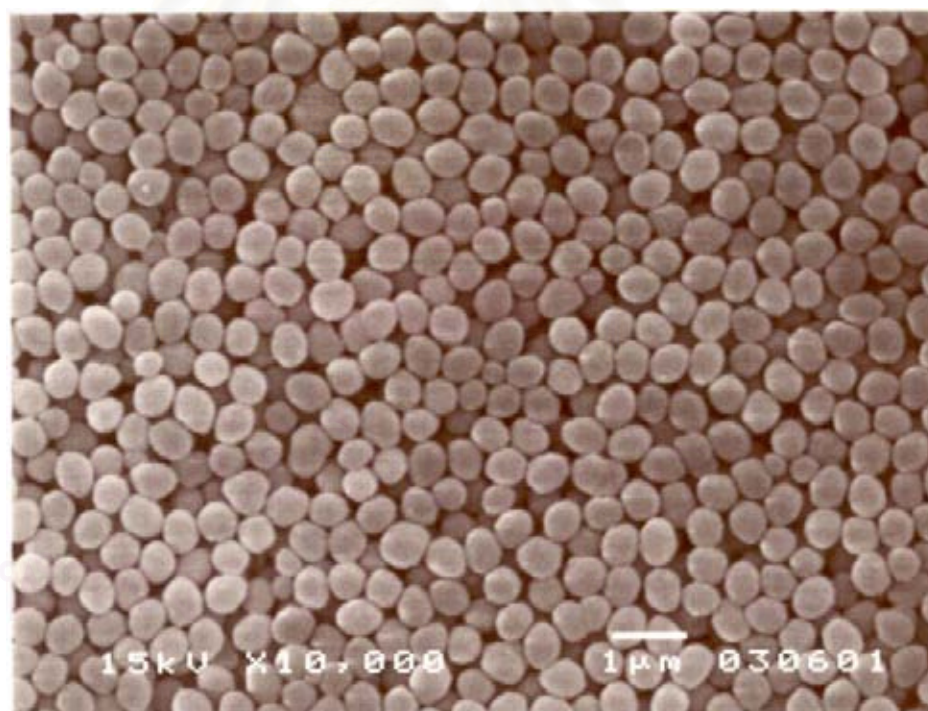


(b)

Figure 5.1 Scanning electron micrographs of H-zeolite beta particle size, (a) 0.2 μm (b) 0.3 μm

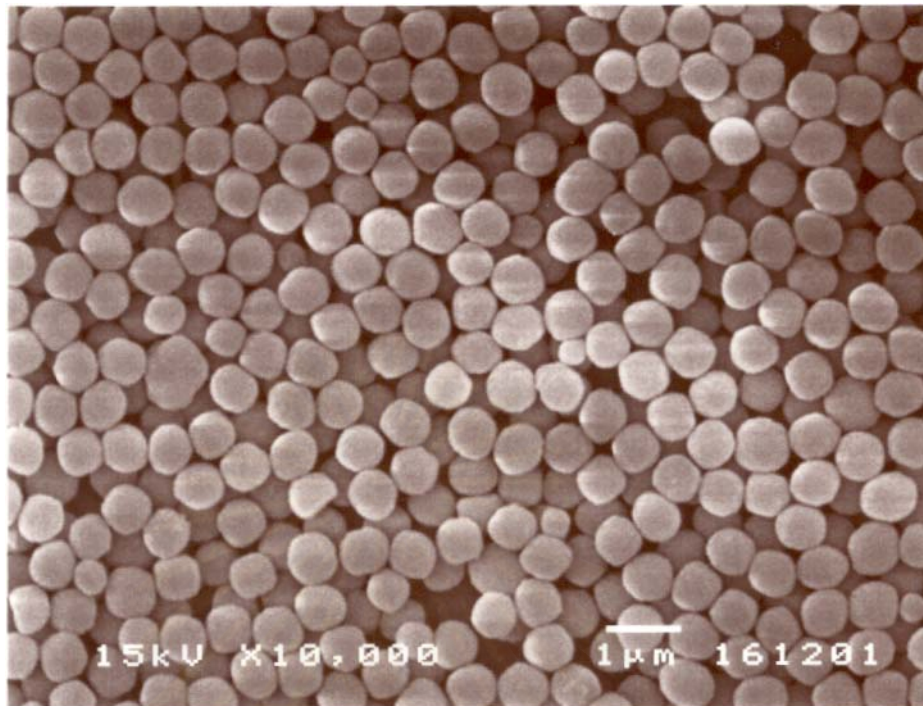


(c)

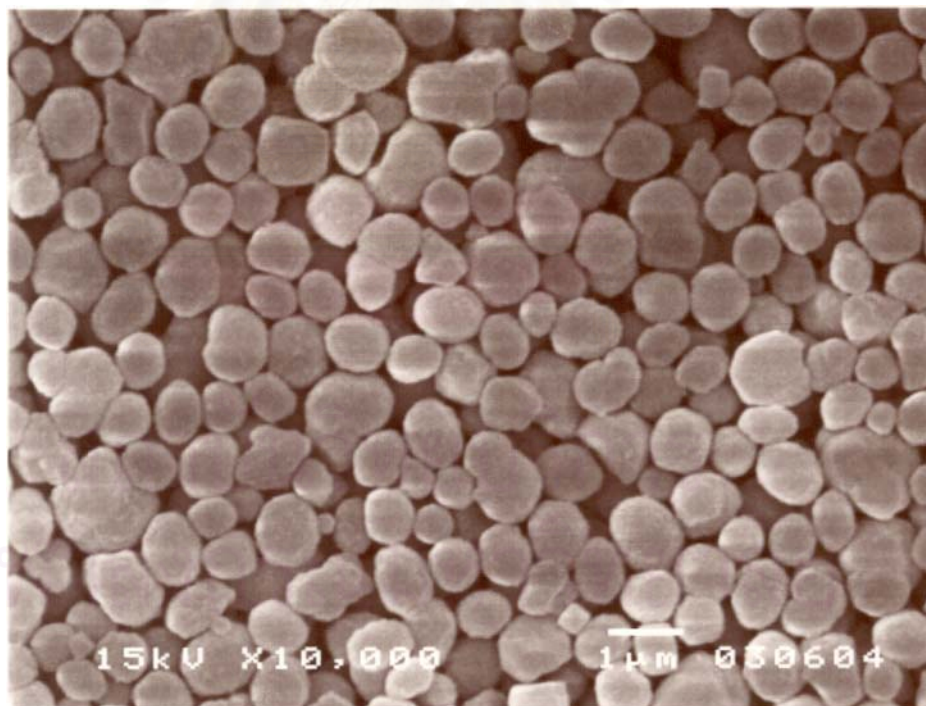


(d)

Figure 5.1 (Cont.) Scanning electron micrographs of H-zeolite beta particle size, (c) 0.4 μm (d) 0.5 μm



(e)



(f)

Figure 5.1 (Cont.) Scanning electron micrographs of H-zeolite beta particle size, (e) 0.7 μm (f) 0.9 μm

Table 5.1 The single point BET surface area and the percent relative crystallinity of zeolite beta, fresh and treated

Particle size (μm)	BET surface area (m^2/g)		% crystallinity after hydrothermal treatment
	fresh catalyst	treated catalyst	
0.2	612	490	95
0.3	579	481	95
0.4	500	459	96
0.5	464	446	97
0.7	382	364	96
0.9	374	355	95

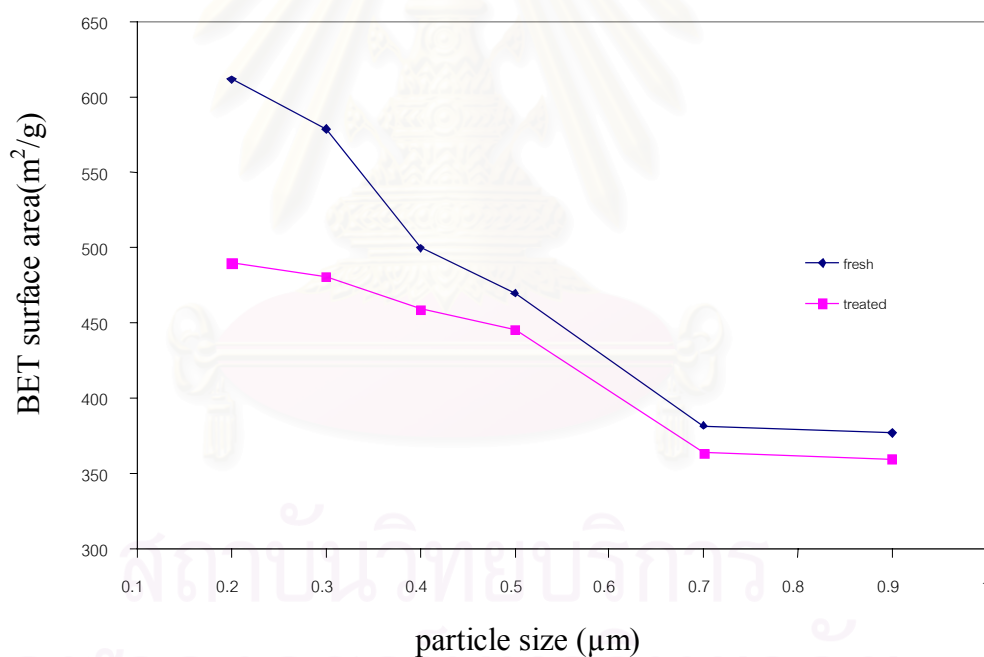


Figure 5.2 Relationship between the single point BET surface area (m^2/g) and the particle size (μm) of H-zeolite beta, both fresh and treated by hydrothermal treatment

5.1.3 Percent relative crystallinity

Figures 5.4-5.9 show the comparative XRD patterns of H-zeolite beta before and after hydrothermal treatment for various crystallize sizes. All the XRD patterns indicate similarly two main peaks of 2θ at 7.8° and 22.4° . This is a unique characteristic of H-zeolite beta in agreement with several works [42]. In addition to identify a catalyst sample, the XRD pattern can indicate the relative crystallinity through integrating the area under curve of the observed peak compared to that of the reference peak. Hence, in this work we define the percent relative crystallinity as the following equation:

$$\% \text{ relative crystallinity} = \frac{\text{Area under the XRD peak of an observed sample} \times 100}{\text{Area under the XRD peak of a reference sample}}$$

However, due to the presence of two distinct peaks of 2θ at 7.8° and 22.4° , the selection of peak to calculate the relative crystallinity is carefully considered. From most of literature reviewed [22, 32, 42], the peak intensity at 22.4° was extensively accepted to be a main characteristic peak of H-zeolite beta and this peak was therefore chosen as a calculated peak. The 22.4° peak of a fresh H-zeolite beta represented a reference sample. The percent relative crystallinities of the treated sample are listed in Table 5.1 and shown in Figure 5.3. To accommodate in observation, the relationship between the percent relative crystallinity and the particle size of H-zeolite beta was graphically plotted in Figure 5.9. It was found that the percent relative crystallinity for all the treated samples decreased slightly. Hence, it was concluded that the crystallinity of the samples after hydrothermal treatment was absolutely retained (more than 95%) and there was no relation between the relative crystallinity and particle size.

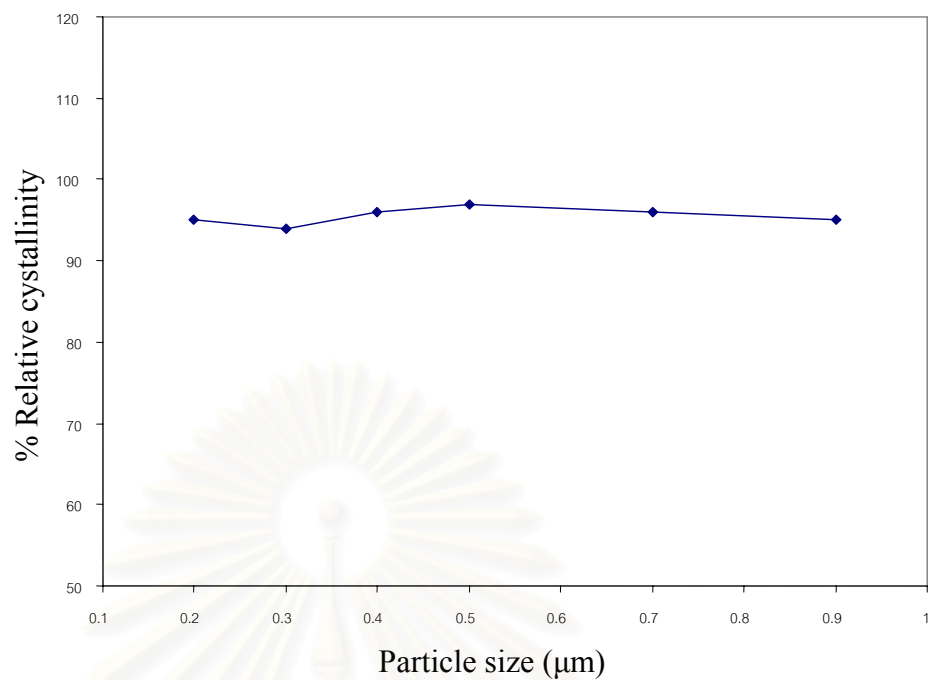


Figure 5.3 The percent relative crystallinity of the treated H-zeolite beta with different size

สถาบันวิทยบริการ
จุฬาลงกรณ์มหาวิทยาลัย

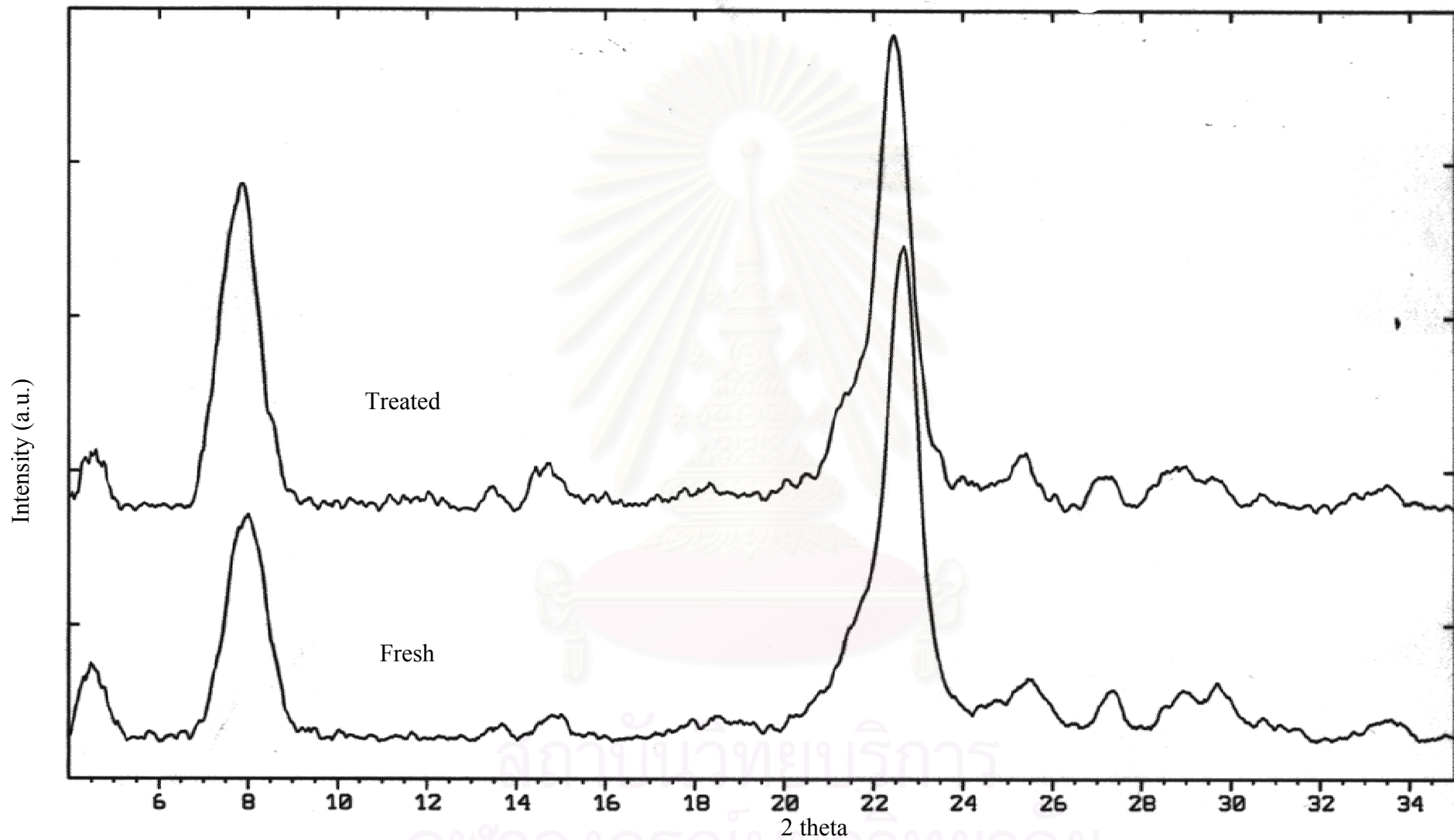


Figure 5.4 XRD spectra of H-zeolite beta particle size 0.2 μm

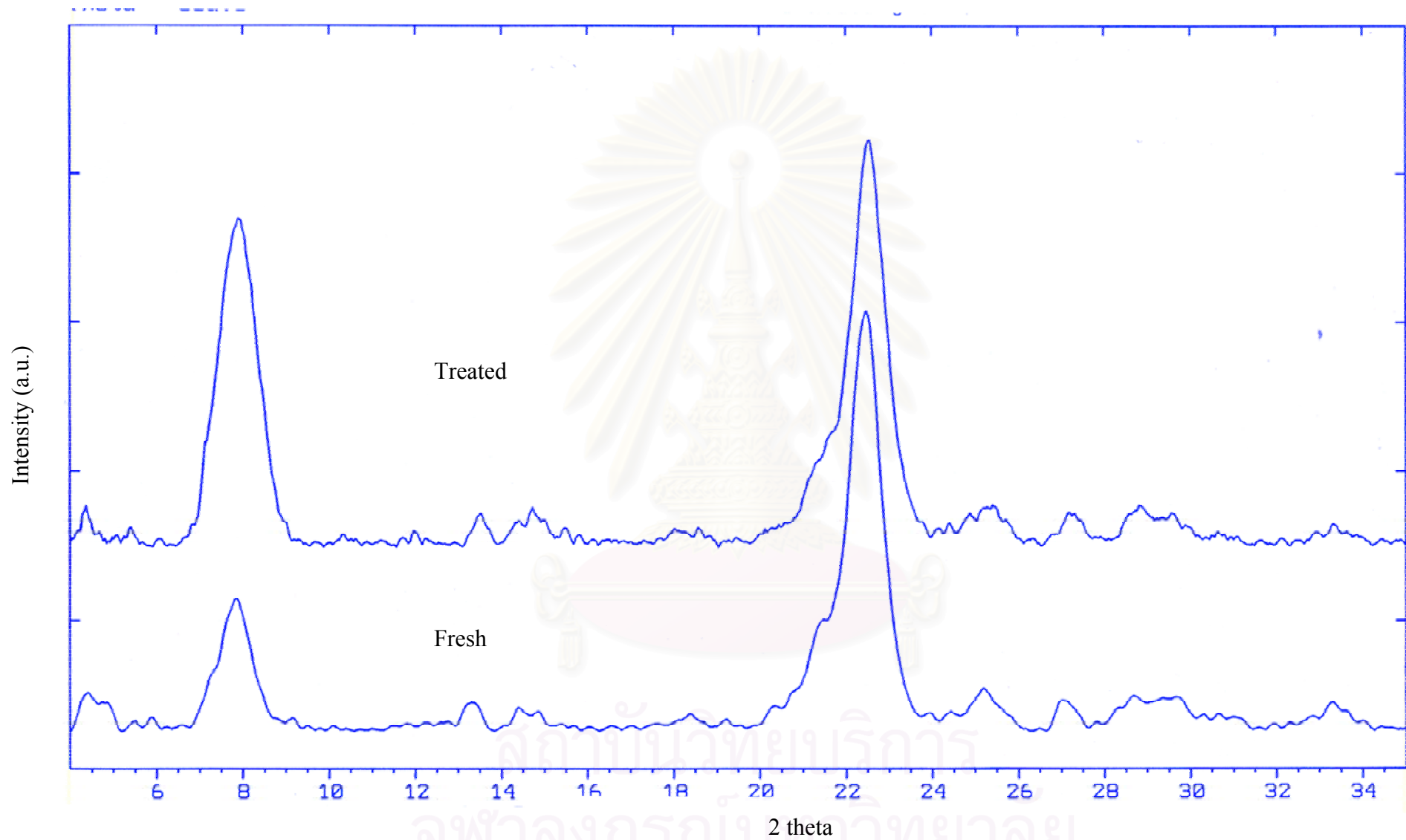


Figure 5.5 XRD spectra of H-zeolite beta particle size 0.3 μm

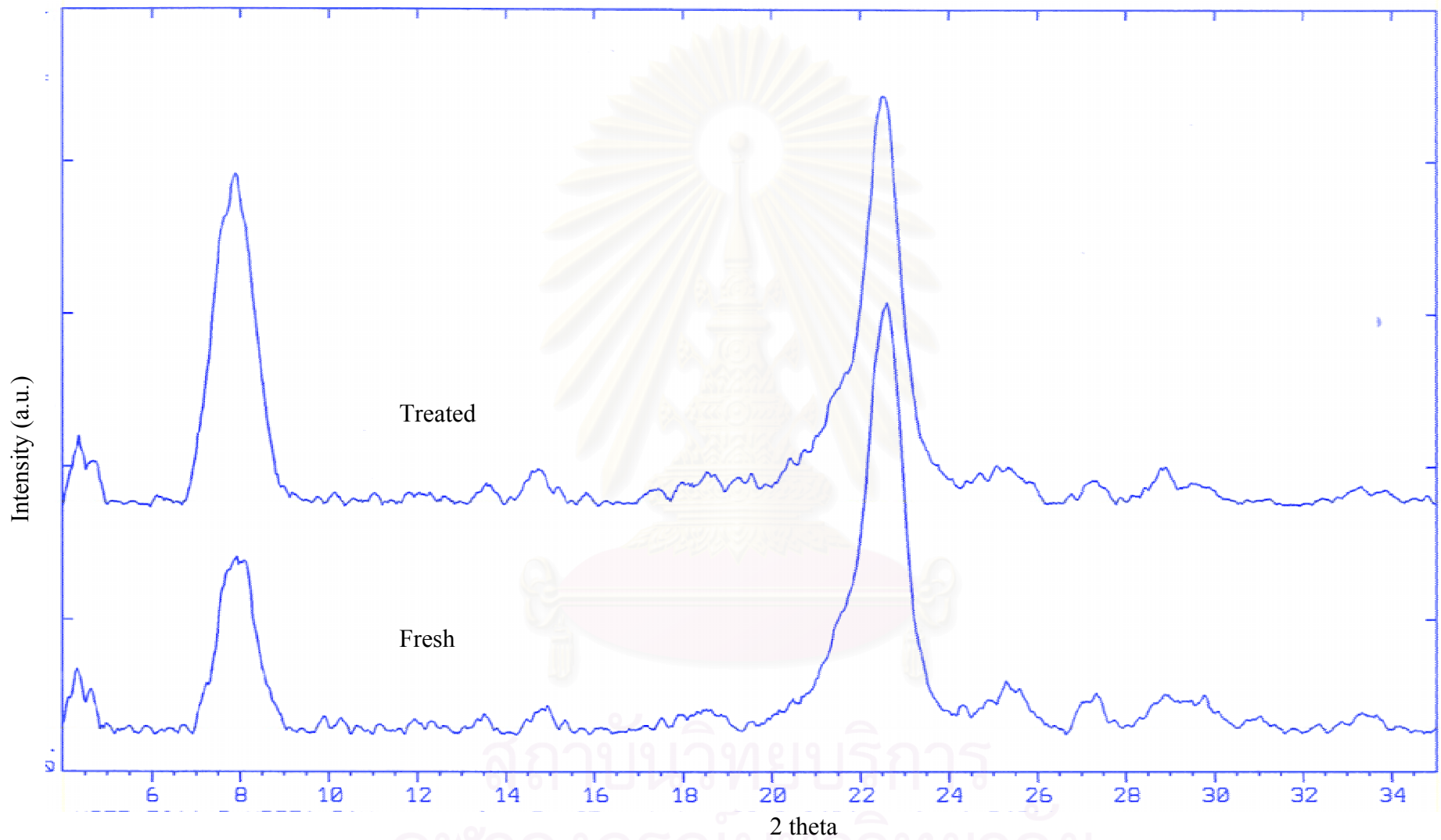


Figure 5.6 XRD spectra of H-zeolite beta particle size 0.4 μm

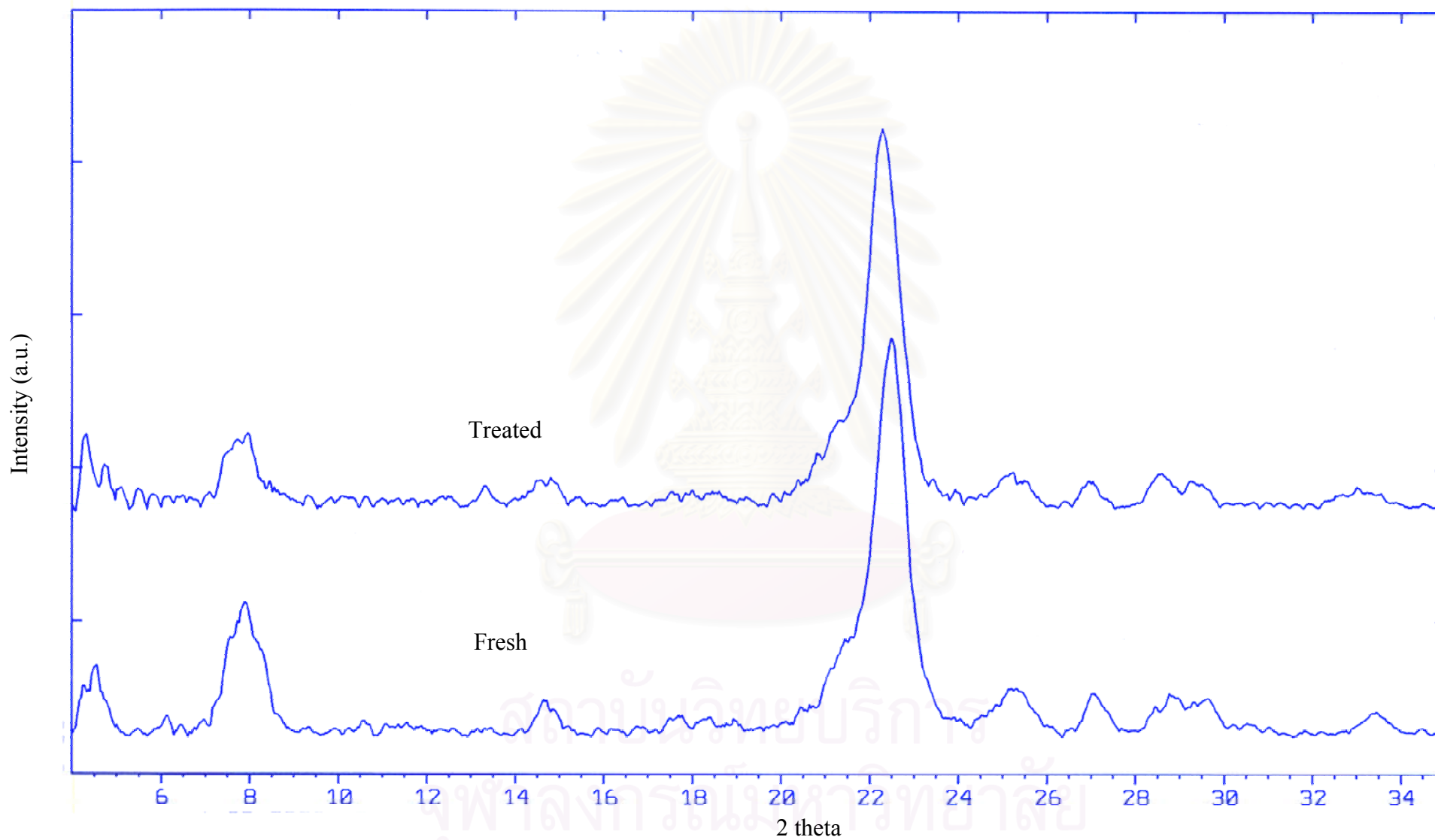


Figure 5.7 XRD spectra of H-zeolite beta particle size 0.5 μm

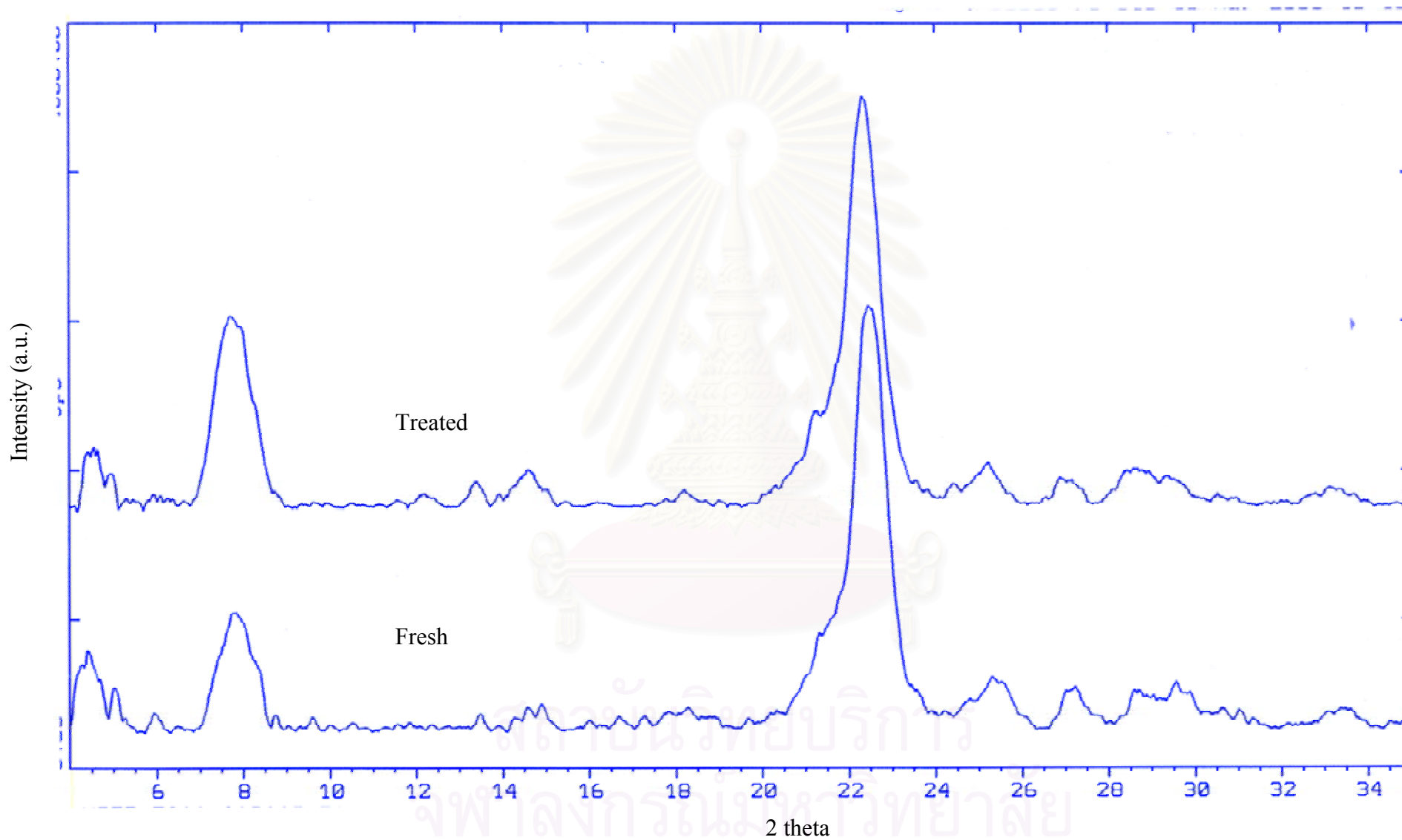


Figure 5.8 XRD spectra of H-zeolite beta particle size 0.7 μm

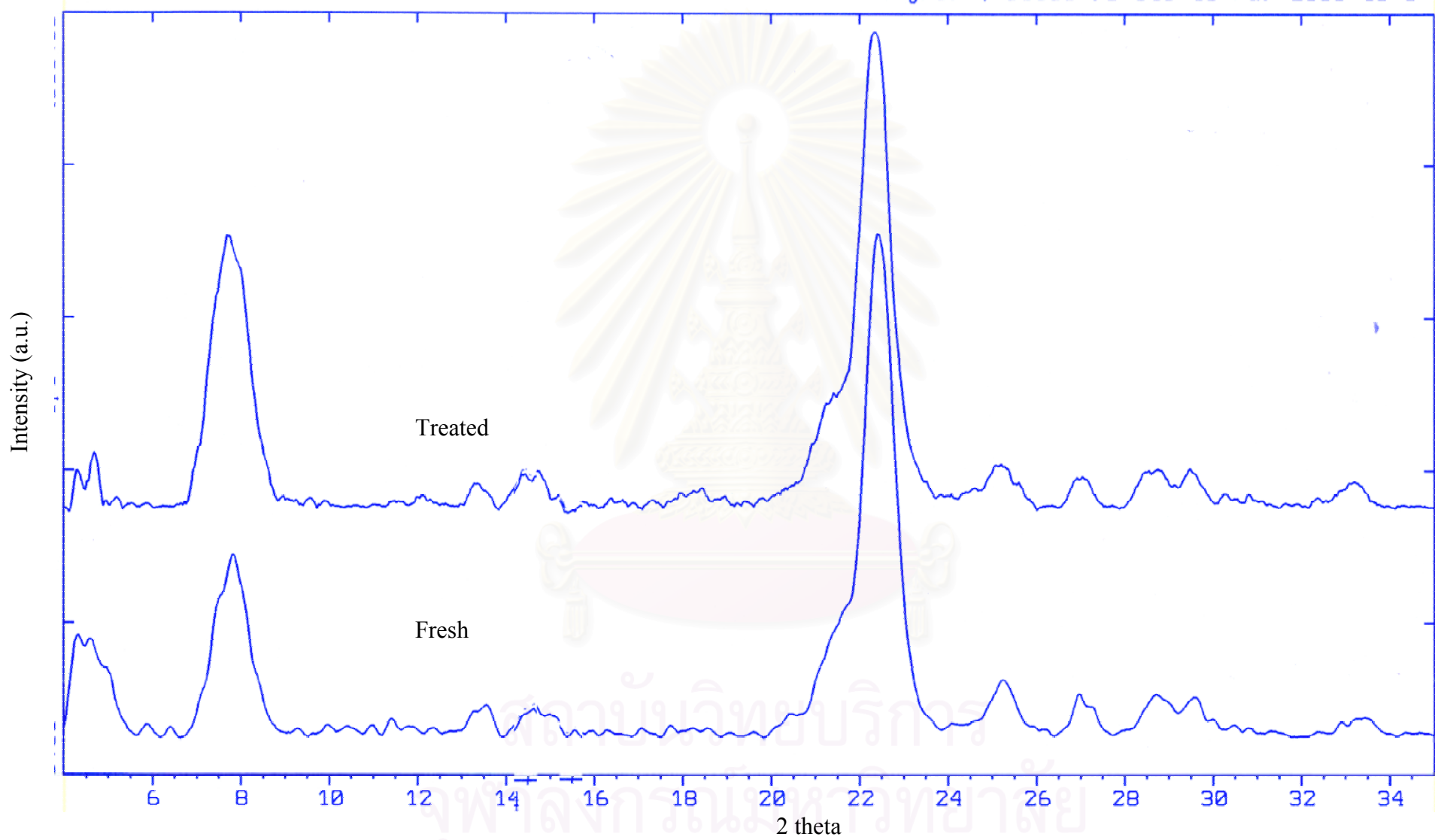


Figure 5.9 XRD spectra of H-zeolite beta particle size 0.9 μm

5.1.4 Framework Al content by ^{27}Al MAS NMR Spectra

Measuring ^{27}Al MAS NMR spectra provides information about the environment of the aluminum atoms in the zeolite sample. Al-tetrahedral presented in the zeolite framework ($\text{Al}(\text{OSi})_4$), displays the NMR feature at ~ 52 ppm. On the other hand, extra-framework aluminum (EFAI) species are usually octahedral coordinates which appear signal at a chemical shift of ~ 0 ppm.

The ^{27}Al MAS NMR spectra for the fresh samples are shown in Figure 5.11 (a)-5.16 (a). The parent sample shows a strong peak at ~ 54 ppm due to tetrahedral coordinated framework Al and a very weak peak at ~ 0 ppm due to octahedral coordinated extra framework Al (EFAI). The EFAI species in the parent sample were formed during the transformation process from as-synthesized to H-form[50] (1st calcination \rightarrow ion exchange with dilute NH_4NO_3 solution \rightarrow 2nd calcinations). Relative amount of tetrahedral and octahedral aluminum atoms can be calculated using ^{27}Al MAS NMR spectra. Figures 5.11-5.16 showed the ^{27}Al MAS NMR spectra of the zeolite beta samples with various size of 0.2 to 0.9 μm before and after hydrothermal treatment. It was found that the ^{27}Al MAS NMR spectra of all samples clearly exhibited the difference between the fresh and the treated samples. The hydrothermal treated samples exhibited the broadening peak at 0 ppm, corresponding to the octahedral aluminum compared to those of the fresh at the same size. In order to quantities and transformation involved, the percent relative area of the peak at 54 ppm and the peak at 0 ppm were evaluated and compared between fresh and treated sample. Hence, in this work we define the percent relative area of tetrahedral aluminum as the following equation:

$$\% \text{ relative area of tetrahedral aluminum} = \frac{\text{integrated area of tetrahedral aluminum}}{\text{integrated area of tetrahedral and octahedral aluminum}}$$

The ratio of integrated area underneath the tetrahedral aluminum and octahedral feature of fresh and treated are compiled in Table 5.2 and the changing of percent relative area ^{27}Al MAS NMR is shown in Figure 5.10.

All treated sample shown the lower relative area of tetrahedral indicated that dealumination occurred after treatment. However the magnitude of dealumination were considerably significantly for the small crystallites size but negligible for in the larger one. Additionally the concentration of tetrahedral in framework after hydrothermal treatment decreased to approximately similar value compared to the value observed before treatment.

Table 5.2 Percent relative area of tetrahedral ^{27}Al NMR signals

Particle size (μm)	The relative area of tetrahedral ^{27}Al (%)		
	fresh	treated	% decrease of tetrahedral ^{27}Al
0.2	94	77	18
0.3	95	78	18
0.4	93	79	15
0.5	88	78	11
0.7	89	81	9
0.9	94	78	7

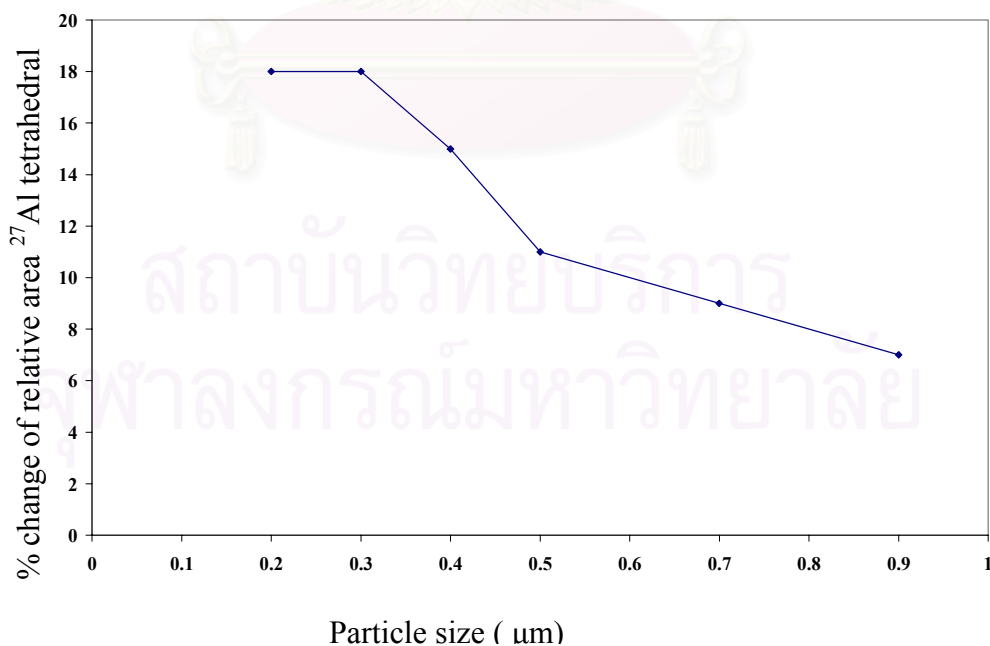


Figure 5.10 Percent change of relative area of tetrahedral ^{27}Al of treated H-zeolite beta with different sizes

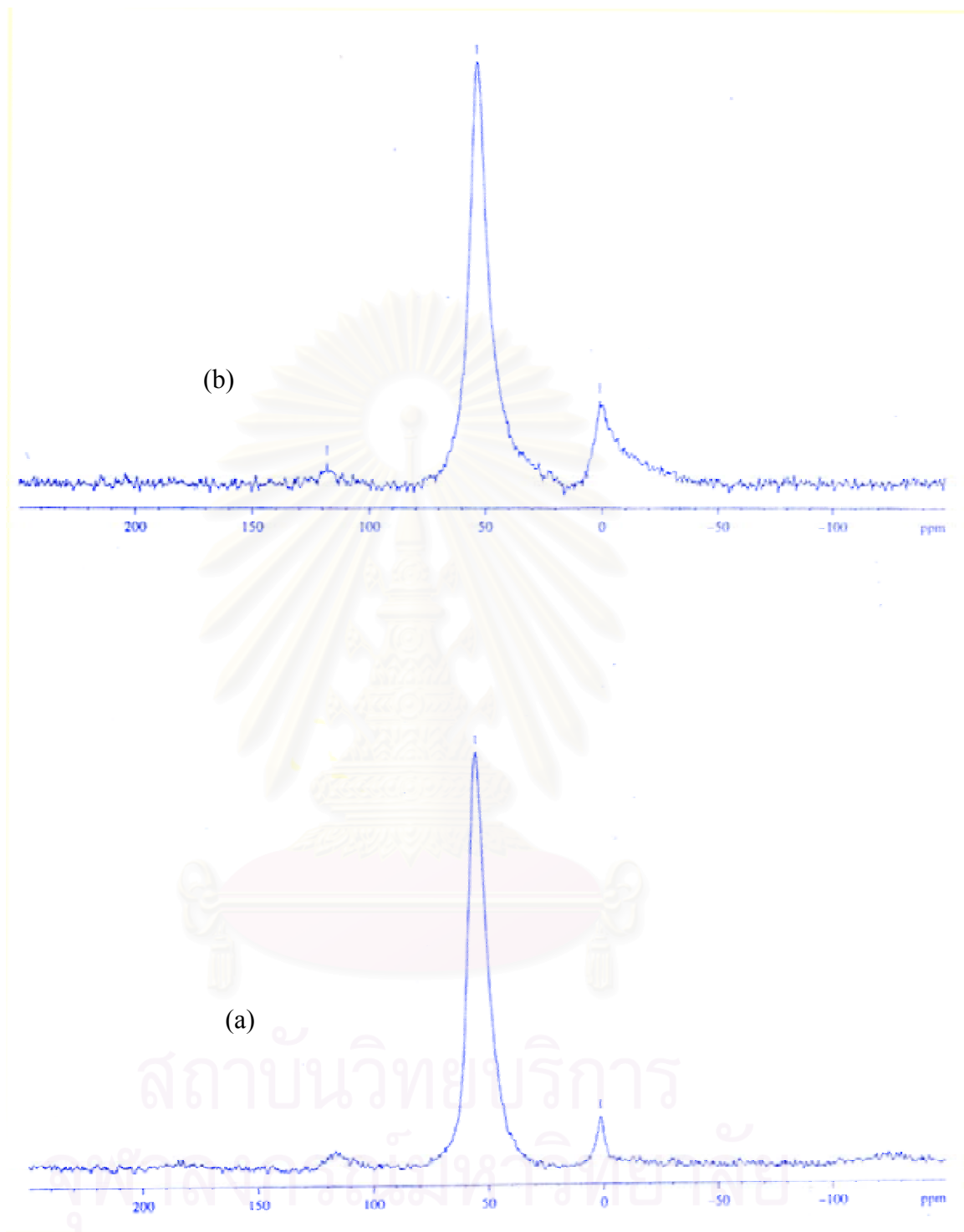


Figure 5.11 ^{27}Al MAS NMR spectra of H-zeolite beta, particle size 0.2 μm
(a) fresh (b) treated

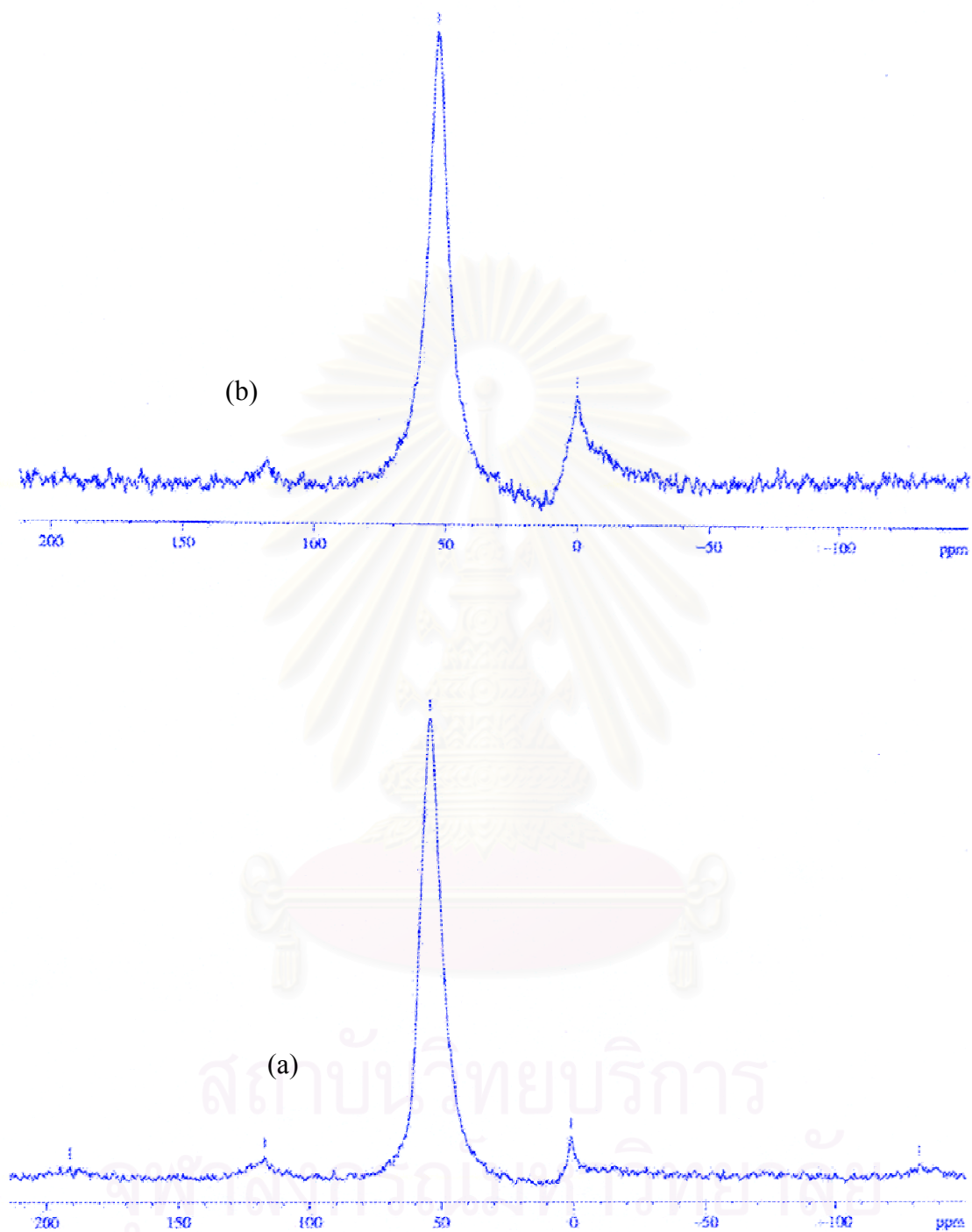


Figure 5.12 ^{27}Al MAS NMR spectra of H-zeolite beta, particle size 0.3 μm
(a) fresh (b) treated

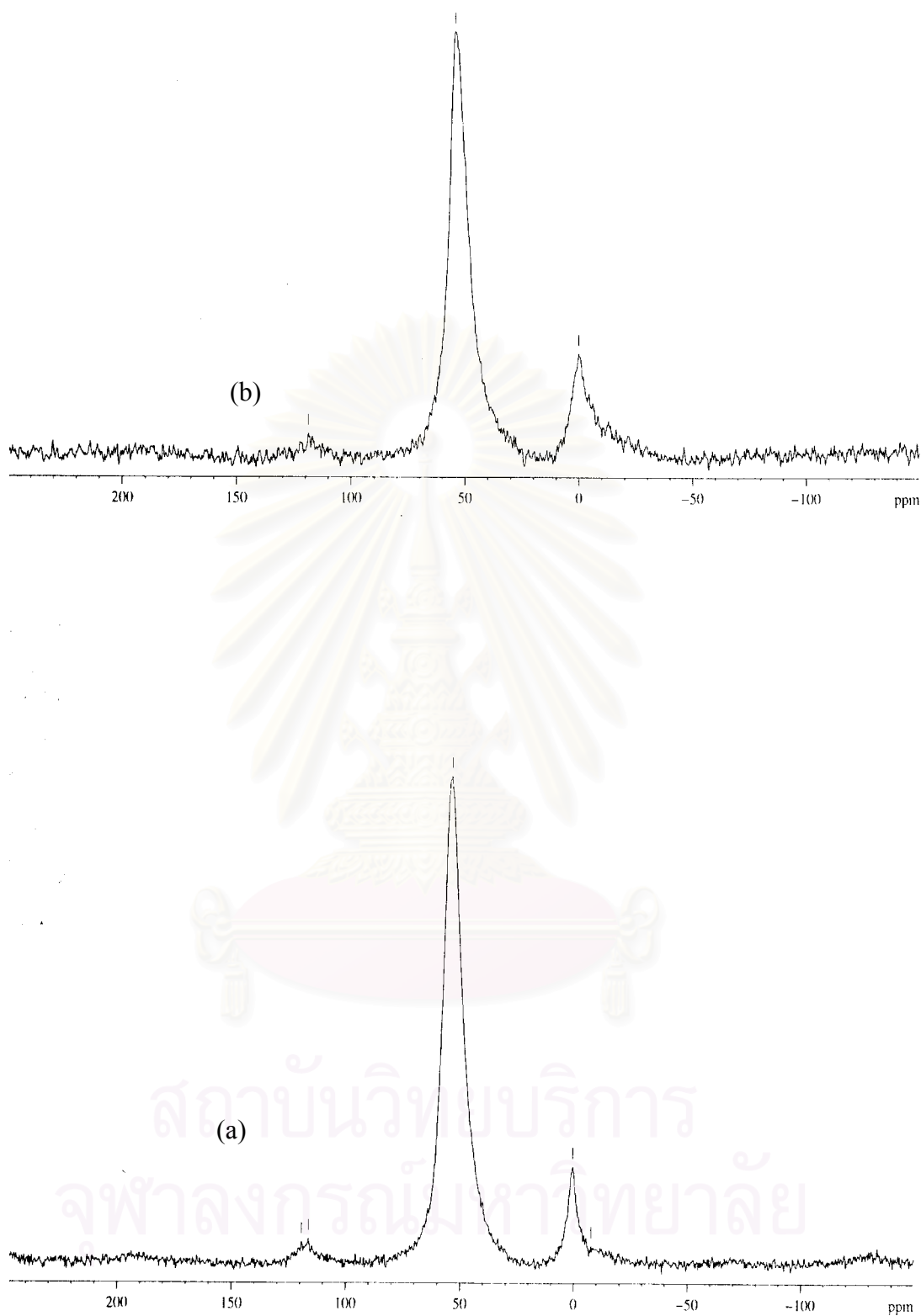


Figure 5.13 ^{27}Al MAS NMR spectra of H-zeolite beta, particle size 0.4 μm

(a) fresh (b) treated

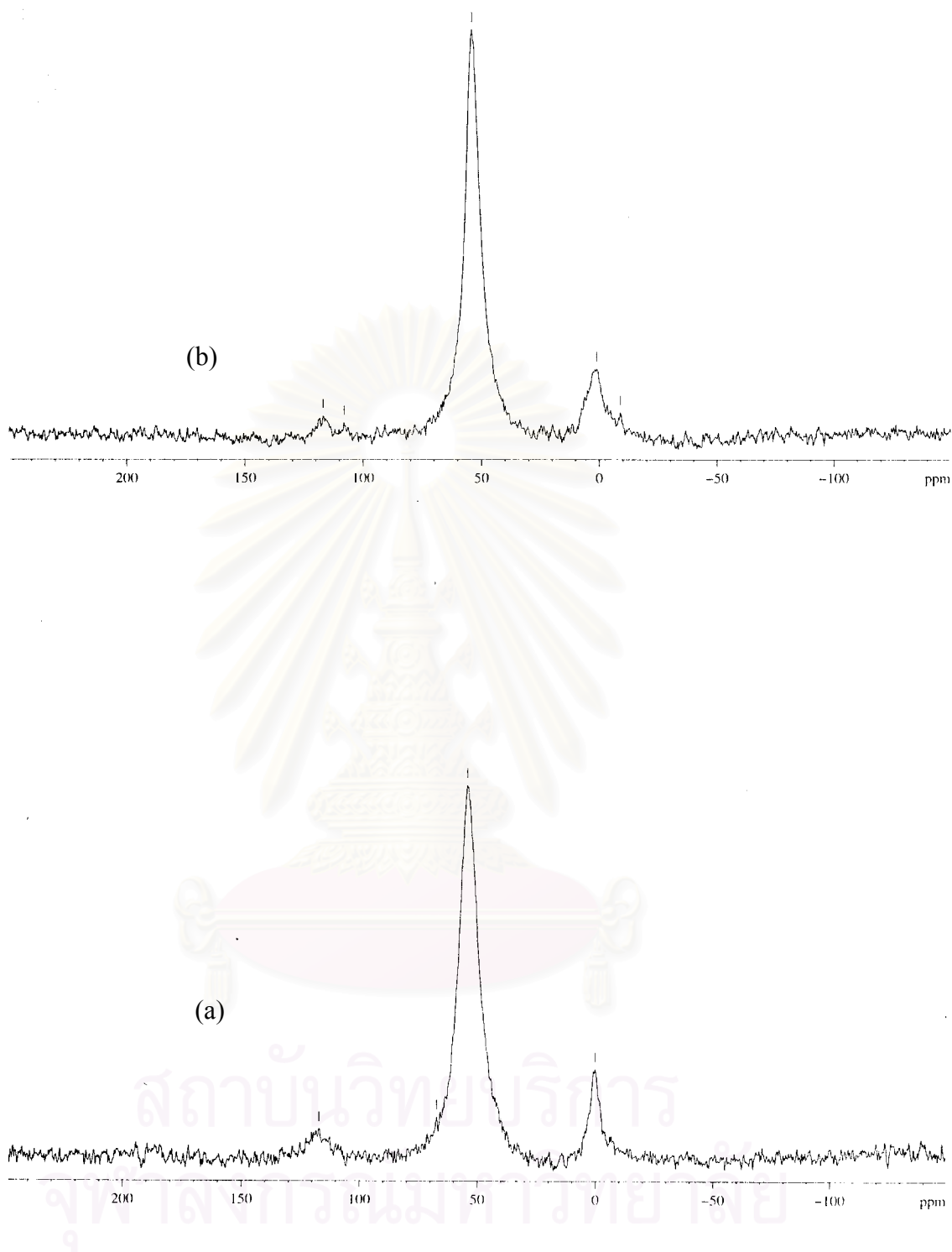


Figure 5.14 ^{27}Al MAS NMR spectra of H-zeolite beta, particle size $0.5\ \mu\text{m}$
(a) fresh (b) treated

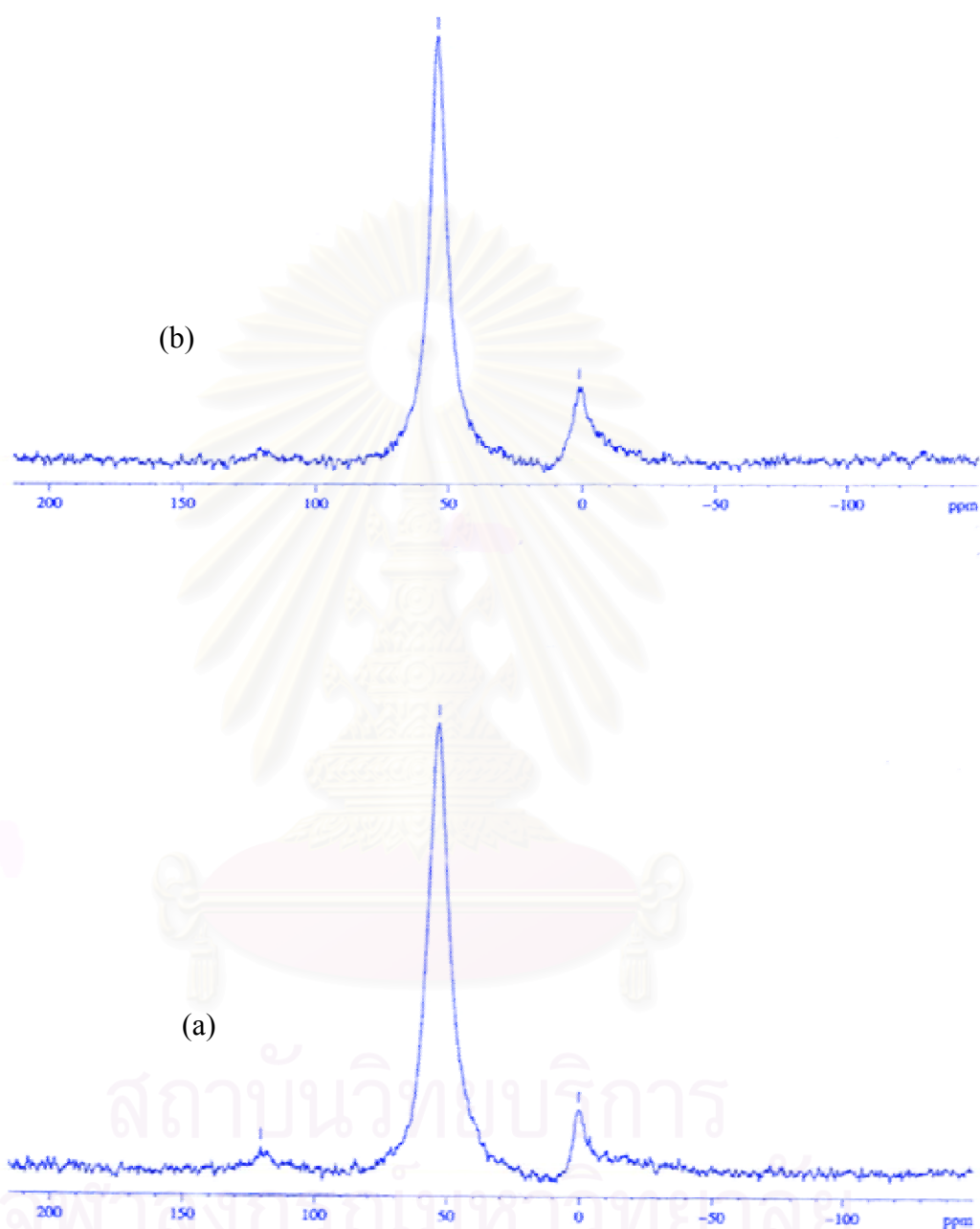


Figure 5.15 ^{27}Al MAS NMR spectra of H-zeolite beta, particle size $0.7\ \mu\text{m}$
(a) fresh (b) treated

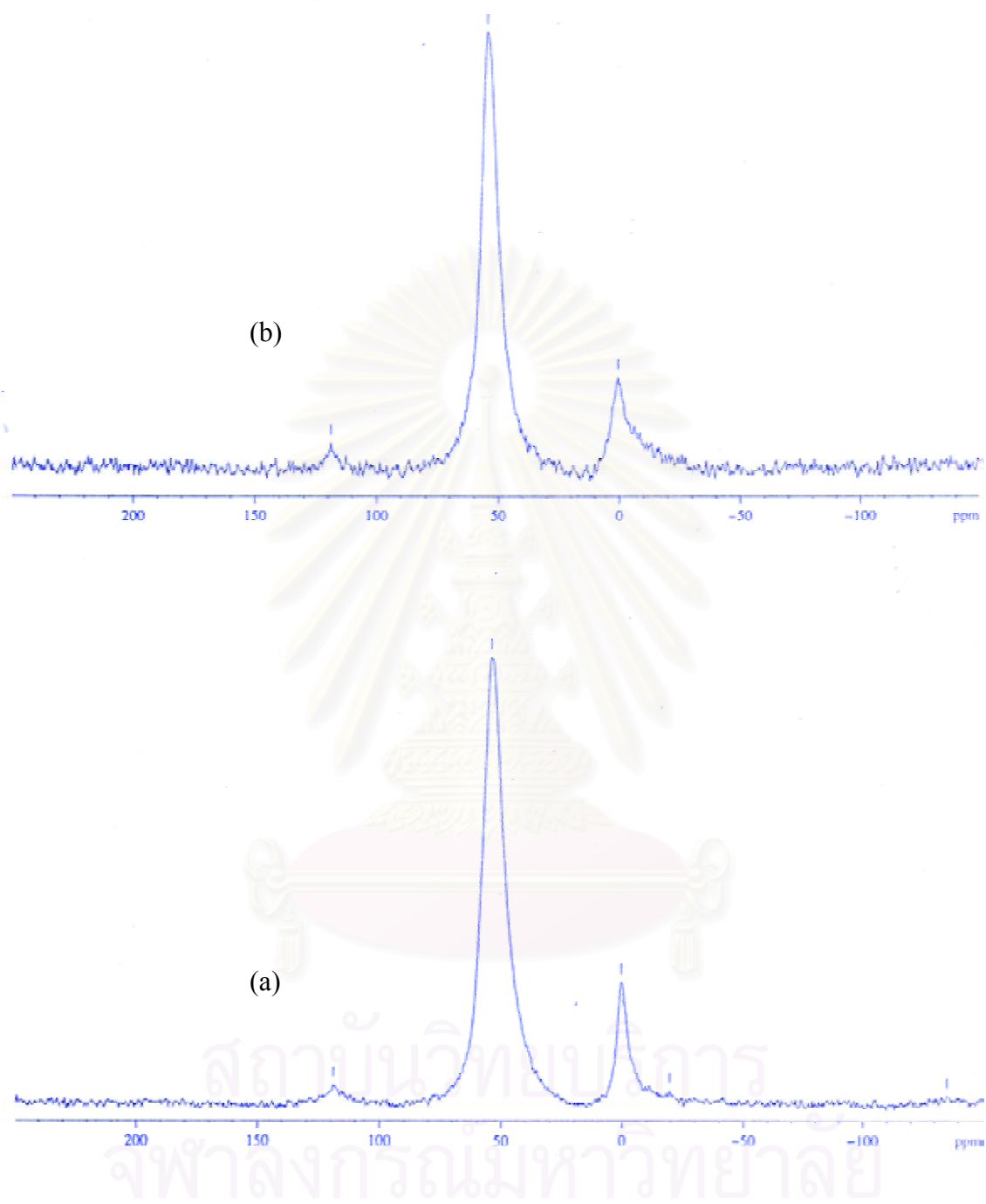


Figure 5.16 ^{27}Al MAS NMR spectra of H-zeolite beta, particle size 0.9 μm

(a) fresh (b) treated

5.1.5 Reaction Testing

The hydrothermal treatment was found to cause dealumination of zeolite framework resulting in a decrease of acidity and catalytic activity of zeolite material [28, 47]. To study the influence of hydrothermal treatment on the catalytic activity, methanol conversion was used as a probe reaction for testing zeolite beta.

Figure 5.17 illustrates the methanol conversion in the course of time over the H-zeolite beta catalysts. Generally, methanol conversion dropped with time on stream and approached to the steady values at approximately 250 min except in case of the fresh catalyst for 0.3 μm of particle size that showed a steady state conversion at 300 min. The small particle size shown higher steady state conversion than the large one for both fresh and treated catalysts. For fresh catalysts, conversion decreased significantly in the range of an initial time on stream and changed slightly after 150 min. On the other hand, a low decreasing rate of conversion was pronounced for the catalysts with hydrothermal treatment prior to testing. A feasible explanation for this may be the structure stability after dealumination of treated catalysts [10, 27, 54]. It was note that although the fresh catalysts exhibited a dramatic decrease of activity in the initial time on stream, the steady state conversion remained to be high compared relatively to the treated catalysts [42].

In summary it was found that the catalysts for small particle size showed higher activity than that for large one. The fresh catalysts gave a high methanol conversion; however, a significant change of activity with time on stream was pronounced. In addition, it was observed that particle size has no a significant effect on methanol conversion at steady state. The above ^{27}Al NMR results that the Si/Al ratio in framework of zeolite beta for all particle size showed the similar value after hydrothermal treatment can support this.

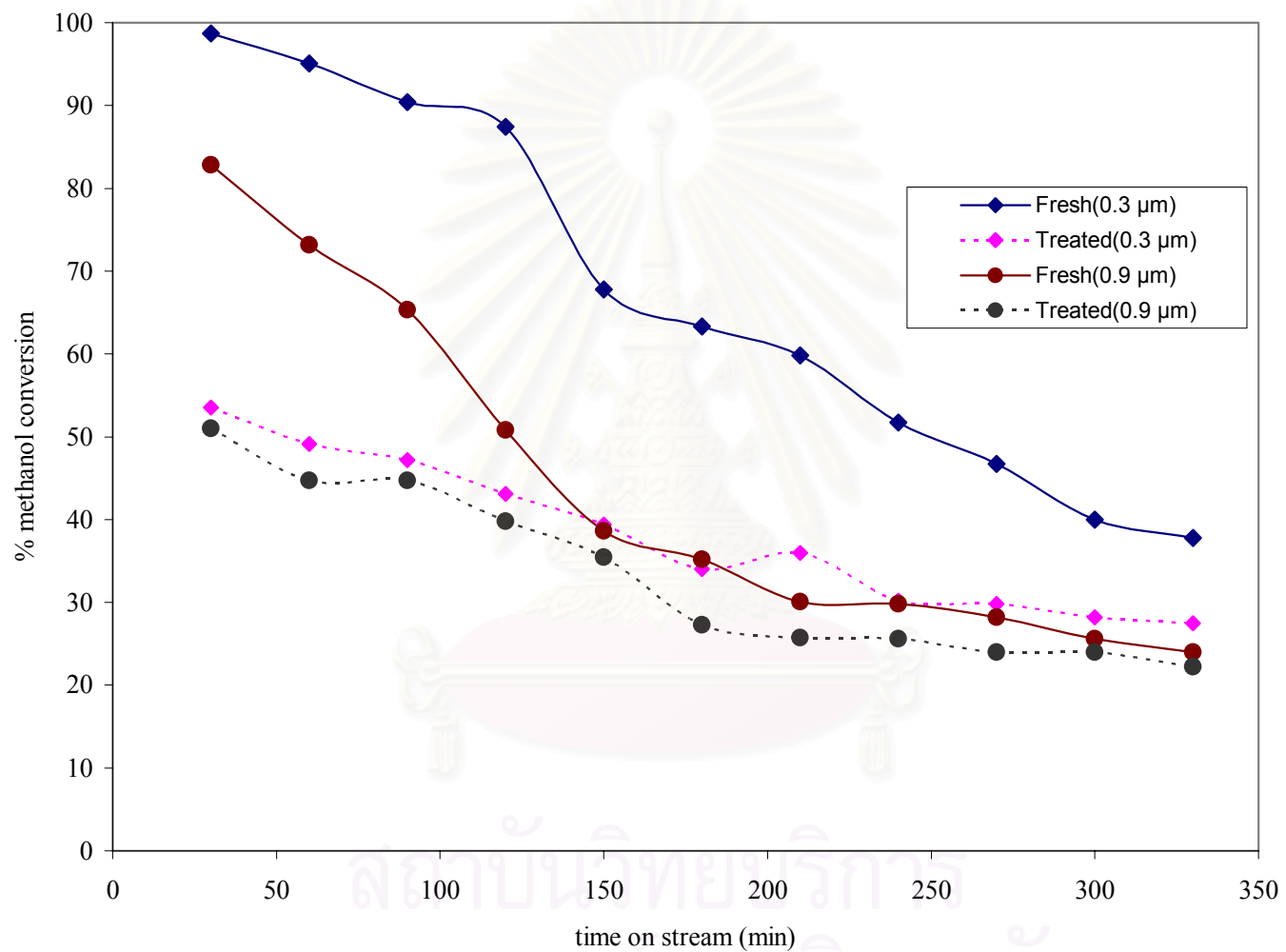


Figure 5.17 Methanol conversion on zeolite beta compared between small and large particle size both fresh and treated

5.2 The effect of silicon to aluminium ratio

5.2.1 silica to alumina ratio by XRF measurement

The result of quantitative analysis by XRF of silicon to aluminium ratio in the synthesized zeolite beta are shown in Table 5.3.

Table 5.3 Si/Al content in zeolite beta

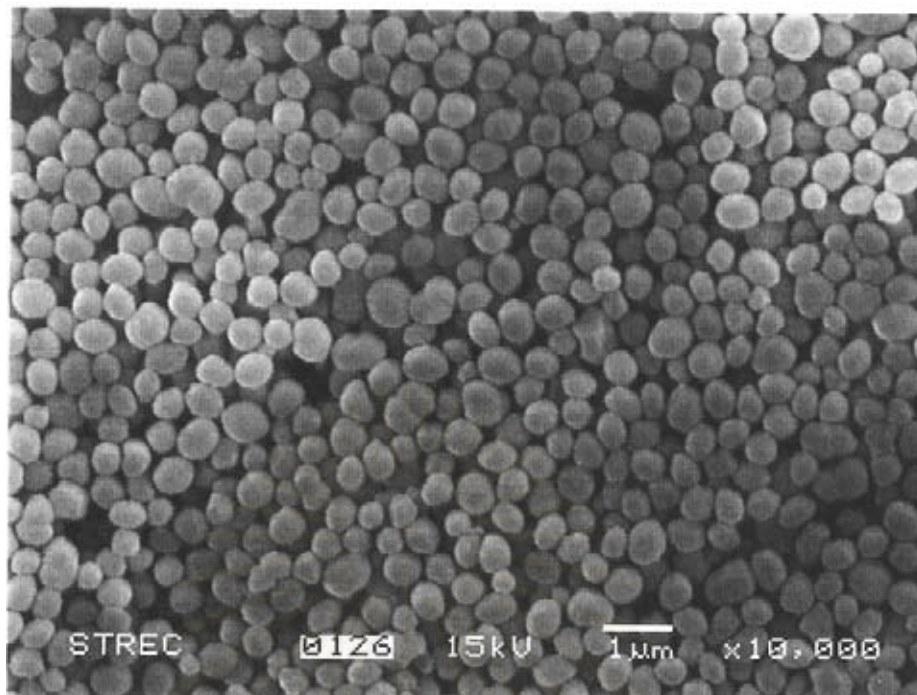
Si/Al molar ratio of beta zeolite in gel	Si/Al molar ratio observed in crystal
30	17
50	27
80	45

5.2.2 The morphology and particle size of H-zeolite beta samples

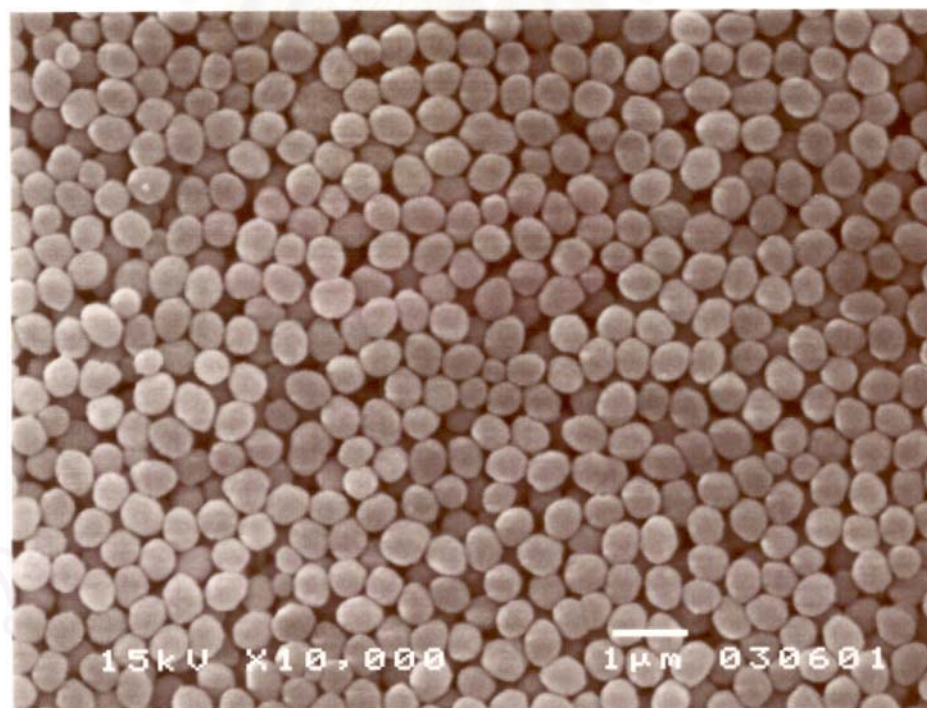
The particle size, average 0.45 μm of silicon to aluminium ratio 17, 27 and 45 can be seen from the scanning electron microscopy (SEM) picture as shown in Figure 5.18 (a), (b) and (c) respectively. The morphology of the crystals were observed in the SEM picture of the treated samples not changed significantly compared to the fresh samples.

5.2.3 The single point BET surface area.

The surface area of H-zeolite beta fresh and hydrothermal treated with 10 % water at difference Si/Al = 27 are displayed in Figure 5.19. It is clear that the BET surface area for all of the H-zeolite beta decrease upon hydrothermal treatment. However, compared with the high Si/Al ratio, the BET surface area of lower Si/Al ratio were decreases more slightly.

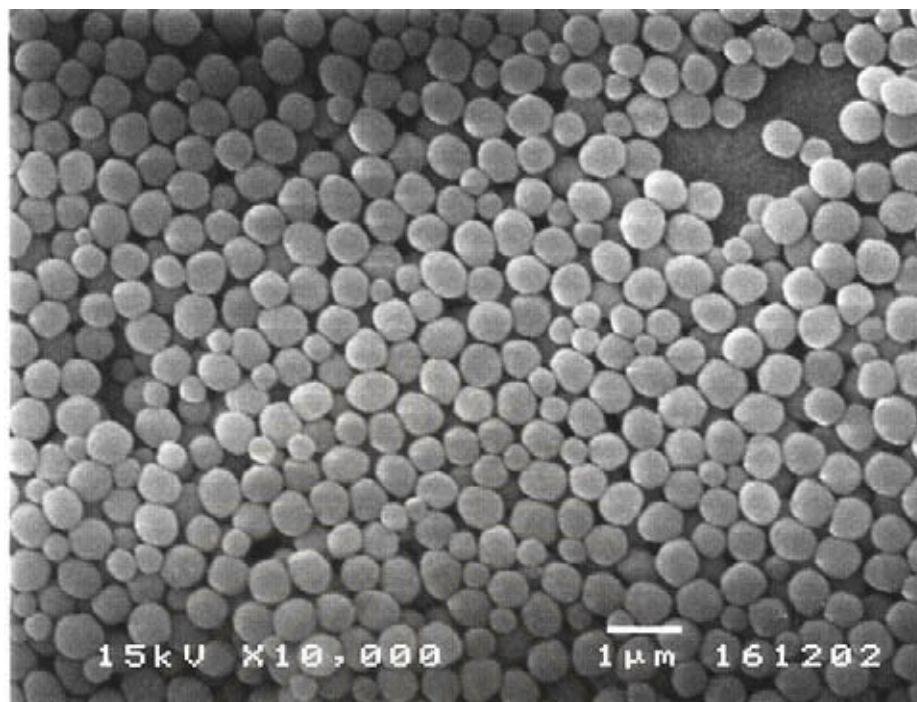


(a)



(b)

Figure 5.18 Scanning electron micrographs of H-zeolite betaparticle size,
(a) Si/Al = 17 (b) Si/Al = 27



(c)

Figure 5.18 (Cont.) Scanning electron micrographs of H-zeolite beta

(b) Si/Al = 47

Table 5.4 BET surface area and percent crystallinity

Si/Al	BET surface area (m ² /g)		% crystallinity of
	Fresh	pretreated	Pretreated
17	478	430	96
27	464	446	97
45	490	474	97

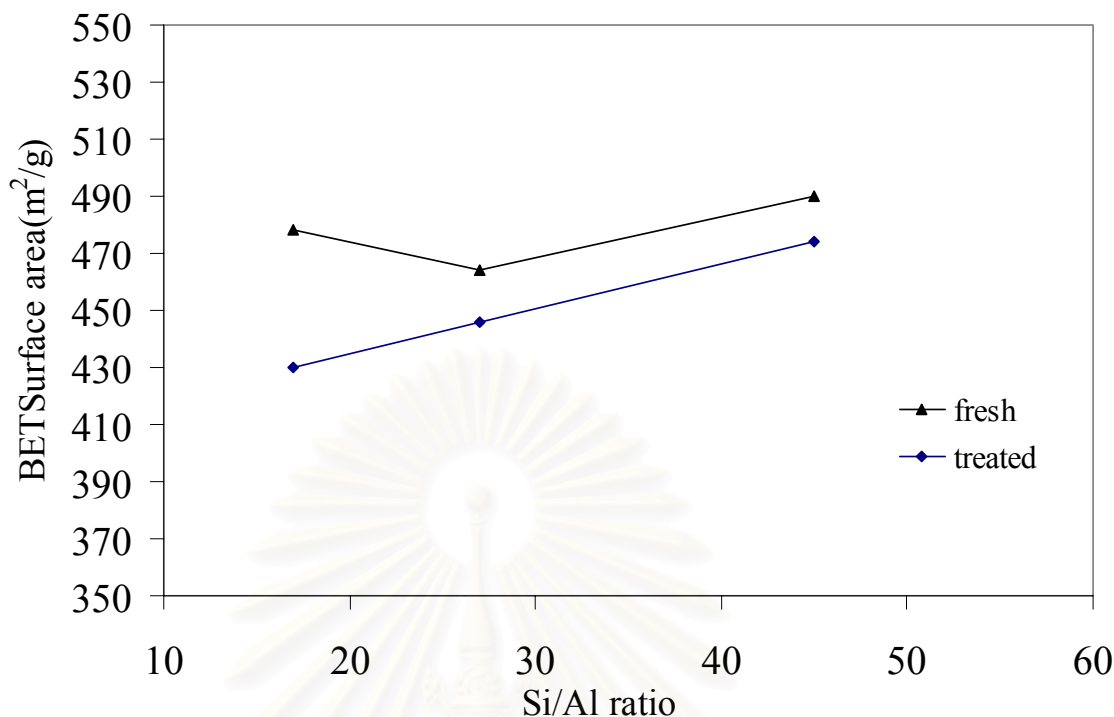


Figure 5.19 Relationship between the single point BET surface area (m²/g) and the Si/Al ratio of H-beta zeolite, both fresh and treated by hydrothermal treatment

5.2.4 Percent relative crystallinity.

The percent relative crystallinity (peak intensity of the $2\theta = 22.4$) of the treated sample measured by XRD are listed in table 5.4. The percent relative crystallinity is calculate from peak area at $2\theta = 22.4$ of fresh per treated sample. The percent relative crystallinity for all sample are slightly decreased in peak area and intensity at $2\theta = 22.4$, showed that the crystallinity of the samples was retained after treated hydro thermally. The XRD patterns of fresh and treated with various Si/Al ratio are showed in Figure 5.20 to 5.22 respectively

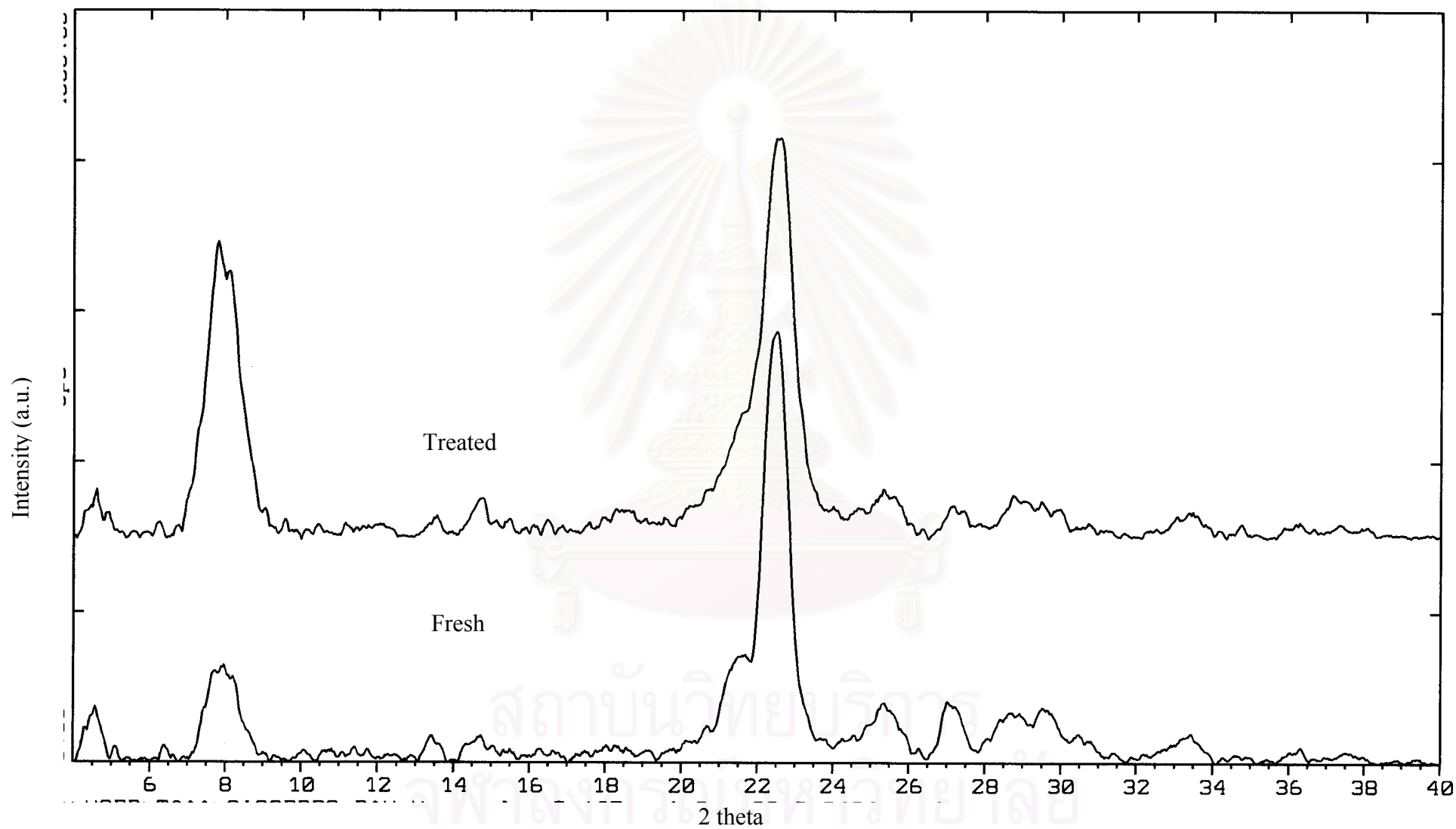


Figure 5.20 XRD spectra of H-zeolite beta, Si/Al ratio = 17

Fresh

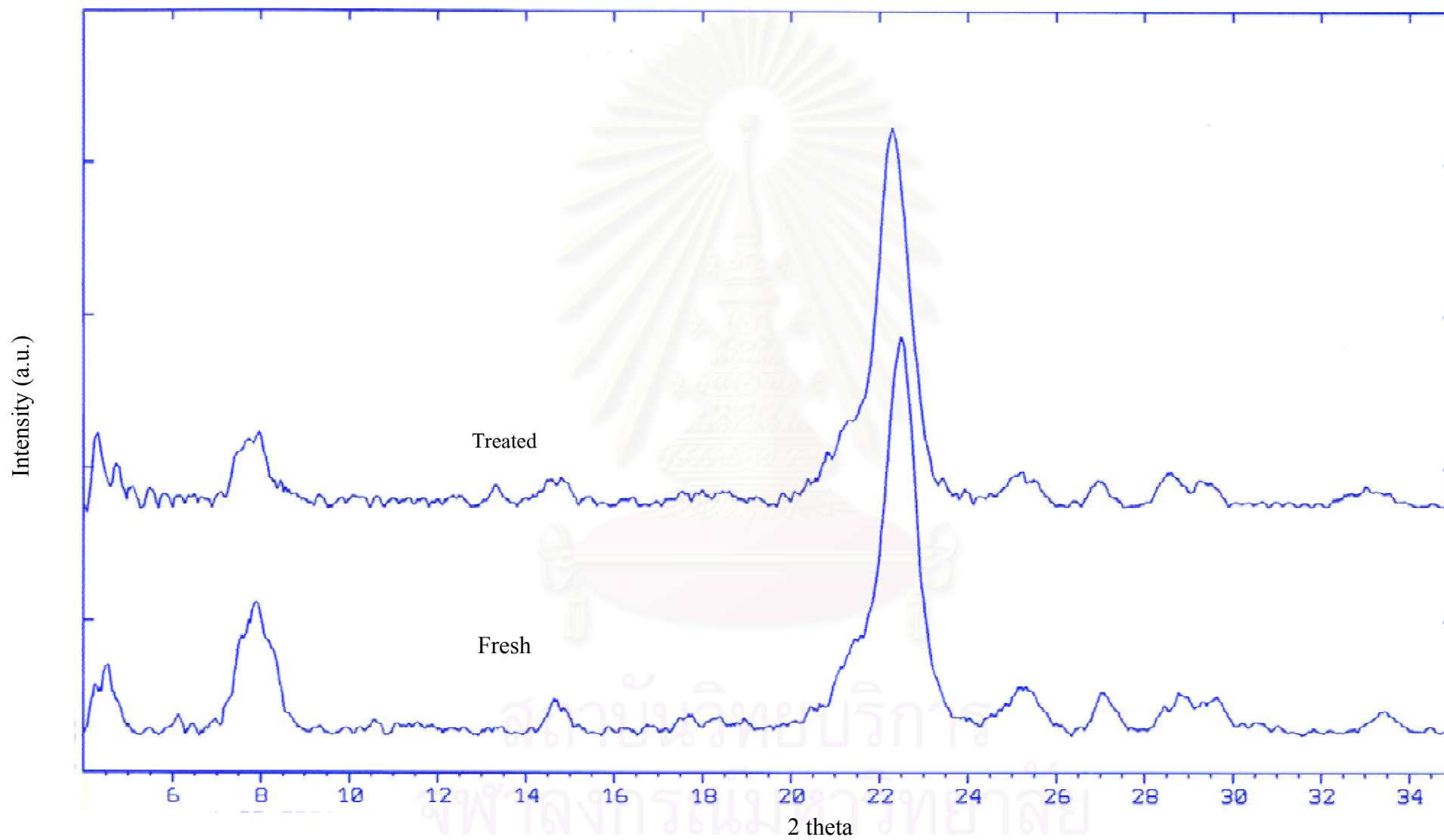


Figure 5.21 XRD spectra of H-zeolite beta, Si/Al ratio = 27

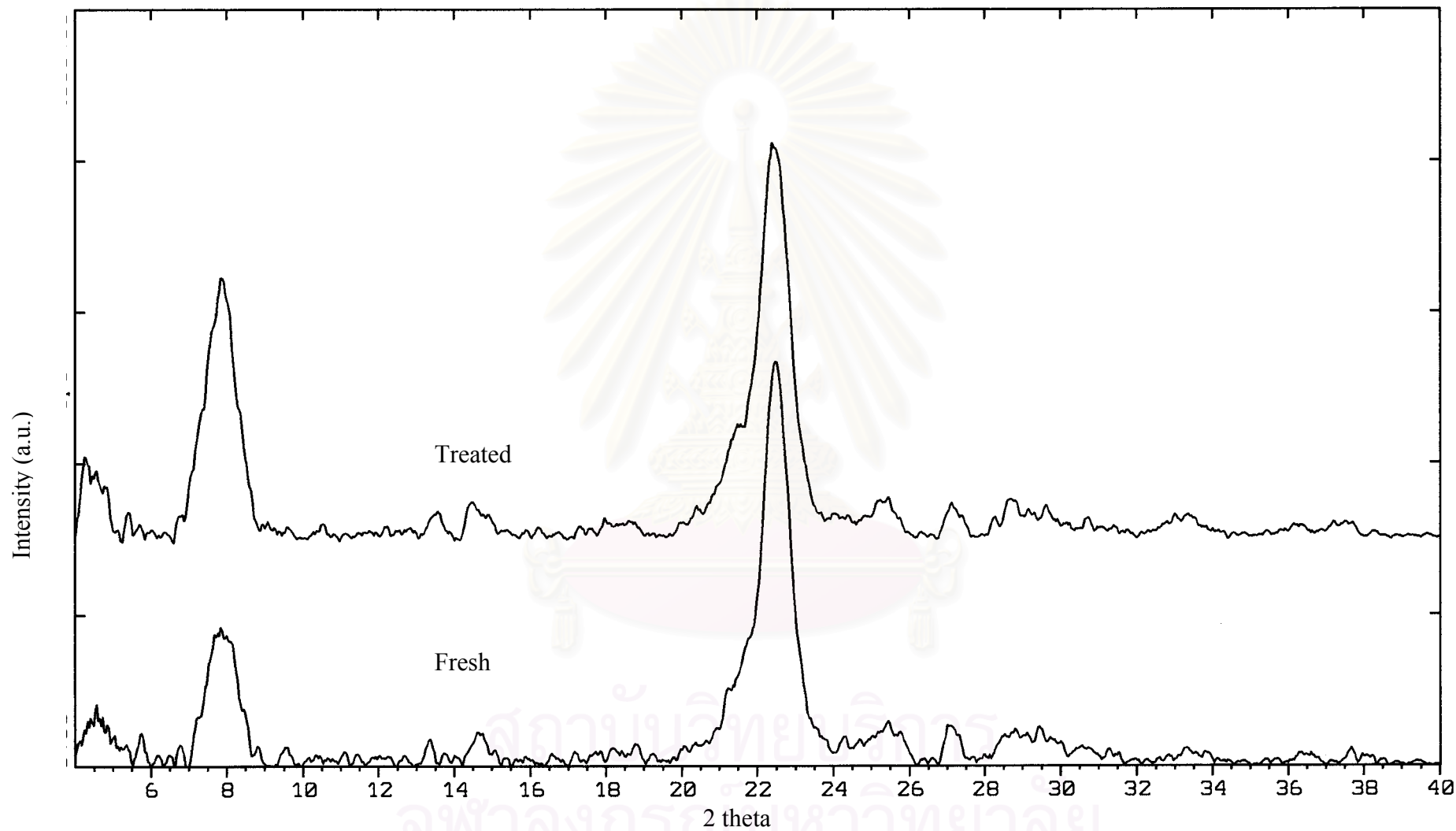


Figure 5.22 XRD spectra of H-zeolite beta, Si/Al ratio = 45

5.2.5 ^{27}Al MAS NMR Spectra

The ^{27}Al MAS NMR spectra for the parent sample as shown in Figure 5.24 (a)-5.26 (a). The parent sample shows a strong peak at ~ 54 ppm due to tetrahedral coordinated framework Al and a very weak peak at ~ 0 ppm due to octahedral coordinated extra framework Al (EFAI). The ^{27}Al MAS NMR spectrum comparison of before and after hydrothermal treatment of zeolite beta with difference Si/Al ratio are shown in Figure 5.24-5.26. It was found that the ^{27}Al MAS NMR spectrum of all sample clearly exhibits the difference between the fresh and treated sample. the ^{27}Al MAS NMR MAS spectra also broadens slightly after hydrothermal treatment. These facts demonstrate that hydrothermal treatment lead to dealumination of the aluminium framework. In order to quantity and transformation involved, the percent relative area of the peak at 54 ppm and the peak at 0 ppm were evaluated and compared between fresh and treated, octahedral aluminum as shown in Table 5.4 and displayed in Figure 5.23. It found that the tetrahedral framework Al of treated H-Beta zeolite for lower Si/Al ratio were decreased more the higher Si/Al ratio. Hence, it was concluded that the extent of dealumination decreased with increase Si/Al ratio, showed that the higher Si/Al ratio of H-beta zeolite more hydrothermal stability than that the low one.

Our results that the dealuminate H-beta zeolite for all sample in this work retain a relative crystallinity higher than 95 % are the agreement with the results observed by Triantafillidis [54] for ZSM-5 zeolite. The phenomena may possible due to, in general, the presence of only less than 3-4 Al atom containing unit cell (92-93 Si atom). Therefore, even when all the Al is removed from its framework, the unit cell do not change significantly and systematically [10,27,54].

An improvement in thermal or hydrothermal stability has been ascribed to the lower density of hydroxyl groups, which id parallel to that of Al content [46]. Dealumination is believed to occur during dehydroxylation. A longer distance between hydroxyl groups decrease the probability of dehydroxylation that generates defects on structure of zeolites.

The hydrothermal treatment of zeolite produce EFAL species which effect the acid catalytic activity of zeolite [10,27,28,32,54]. This behavior has also been recognized and is even more pronounced in the case of Y-type dealuminated zeolite. Furthermore, it has been shown that both the amount and the type of EFAl or Si-Al species are important in defining the acidity and catalytic activity of catalyst.

Table 5.5 Percent relative area of tetrahedral ^{27}Al NMR signals

Si/Al	The relative area of tetrahedral ^{27}Al (%)		
	fresh	treated	% decrease of tetrahedral ^{27}Al
17	92	76	18
27	88	78	10
45	92	86	6

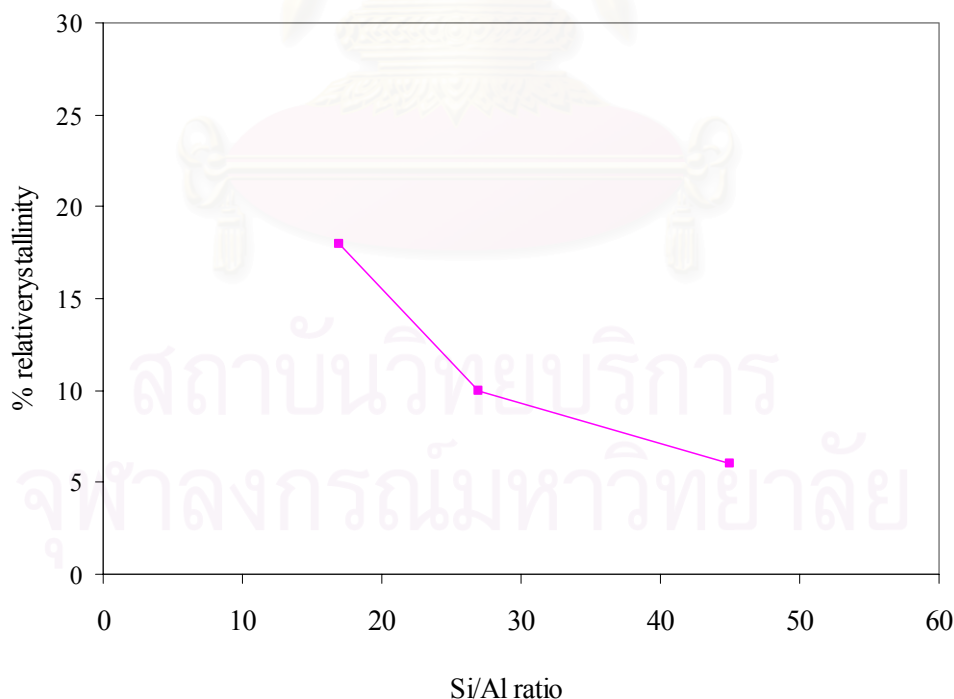


Figure 5.23 Percent relative area of tetrahedral ^{27}Al NMR changed of treated H-Beta zeolite with different Si/al ratio

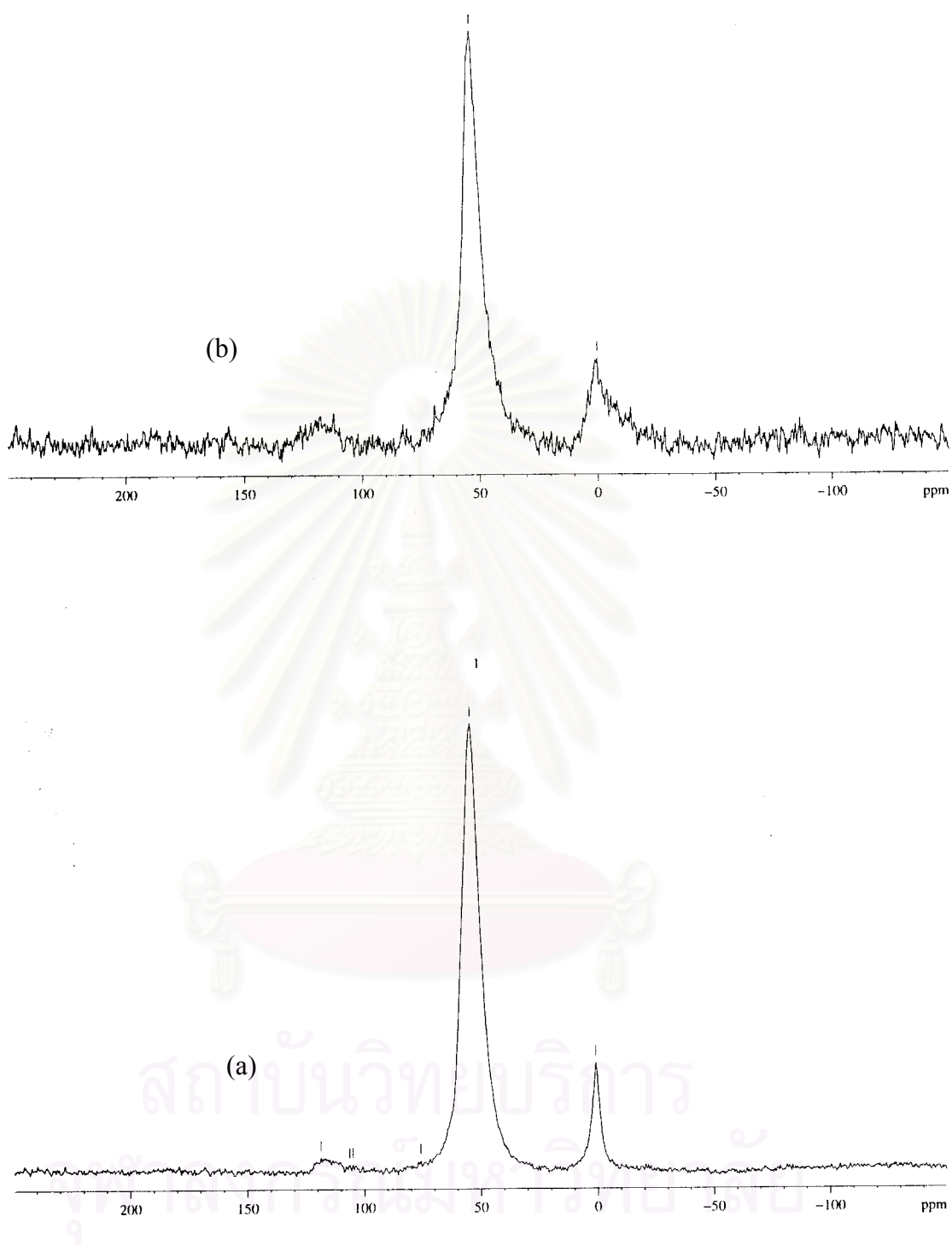


Figure 5.24 ^{27}Al MAS NMR spectra of H-zeolite beta, Si/Al ratio = 17
(a) fresh (b) treated

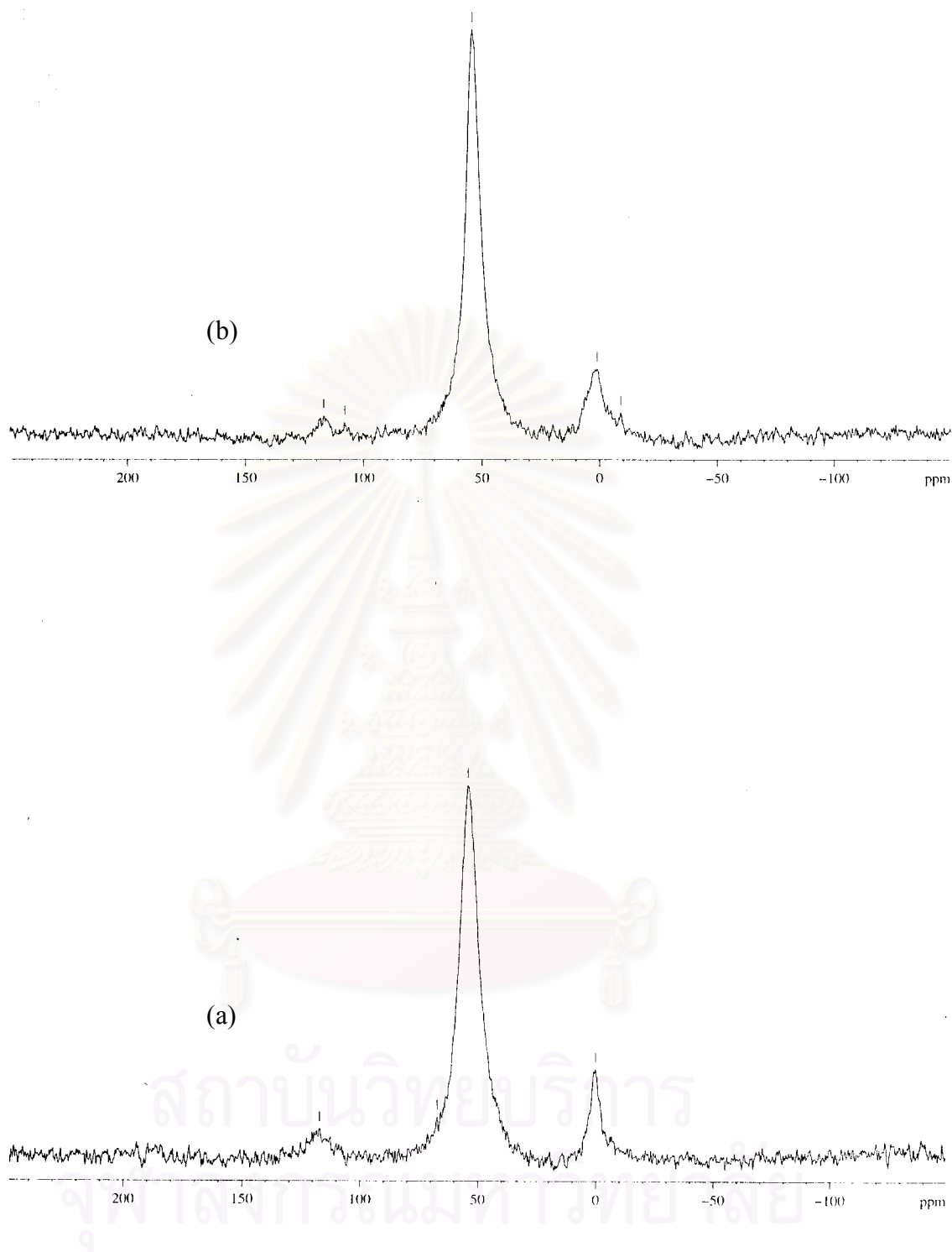


Figure 5.25 ^{27}Al MAS NMR spectra of H-zeolite beta, Si/Al ratio =27
(a) fresh (b)treated

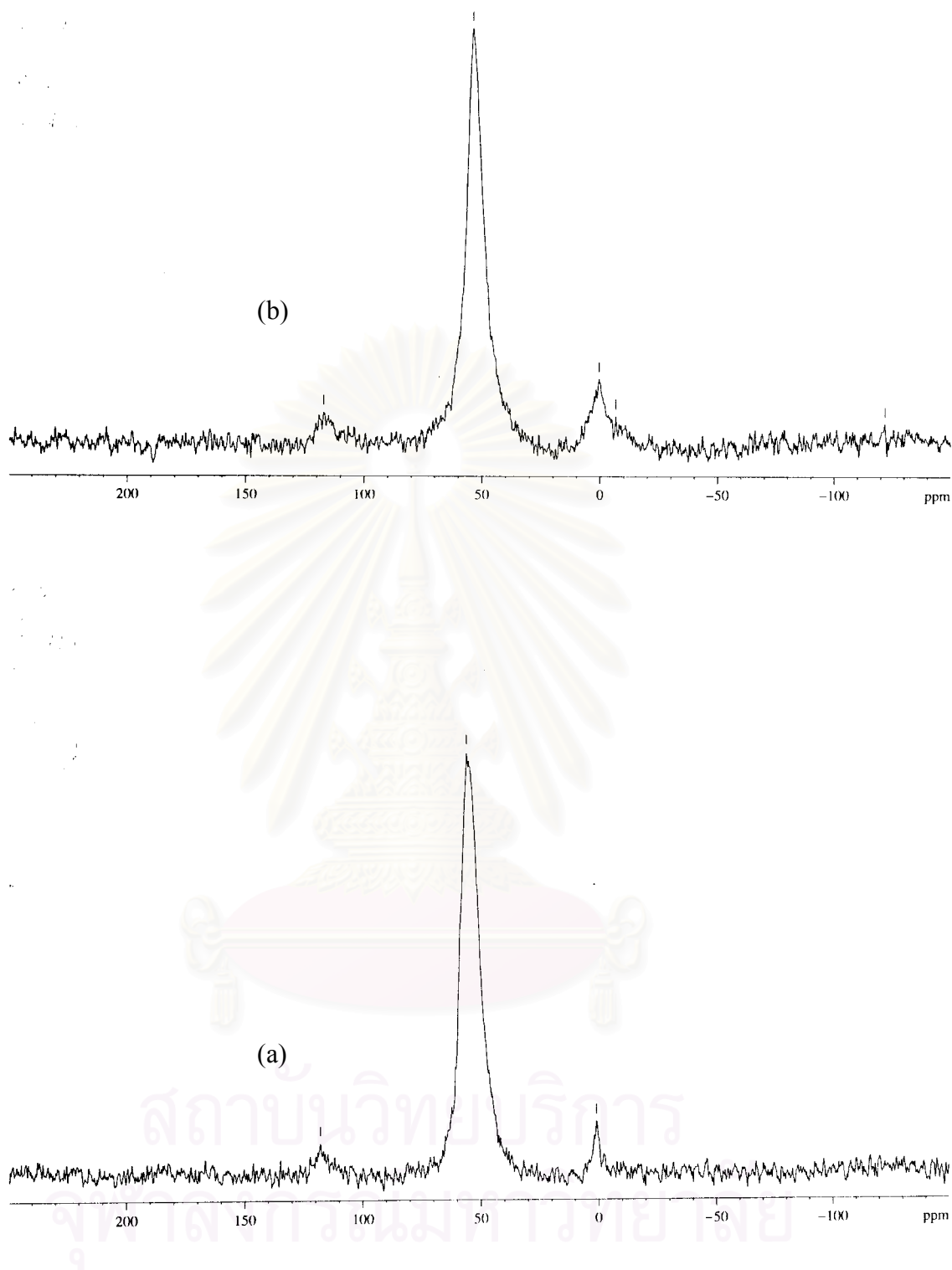


Figure 5.26 ^{27}Al MAS NMR spectra of H-zeolite beta, Si/Al ratio =45
(a) fresh (b)treated

CHAPTER VI

CONCLUSION AND RECOMMENDATION

This thesis has described the study of effect of particle size and silica to alumina ratio on the hydrothermal stability of zeolite beta. The conclusions of this research can be summarized as follows:

1. The extent of dealumination of zeolite beta decreases with increasing of particle size.
2. The concentration of tetrahedral in zeolite framework after hydrothermal treatment decreased to the same value.
3. The zeolite beta with higher silicon to aluminium ratio is more stable on dealumination under hydrothermal treatment.

From this research, the recommendations for further study are as follows:

1. Further studies of the effect of particle size on the hydrothermal stability should be investigated.
2. The acidity of H-zeolite beta before and after hydrothermal treatment should be studied

สถาบันวิทยบริการ
จุฬาลงกรณ์มหาวิทยาลัย

REFERENCES

1. Wadlinger, R.L.; Kerr, G. T. and Rosinski, E.J. US Patent 3 308 068 (1967).
2. Wedlinger, R. L.; Kerr, G. T. and Rosinski, E. US Pat. 3 308 069 (1967); and reissued US Pat. Re. 28 341 (1975).
3. Maria wima N.C. and Cardoso, D. Stud. Surt. Sci Catal; 105(1997): 349-356
4. Pardillos, J.; Brunel, D.; Coq, B.; Massiani, P.; De Menorval, C. and Figueras, A. J. Am. Chem. Soc. (1991): 69, 125.
5. Perez Pariente, J.; Sastre, E.; Fornes, V.; Martens, J. A.; Jacobs, P. A. and Corma, A. Appl. Catal. (1991): 69, 125.
6. Reddy, K. S. N.; Rao, B. S. and Shiralker, V. P. Appl. Catal. 95 (1993): 53.
7. Keading, W. W. J. Catal. 67, (1981): 159.
8. Bonetto, L.; Cambor, M. A.; Corma, M. and Perez-Pariente, J. Anales del 13^o Simposio Ibero Americano de Catalisis. (1992): 759.
9. Francesco Di Renzo, Catl. today. 41 (1998): 37-40.
10. Zhang, W.; Han, X.; Lin. X. and Bao, X. Microporous and Mesoporous Meter 50(2001): 13-23
11. Haw, J. F.; Bell, A. T. and Pines, A. NMR Techniques in Catalysis New York: Dekker, (1994): 139.
12. Hunger, M. Catal. Rev. Sci. Eng. 39 ,(1997): 345.
13. Rao, L. F.; Pruski, M. and King, T.S. J. Phys. Chem. B 101, (1997): 5717.
14. Hari, P. R.; Ueyama, K. and Matsukata, M. Appl. Catal A. 166 (1998): 97-103.
15. Perez-Pariente, J.; Martens, J. A. and Jacobs, P. A. Zeolites 8 (1988): 46.
16. Lohse, U.; Altrichter, B.; Donath, R.; Fricke, R.; Jancke, K.; Parlitz, B. and Schreier, E. J. Chem. Soc. Faraday Trans. (1996): 159.
17. Lepage, L. F.; Ertl, G.; Knozinger, H. and Weitkamp, J. Preparation of solid Catalysts, Wiley-VCH, Weinheim (1999): 4.
18. Lohse, U. and Altrichter, B. J. Chem. Soc. Faraday Trans. 92,1 (1996): 159-165.
19. Lohse, U. and Altrichter, B. J. Chem. Soc. Faraday Trans. 93,3 (1997): 505-512.
20. Perez Pariente, J.; Matartens, J. A. and Jacobs, P.A. Zeolites 8 (1988): 46-53.
21. Bellussi, G.; Pazzuconi, G.; Perego, C.; Girotti, G. and Terzoni, G. J.Catal. 157, (1995): 227-234.
22. Camiloti, A. M.; Jahn, S. L.; Velasco, N.D.; Moura, L.F. and Cardoso, D. Appl.

- Catal. A 182 (1999): 107-113.
23. Chang, C. D. and Chu, C. T. European Patent (1984): 123449.
 24. Persson, A. E.; Schoeman, B. J. and Otterstedt, J. E. Zeolites 14 (1994): 557.
 25. Bourgeat-Lami, E.; Massiani, P.; Di Renzo, F.; Espiau, P. and Fajula, F. Appl. Catal. 72 (1991): 139-152.
 26. Muller, M.; Harvey, G. and Prins, R. Microporous and Mesoporous Mater 34 (2000): 281-290.
 27. Muller, M. and Harvey, G. Microporous and Mesoporous Mater 34, (2000): 135-147
 28. Cambell, S. M. and Bibby, D. M. J. of Catalysis 161 (1996): 338-349.
 29. Reschetilowski, W. and Einicke, W. D. Appl. Catal. A. 56 (1989): L15-L20.
 30. Guisnet, M. and Ayrault, P. J. Chem. Soc. Faraday Trans. 93(8) (1997): 1661-1665.
 31. Apelian, M. R. and Fung, A. S. J. Phys. Chem. 100 (1996): 16577-16583.
 32. Kunkeler, P. J.; Zuurdeeg, B. J.; Van der Waal, J.C.; Van Bokhoven, J.A.; Koningsberge, D.C. and Bekkun Van, H. J. of Catal. 180 (1998): 234-244.
 33. Datka, J. and Tuznik, E. J. Catal. 43 (1986): 102
 34. Halgeri, A. B. and Das, J. Appl. Catal. A. 181 (1999): 347-354.
 35. Vandry, F.; Renzo, F.D; Fajula, F. and Schulz, P. J. Chem. Soc., Faraday Trans., 1998, 94(4), 617-627.
 36. Cambor, M. A. and Corma, A. Stud. Surf. Sci. Catal. 105 (1997): 341.
 37. Bonetto, L.; Cambor, M. A. and Corma, A. Appl. Catal. A. 82 (1992): 37-50.
 38. Barrer, R.M. Hydrothermal Chemistry of Zeolites, London: Academic Press, 1982.
 39. Arribus, M. A. and Martinez, A. Catal. Today 65 (2001): 117-122.
 40. King, R. B. Encyclopedia of Inorganic Chemistry, vol. 7. Wiley & Sons, (1994): 4365-4391
 41. Bekkum, H.V.; Flanigen, E.M. and Jansen, J.C. Stud. Surf. Sci. Catal. 578 (1991).
 42. Szoztak, R. Molecular Sieve Principles of Synthesis and Identification, pp. 1-50, New York: Van Nostrand Reinhold, 1989.
 43. Satterfield, C.N. Heterogeneous Catalysis in Industrial Practice, 2nd ed., pp. 226-259, New York: McGraw-Hill, 1991.
 44. Meier, W.M. and Olson, D.H. Atlas of Zeolite Structure Types, 3rd revised ed., int. Zeolite Assoc., Boston: Butterworth-Heinemann, 1992.
 45. Tsai, T.; Lui, S. and Wang, I. Appl. Catal. A 181 (1991): 355-3698.
 46. Barthoment, D. "Acidic catalysts with Zeolites", Zeolites Science and Technology (Rebeira, F.H. et al.), Martinus Nijhoff Publishers, The Hange, 1984.

47. Ashton, A.G.; Batamanian, S. and Dwyer, J. "Acid in Zeolite" (Imelik, B. et al.), Catalysis by Acid-Bases, Amsterdam: Elsevier, 1985.
48. Sano, T.; Fujisawa, K. and Higihara, H, "High Stream Stability of H-ZSM-5 Type Zeolite Containing Alkaline Earth Metals" Catalyst Deactivation, (Delmon, B. and Froment, G.R. eds), Stud. Surf. Sci. Catal., p 34, Amsterdam: Elsevier, 1987.
49. Tanaka, K.; Misono, M.; Ono, Y. and Hattori, H. "New Solid Acids and Bases" (Delmon, B. and Yates, J.T. et al.), Stud. Surf. Sci. Catal., p 51, Tokyo: Elsevier, 1989.
50. Ramesh, B.B. and Perez Clearfield, A. J. Phys. Chem. 96 (1992): 6729-6737.
51. Ratnasamg, P.; Bhat, R. N.; Pokhrrigak, S. K.; Hegde, S. G. and Kumar, R. J. Catal. 199 (1989): 65
52. Chen, N. Y.; Garwood, W. E.; Dwyer, F. G. Shap Selective Catalyst in Industrial Applications, 2nd ed., New York: Marcel Dekker, 1996.
53. McDaniel, C. V. and Maher, P.K. American Chemical Society, ACS Monograph 171 (1976): 285
54. Costa, C.T.; Athanasios, G.V.; Nalbandian, L. and Nicholas P.E. Microporous and Mesoporous Mater 47 (2001): 369-388.



APPENDICES

สถาบันวิทยบริการ
จุฬาลงกรณ์มหาวิทยาลัย

APPENDIX A

SAMPLE OF CALCULATIONS

A-1 Calculations of Si/Al Atomic for Beta Zeolite Preparation

The calculation is based on weight of Sodium Aluminate (Al/NaOH = 0.78) in gel preparation.

$$\text{Molecular Weight of Al} = 26.9815$$

$$\text{Molecular Weight of NaAlO}_2 = 81.97$$

Using Sodium Aluminate (NaAlO₂) 0.702 g as gel preparation.

$$\begin{aligned} \text{Mole of Al used} &= \text{wt} \times \frac{(\%)}{100} \times \frac{(\text{M.W. of Al})}{(\text{M.W. of NaAlO}_2)} \times \frac{(1 \text{ mole})}{(\text{M.W. of Al})} \\ &= (0.702)(0.78) (1/81.97) \\ &= 6.680 \times 10^{-3} \text{mole} \end{aligned}$$

For example, to prepare zeolite beta at Si/Al atomic ratio of 80 by using cataloid (SiO₂ 30% wt in water) for silicon source.

$$\text{Molecular Weight of Si} = 28.0855$$

$$\text{Molecular Weight of SiO}_2 = 60.0843$$

Si/Al atomic ratio of 80

$$\begin{aligned} \text{Mole of SiO}_2 \text{ required} &= (6.680 \times 10^{-3})(80) \\ &= 0.5344 \text{ mole} \end{aligned}$$

$$\begin{aligned} \text{Amount of SiO}_2 &= (0.5344)(60.0843) \\ &= 32.1090 \text{ g} \end{aligned}$$

$$\begin{aligned} \text{Amount of Cataloid} &= \frac{(100)}{(30)} \times (32.1090) \\ &= 107.0301 \end{aligned}$$

This is the amount of NaAlO₂ and SiO₂ used in gel preparation.

A-2 Calculation of vapor pressure of water

Set the partial vapor pressure of water to the requirement by adjusting the temperature of saturator according to the antoine equation

$$\log P = A - \frac{B}{(T + C)}$$

When P = vapor pressure of water, mbar

T = temperature, °C

A, B and C is constants

Range of temperature that applied ability –20 –126 °C

The values of constants.

Reactant	A	B	C
Water	8.19625	1730.630	233.426

A-3 Calculation of % crystallinity

$$\% \text{ Crystallinity} = \frac{\text{Area under XRD pattern}(2\theta=22.4)\text{of sample} \times 100}{\text{Area under XRD pattern}(2\theta=22.4)\text{of reference}}$$

Reference is the fresh zeolite beta for the same size.

For example:

Area under XRD pattern of treated = 1132

Area under XRD pattern of fresh = 1175

$$\% \text{ Crystallinity} = \frac{1132 \times 100}{1175} = 96$$

A-4 Calculation of the relative area of tetrahedral aluminum(%)

$$\text{The relative area of tetrahedral aluminum (\%)} = \frac{\text{Area of tetrahedral Al} \times 100}{\text{Total Area}}$$

Area of tetrahedral Aluminum is a peak at a chemical shift of around 54 ppm.
Total area is the total summation area of tetrahedral and octahedral aluminum(0 ppm).

For example:

Area of tetrahedral Al = weight of paper under peak area at 54 ppm = 0.0867

Area of octahedral Al = weight of paper under peak area at 0 ppm = 0.0225

$$\text{The relative area of tetrahedral aluminum (\%)} = \frac{0.0867 \times 100}{(0.0867 + 0.0225)} = 84$$

A-5 Calculation of the specific surface area

From Brunauer-Emmett-Teller (BET) equation

$$\frac{p}{n(1-p)} = \frac{1}{n_m C} + \frac{(C-1)p}{n_m C} \quad (\text{A-5-1})$$

Where, p = Relative partial pressure of adsorbed gas, P/P_0

P_0 = Saturated vapor pressure of adsorbed gas in the condensed state at the experimental temperature, atm

P = Equilibrium vapor pressure of adsorbed gas, atm

n = Gas adsorbed at pressure P , ml. At the NTP/g of sample

n_m = Gas adsorbed at monolayer, ml. At the NTP/g of sample

$C = \text{Exp} [(H_c - H_1)/RT]$

H_c = Heat of condensation of adsorbed gas on all other layers

H_1 = Heat of adsorption into the first layer

Assume $C \rightarrow \infty$, then

$$\frac{p}{n(1-p)} = \frac{p}{n_m}$$

$$n_m = n(1-p) \quad (\text{A-5-2})$$

The surface area, S , of the catalyst is given by

$$S = S_b \times n_m \quad (\text{A-5-3})$$

From the gas law

$$\frac{P_b V}{T_b} = \frac{P_t V}{T_t} \quad (\text{A-5-4})$$

Where, P_b = Pressure at 0 °C

P_t = Pressure at t °C

T_b = Temperature at 0 °C = 273.15 K

T_t = Temperature at t °C = 273.15 + t K

V = Constant volume

Then, $P_b = (273.15/T_t) P_t = 1 \text{ atm}$

Partial pressure

$$p = \frac{[\text{Flow of (He + N}_2) - \text{Flow of He}]}{\text{Flow of (He + N}_2)}$$

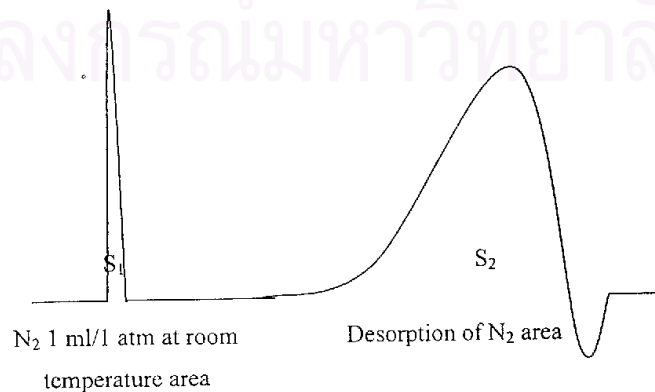
$$= 0.3 \text{ atm}$$

For nitrogen gas, the saturated vapor pressure equals to

$$P_o = 1.1 \text{ atm}$$

Then, $p = P/P_o = 0.3 / 1.1 = 0.2727$

To measure the volume of nitrogen adsorbed, n



$$n = \frac{S_2}{S_1} \times \frac{1}{W} \times \frac{273.15}{T} \text{ ml. / g of catalyst} \quad (\text{A-5-5})$$

Where, $S_1 = N_2$ 1 ml/ 1 atm at room temperature area

$S_2 =$ Desorption of N_2 area

$W =$ Sample weight, g

$T =$ Room temperature, K

Therefore,

$$n_m = \frac{S_2}{S_1} \times \frac{1}{W} \times \frac{273.15}{T} \times (1 - p)$$

$$n_m = \frac{S_2}{S_1} \times \frac{1}{W} \times \frac{273.15}{T} \times 0.7273 \quad (\text{A-5-6})$$

Whereas, the surface area of nitrogen gas from literature equal to

$$S_b = 4.373 \text{ m}^2 / \text{ml of nitrogen gas}$$

Then,

$$S = n_m = \frac{S_2}{S_1} \times \frac{1}{W} \times \frac{273.15}{T} \times 0.7273 \times 4.343$$

$$S = n_m = \frac{S_2}{S_1} \times \frac{1}{W} \times \frac{273.15}{T} \times 3.1582 \text{ m}^2 / \text{g} \quad (\text{A-5-7})$$

A-6 Calculation of reaction flow rate

The used catalyst = 0.1000 g

Pack catalyst into quartz reactor (inside diameter = 0.6 cm).

Determine the average high of catalyst bed = H cm, so that,

$$\text{Volume of bed} = \pi (0.3)^2 \times H \text{ ml-cat.}$$

Use Gas Hourly Space Velocity (GHSV) = 4000 h⁻¹

$$\text{GHSV} = \frac{\text{Volumetric flow rate}^1}{\text{Volume of bed}}$$

$$\text{Volumetric flow rate}^1 = 4000 \times \text{Volume of bed ml/h}$$

$$= \underline{4000 \times \pi (0.3)^2 \times H} \text{ ml/min}$$

A-7 Calculation of methanol conversion reaction

Methanol conversion activity was evaluated in term of conversion of methanol into other hydrocarbons

$$\text{Methanol conversion (\%)} = \frac{(\text{methanol}_{\text{in}} - \text{methanol}_{\text{out}}) \times 100}{\text{methanol}_{\text{in}}}$$

For example:

From data of Shimadzu GC 8A (Porapack-Q column)

$$\text{Methanol conversion(\%)} = \frac{(238360 - 113960) \times 100}{238360} = 49$$



สถาบันวิทยบริการ
จุฬาลงกรณ์มหาวิทยาลัย

APPENDIX B

B-1 The result of hydrothermal treatment condition: 600 °C, 24 h with 10 mole percent of water

Particle size (μm)	BET surface area (m^2/g)		%crystallinity of treated	%decreased of Al tetrahedral
	Fresh	Treated		
0.3	579	492	93	6
0.4	500	474	98	4
0.5	464	451	94	4
0.7	382	370	97	3

B-2 The result of hydrothermal treatment condition: 700 °C, 24 h with 10 mole percent of water

Particle size (μm)	%crystallinity of treated
0.2	99
0.3	96
0.4	98
0.5	94
0.7	95
0.9	97

VITA

Miss Usnee Toophorm was born on April 8, 1971 in Petchaboon, Thailand. She received the Bachelor Degree of Chemical Industrial from Faculty of Science, Chang mai University in 1993.



สถาบันวิทยบริการ
จุฬาลงกรณ์มหาวิทยาลัย